2013-01-01

Manufacturing Nerve Guidance Conduits by Stereolithography for Use in Peripheral Nerve Regeneration

Mireya Aidee Perez
University of Texas at El Paso, mireyapz1432@hotmail.com

MANUFACTURING NERVE GUIDANCE CONDUITS BY STEREOLITHOGRAPHY FOR USE IN PERIPHERAL NERVE REGENERATION

MIREYA AIDEE PEREZ

Biomedical Engineering

APPROVED:

Ryan B. Wicker, Ph.D., Chair

Thomas Boland, Ph.D.

Kristin L. Gosselink, Ph.D.

Benjamin C. Flores, Ph.D.
Dean of the Graduate School

Dedication

This Thesis is dedicated to my Family

MANUFACTURING NERVE GUIDANCE CONDUITS BY STEREOLITHOGRAPHY FOR USE IN PERIPHERAL NERVE REGENERATION

by

MIREYA AIDEE PEREZ, B.S.

THESIS

Presented to the Faculty of the Graduate School of

The University of Texas at El Paso

in Partial Fulfillment

of the Requirements

for the Degree of

MASTER OF SCIENCE

Biomedical Engineering

THE UNIVERSITY OF TEXAS AT EL PASO

December 2013

Acknowledgements

First of all, I wish to thank Dr. Ryan B. Wicker, director of the W.M. Keck Center of 3D Innovation for guiding me during the entire duration of this research and for providing me all of the tools I needed to conduct the tests you will read about in these chapters. I wish to thank the other members of my committee, Dr. Thomas Boland and Dr. Kristin Gosselink for agreeing to participate in this process and for their support. I especially wish to thank Dr. Karina Arcaute, for having the patience to train me during the initial stages of my research and for continuing to be a mentor and lifelong friend. I wish to thank Dr. Brenda Mann from the University of Utah for her guidance and help during the NGF-release tests that were conducted. I also wish to thank Drs. Gregory Evans and Maristella Evangelista from the University of California, Irvine for their collaboration and dedication to the *in vivo* portion of this research. From the Department of Biology, I wish to thank Dr. Kristin Garza and her student Adam Villalba for allowing me to observe an ELISA procedure as well as Lani Alcazar, and Emma Arigi for helping me use the ELISA plate reader. I wish to thank David Espalin and Mahesh Tonde for their contributions in the design of the retrofitted small-beam laser as well as Frank Medina, Luis Ochoa, and all of the other members of the Keck Center team for being there to help me and answer any questions I may have ever had. Other students who deserve recognition are Elaine Maestas, for her help with the ELISAs, and Lizette Mendiola, for helping me with cell counts.

I wish to thank all of the friends who supported me during this endeavor and who encouraged me to keep going. Most importantly, I would like to thank my parents, Gustavo Perez and Rosaura C. Perez, and my brothers, Daniel and Alan, for always providing me the love and encouragement necessary to succeed in life and for their continued support of all my endeavors.

The work conducted in this thesis was funded primarily by the National Science Foundation under Grant No. CBET-0730750.

Abstract

Nerve regeneration techniques have been studied in great depth in recent years. Peripheral nerve injuries, in particular, can be caused by accidents, falls, athletic injuries, etc. Current methods of repair include direct suturing of the 2 injured nerve ends or the use of autografts, when a nerve section is taken from another area of the body. Both methods have a series of limitations which have led researchers to study alternative methods of repair. Nerve guidance conduits may provide a viable solution because they can be modified and adapted to the patient's needs. Some conduits already exist on the market and are manufactured using FDA-approved biomaterials. Poly(ethylene glycol) (PEG) is an FDA-approved biomaterial not currently used in market-available conduits. It possesses many qualities that would make it a desirable material for nerve regeneration. It does not interfere with activity of peptides that can be used to make the material bioactive and biodegradable. It is also photocrosslinkable through exposure to ultraviolet (UV) light. One such method that does this is stereolithography (SL). SL is an additive manufacturing technology that runs a UV laser over the surface of a photocrosslinkable resin, solidifying the resin into a desired shape. SL provides one of the best surface finishes of any additive manufacturing technology. In the case of PEG, SL forms a hydrogel. This allows the material to resemble soft tissue. A series of tests were conducted for this thesis to study the use of PEG in the construction of nerve guidance conduits via SL.

First, it was important to test how growth factors can be integrated into a nerve guidance conduit to promote neurite extension, improving the prospect of regeneration. For this, nerve growth factor (NGF) was incorporated into PEG scaffolds through encapsulation and conjugation of the protein. The rate of release of NGF by the scaffold was tested over a 35-day period using 2 molecular weights of PEG. The bioactivity of NGF was tested by seeding PC-12 cells with it and analyzing neurite extension. Then, cells were seeded directly on a PEG surface to test if they can attach to the material through the use of a cell adhesion peptide, RGDS. In addition, NGF was added to already-attached cells to verify that neurite extension can also be accomplished on a PEG surface. These results were compared to those achieved by growing cells on tissue culture-treated plastic. *In vivo* tests were conducted by implanting single-lumen and multi-lumen conduits into Sprague-Dawley rats. Histomorphological

analysis compared axonal regeneration in proximal, middle, and distal portions of the conduit to that found in healthy, uninjured, nerve. These tests were also used to compare the efficiency of single and multi-lumen conduits. Cell attachment to PEG may be increased if the surface area available for attachment is increased. For this, an alternative construction method was studied using a modified SL system. A commercial SL system was retrofitted in a biosafety cabinet and the optical system was changed to decrease the diameter of the laser beam. The decrease in diameter would permit construction of nerve guidance conduits of an increased number of lumens by reducing the diameter. Construction of 14, 16, and 18-lumen samples was attempted using this new, modified, SL system.

The NGF proved to be bioactive in that it promoted neurite extension in PC-12 cells. When encapsulating NGF, a greater release was seen using a higher molecular weight of PEGda. On the other hand, when conjugating NGF, a greater release was seen from a lower molecular weight. A quick initial burst was present from all of the samples. RGDS did, in fact, produce attachment of cells to a PEG surface. However, the amount of cells attached was less than that seen on tissue-culture treated plastic. Addition of NGF promoted neurite extension on both surfaces with a greater percentage of cells extending neurites on the PEG surface. This is most likely due to the fact that neurites extend better on more flexible surfaces as less tension is required. *In vivo* tests showed that nerve regeneration can be achieved by using SL-fabricated PEG conduits. Upon histomorphological analysis, single-lumen conduits yielded results comparable to controls as seen in axon diameter, myelin thickness, and total number of fibers. On the other hand, histomorphological analysis of multi-lumen conduits could not be achieved due to problems in the staining and sectioning of the sections. Finally, when using the modified SL system, it was also possible to produce conduits with (or conduit sections) sections containing as many as 18 lumens. Calculations of samples in a swollen state showed 7-lumen conduits had a surface area of 125.6 mm^2 while 18-lumen conduits had an increased surface area of 193.5 mm^2.

Nerve injuries can be very debilitating and can interrupt a person's lifestyle significantly. This research studied SL as a means for constructing PEG nerve guidance conduits as an alternative to current methods of repair. As a building technique, SL offers several advantages in the design and finish of the product. Results achieved in this thesis demonstrated that PEG can be made bioactive

through addition of RGDS, a cell adhesion peptide, and NGF, a protein that stimulates neurite extension. *In vivo* tests showed that regeneration can be achieved using single-lumen conduits. More tests are required to study regeneration using multi-lumen conduits as problems in the histological preparation hindered the analysis of such. Multi-lumen conduits (containing up to 18 lumens) can, however, be built using a laser of reduced diameter, increasing the surface area available for cell attachment. Although more tests are required, the ability to regenerate injured nerves using SL is possible.

Table of Contents

List of Tables

List of Figures

Chapter 1: Introduction

1.1 THE NERVOUS SYSTEM

The nervous system is the system that allows the body to react to external and internal environmental changes. It establishes coordination and integration of activities amongst other systems in the body, such as that which occurs between the circulatory and respiratory systems. The nervous system can be divided into two structural components: the central nervous system (CNS) and the peripheral nervous system (PNS). The CNS consists of the brain and the spinal cord while the PNS consists of exterior fibers that send impulses to and away from the CNS. There are two main cell types making up the nervous system: neurons and neuroglia, also known as glial cells. Neurons are the functional units of the nervous system [1]. They communicate with each other using a combination of electrical and chemical signals. Because most neurons are electrically excitable, they can convey electrical signals rapidly and accurately. This is the way a human body organizes and directs physiological responses. Neurons are composed of a cell body with dendrites, and an axon. Axons are what carry the nerve impulses, known as action potentials, away from the cell body [2]. Large segments of axon are insulated by a myelin sheath, formed by overlapping layers of myelin, a type of fatty membrane made of lipid and protein [1]. Myelin serves two purposes: to increase the effective transmembrane resistance and decrease the effective membrane capacitance. This greatly increases the length constant of the axon membrane covered by myelin. Therefore, enhancing the efficiency with which current spreads in a longitudinal direction. However, in order for this to happen, myelin must leave some segments of the axon exposed. Such segments are known as nodes of Ranvier. Wrapped segments of axon can range from 200 μm to 2 mm in length; whereas nodes of Ranvier are only about 10 μm. This results in an inconsistent propagation of action potentials along the axonal membrane. Instead, action potentials are only produced in the nodes of Ranvier, resulting in a phenomenon known as saltatory conduction. This greatly enhances the velocity of signal transmission. A single nerve can contain many unmyelinated axons of different diameters. As a result, signals travel at different velocities within the same nerve [2]. The second cell type, neuroglia, are more abundant than neurons; about five times more. They are present because they form the scaffolding of the nervous tissue. They

are nonneuronal and nonexcitable [1]. Two types of neuroglia are Schwann cells and oligodendrocytes. Schwann cells are the cells that lay down myelin around axons in the PNS while oligodendrocytes do so in the CNS. All of these components are illustrated in Figure 1.1.

As previously mentioned, cell bodies are surrounded by dendrites. Dendrites are branches that serve as receivers to gather information from other neurons and carry them toward the cell body. At the opposite end of a neuron, lie the axon terminals. The specialized location where a dendrite from a neuron meets an axon terminal from another neuron is called a synapse [See Figure 1.1]. Presynaptic and postsynaptic cells pass and receive information across a synapse, respectively. The majority of synaptic transmission is done by chemical neurotransmitters, specific molecules released from the axon terminals of a presynaptic neuron in response to an action potential in its axon [2].

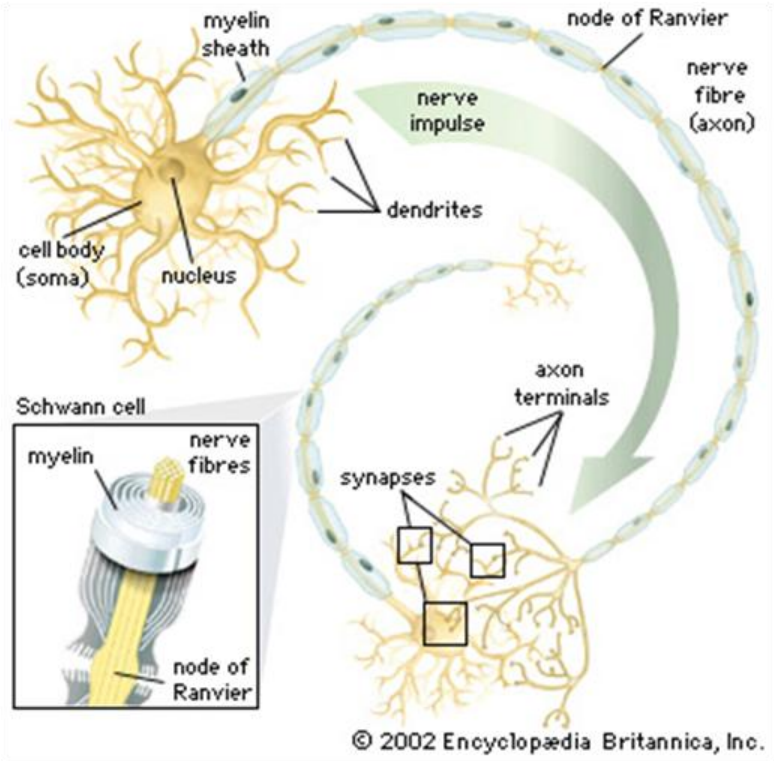

Figure 1.1: Anatomy of a neuron. By courtesy of Encyclopaedia Britannica, Inc., copyright 2002; used with permission [3].

1.1.1 The Peripheral Nervous System

The purpose of PNS is to connect peripheral structures to the CNS. Peripheral nerves are made up of bundles of nerve fibers, their connective tissue coverings, and blood vessels. The neurolemma of a myelinated nerve fiber consists of a myelin sheath surrounding an individual axon, along with the Schwann cells forming such myelin. The neurolemma of unmyelinated nerve fibers consists of multiple axons embedded within the cytoplasm of non-myelin-producing Schwann cells. Peripheral nerves are protected by three types of connective tissue coverings and are therefore, fairly strong. The endoneurium surrounds the neurolemma cells and axons. The perineurium surrounds a fascicle, or bundle of nerve fibers. Finally, the epineurium encloses a bundle of fascicles and also forms the outermost covering of a nerve. It can also include fatty tissue, blood vessels, and lymphatics [1]. The various connective tissue coverings can be seen in Figure 1.2.

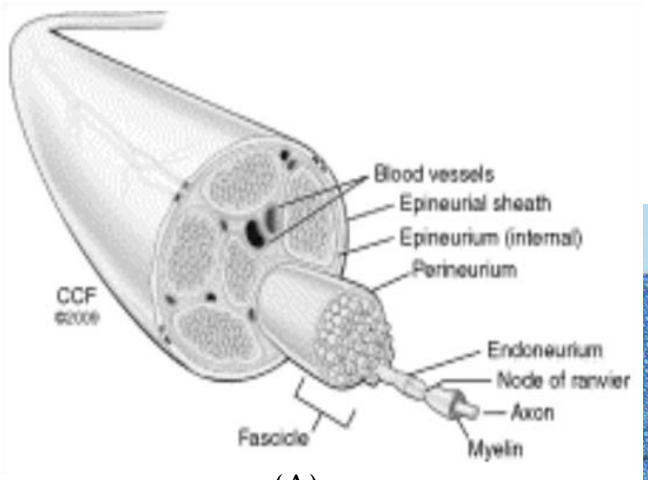

(A)

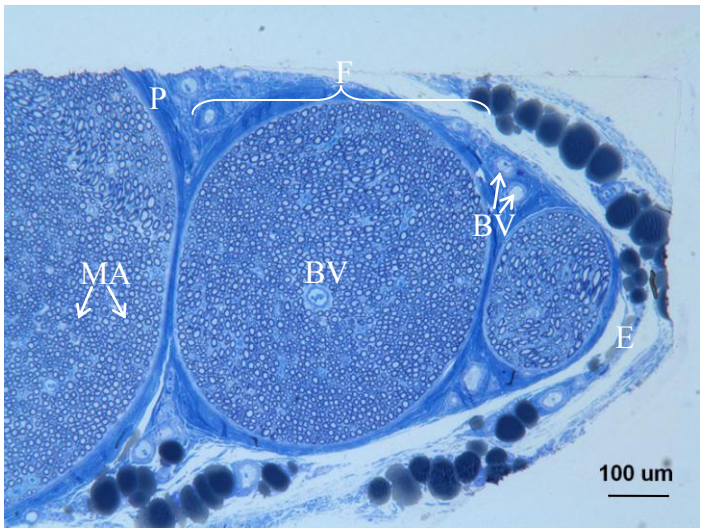

(B)

Figure 1.2: Arrangement of a Peripheral Nerve; (A) Illustration showing connective tissue coverings. Used with permission [4]; (B) Cross-sectional view of a nerve, F = Fascicle, P = Perineurium, MA = Myelinated axons, BV = Blood vessels, E = Epineurium

1.1.2 Peripheral Nerve Injuries

While injuries to the spinal cord can have severe consequences, such as paraplegia or quadriplegia, peripheral nerve injuries can have series results as well. They can occur as a result of automobile accidents, work accidents, falls, athletic injuries, etc. Peripheral nerve injuries interfere with the brain's ability to communicate with muscles and organs. They are a significant source of morbidity in trauma patients. According to a 10-year study conducted by Noble *et al.*, peripheral nerve injuries affect 2.8% of all trauma cases [5]. Each year in the U.S., approximately 360,000 people are affected by upper extremity paralytic syndromes [6]. This, in turn, results in lost work due to days of restricted activity and bed rest. The most severe form of injury is when a nerve is completely severed. Because it is no longer receiving metabolic support from the cell bodies, the distal portion begins to degenerate through a process known as Wallerian degeneration [7]. First, the cytoskeleton breaks down and the cell membrane begins to dissolve. Then, Schwann cells shed their myelin lipids [8]. Although it is debated that Schwann cells do not participate in clearance of myelin debris, studies conducted by Stoll, *et al*. support evidence showing that Schwann cells, aided by phagocytic cells such as macrophages, clear myelin and other axonal debris [9]. Following debris clearance, these cells can also produce cytokines to enhance axonal regeneration. New axons are usually born at the nodes of Ranvier of existing axons. Regeneration begins at the proximal end, continues in the distal direction, and is complete once axons reach the distal target. Axonal regeneration in humans occurs at an approximate rate of 2 – 5 mm/day [8] [See Figure 1.3].

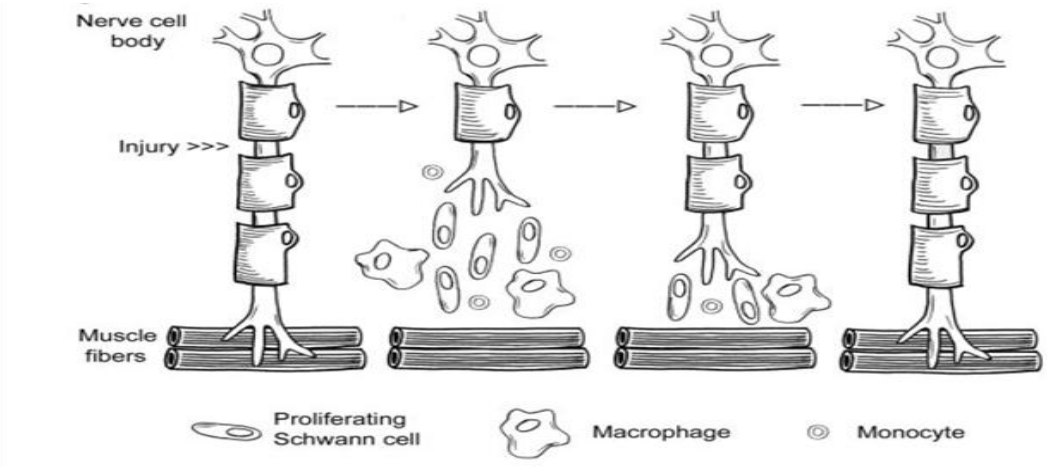

Figure 1.3: Physiological response to a peripheral nerve injury. Used with permission [8].

1.1.3 Current Methods of Peripheral Nerve Repair

Recent technology has allowed for many advances in the repair of nerve injuries; two forms being direct repair and autograft repair [10]. Neurorrhaphy, a type of direct repair, consists of direct surgical reconnection of the proximal and distal nerve ends [See Figure 1.4 (A)]. Such repair can only be performed when the defect is less than 5 mm [11]. It is not effective if the nerve gap is too large because introducing tension into the nerve can result in loss of function [10]. Wall, *et al*. showed that the tibial nerve can regain almost all function when stretched only by 6%. Yet, when stretched by 12%, there is complete loss of function [12]. Autograft repair, on the other hand, uses a nerve graft taken from a donor site [10] [See Figure 1.4 (B)]. Autografts are more likely to be biocompatible than synthetic materials. For this reason, they are the current standard of care for peripheral nerve injuries too large to be treated by direct repair [11]. However, there are several limitations to autograft repair. There is always a risk for donor site morbidity such as scarring or loss of sensation. There is also a limited supply of donor tissue, especially when treatment of long nerve gaps is required [11]. There is no guarantee for full functional recovery at the site of injury. In fact, only about an 80% clinical functional recovery rate is achieved through autograft repair [8]. Such deficiencies in direct and autograft repair have led researchers to look for other methods to treat peripheral nerve injuries. A nerve guidance conduit can provide a promising alternative to the previously mentioned methods [10, 11, 13].

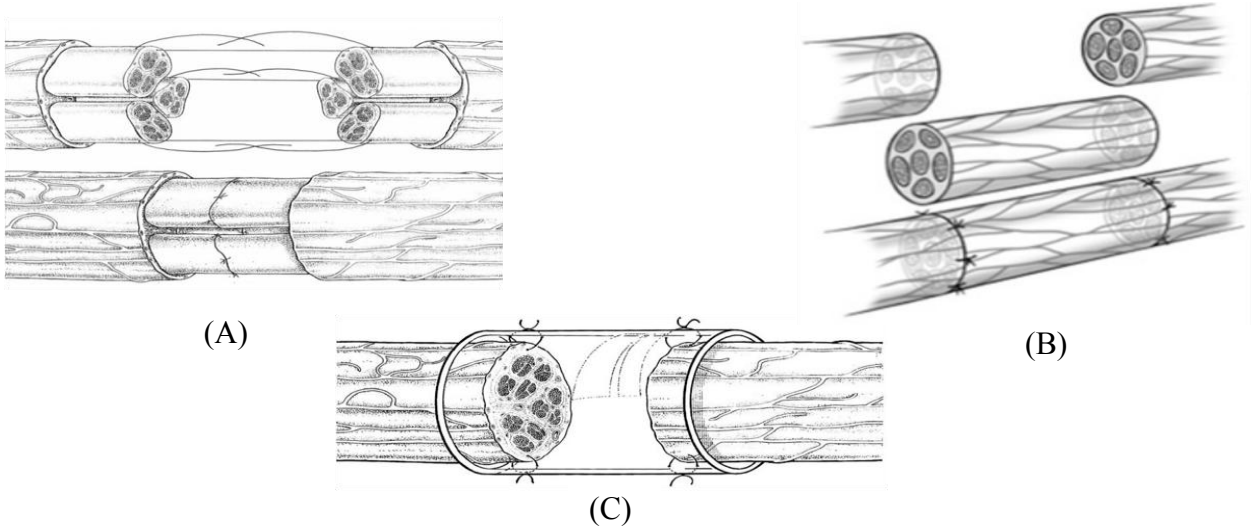

Figure 1.4: Methods of peripheral nerve repair; (A) Direct surgical reconnection [7]; (B) Autograft nerve repair [14]; (C) Nerve guidance conduit [7]. All images used with permission.

1.1.4 Nerve Guidance Conduits

Nerve guidance conduits are scaffolds used to guide nerve regeneration. They are typically designed as tubular conduits to which nervous tissue can be sutured at each end. Unlike using an autograft, they eliminate the need for a second surgical site. Therefore, donor site morbidity is not a factor. A nerve guidance conduit should possess three essential properties. It must be readily manufactured having the desired dimensions, must be easily implantable, and must be easily sterilizable [15]. In addition, there are other properties a conduit may possess to make it an ideal candidate for nerve repair: biodegradability and porosity of its walls, controlled release of bioactive factors, the ability to incorporate support cells, an internal matrix that allows for cell migration, intraluminal channels that mimic the internal structure of fascicles, and electrical activity [See Figure 1.5] [15].

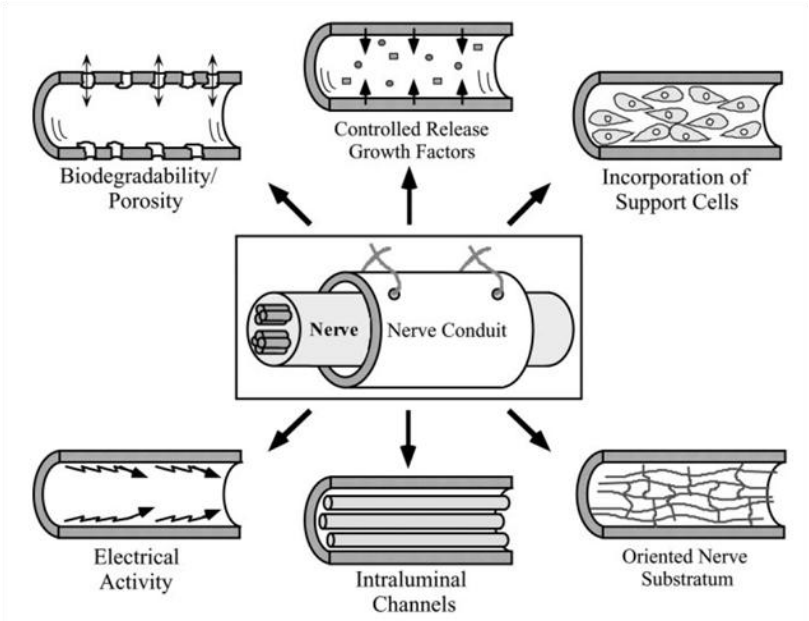

Figure 1.5: Properties of an ideal nerve guidance conduit. Used with permission [15].

Certain materials have already received approval by the US Food and Drug Administration (FDA) for use in peripheral nerve repair. These include both natural and synthetic materials. The Neurotube® is a conduit made of polyglycolic acid (PGA) that received FDA approval in 1999. It has a degradation period of 3 months and works with gaps of 2-4 cm. The NeuraGen®, Neuroflex™, and NeuroMatrix™ tubes are all made from type I collagen and were approved in 2001. NeuraGen® has a

36-48 month degradation period and can be used for gaps of 2-3 cm. On the other hand Neuroflex™, and NeuroMatrix™ have a degradation period of 4-8 months and work for gaps of 2.5 cm. The Neurolac® was approved in 2003. It is made from poly(α-lactide-ε-caprolactone) (PCL) and has a 16 month degradation. It works with gaps of 3 cm. The AxoGuard™ Nerve Connector is made from porcine small intestine submucosa (SIS). It was also approved in 2003. It works with 10 mm gaps and has a degradation period of 3 months. Finally, the SaluTunnel™ Nerve Protector™, made from polyvinyl alcohol (PVA), was approved in 2010. It is non-absorbable and works with 6.35 cm gaps [16].

There are some downsides to working with these implants. The high rate of degradation of some of these materials, such as PGA, type I collagen, and SIS, causes a contiguous reduction of short term mechanical properties as well as acidic degradation products. On the other hand, conduits that degrade over too long (NeuraGen®) or those that do not degrade at all (Nerve Protector™) may lead to nerve compression and tension at the suture lines once regeneration has occurred. The Neurolac conduit, made from PCL, is very rigid. Previous studies of this conduit have shown frequent needle breakage during suturing. This may also lead to the nerve stumps being torn out of the conduit as a result of inflexibility. Finally, natural materials, such as type I collagen or SIS, may cause undesirable immune responses. Therefore, immunosuppressive drugs may be required. Batch-to-batch variations may also diminish the reproducible performance of these devices [16].

1.2 STEREOLITHOGRAPHY

Stereolithography (SL) is an additive manufacturing technology in which three-dimensional (3D) parts are built in a layer by layer basis when a laser beam scans the surface of a photocrosslinkable liquid resin. First, a computer-aided design (CAD) of the desired part is created. The user must convert the file into .stl format and import it into the SL system. In a commercial SL system, a large vat is filled with liquid resin. A computer-controlled optical scanning system directs a helium-cadmium (HeCd) ultraviolet (UV) laser via a specific path outlined by the CAD file. The laser cures a thin layer of resin near the surface. The build platform is then lowered by an elevator and a sweeper blade coats a new layer of resin on the surface. The laser travels across the surface again and a new layer is similarly

formed. The process continues until all of the layers are built and the part is finished. The vat can be drained to remove the part for additional processing if necessary [17]. These components are illustrated in Figure 1.6.

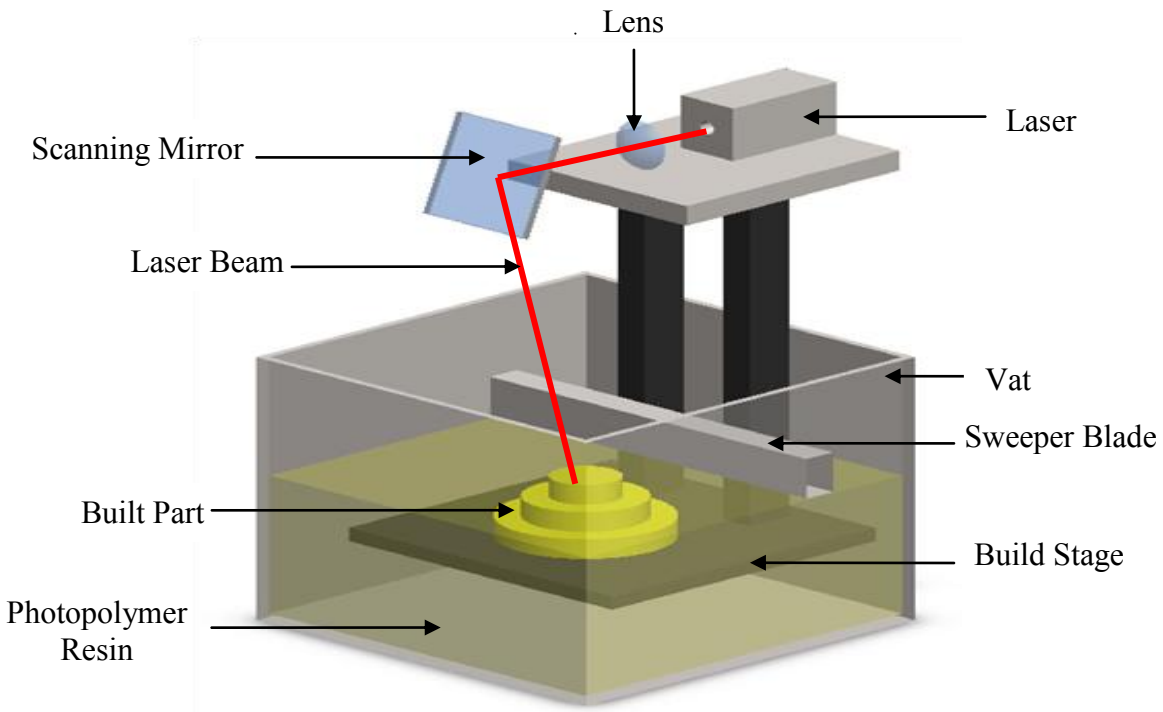

Figure 1.6: Commercial set-up of a stereolithography system

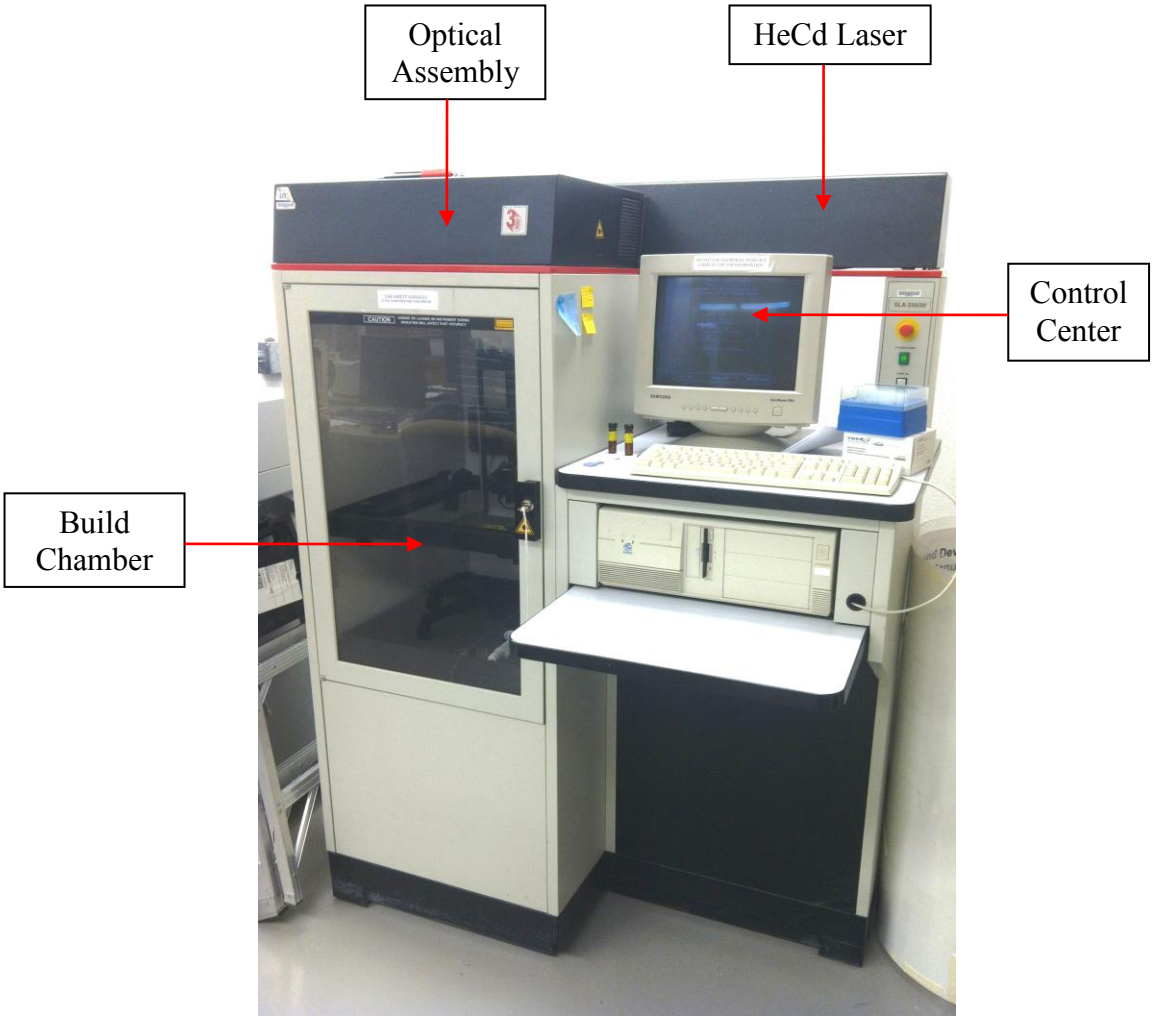

(A)

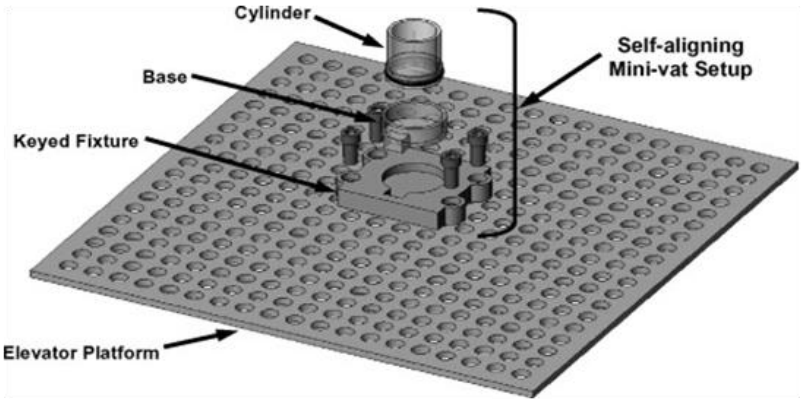

(B)

Figure 1.7: 3D Systems SLA 250/50 (Valencia, CA); (A) Exterior view; (B) Modified mini vat design. Used with permission [18].

1.2.1 Mini Vat Design

The SLA 250/50 from 3D Systems (Valencia, CA) pictured in Figure 1.7 (A), was utilized for most of the tests in the chapters that follow. The design of a typical SL system was not practical for use in these tests as the vat that holds the liquid polymer was too large. Therefore, it was slightly modified to use a mini vat [See Figure 1.7 (B)]. A keyed fixture was secured to the already existing elevator platform. The mini vat consisted of two parts: a base and cylinder. The cylinder snaps into the base creating a tight fit. The base then fits into the keyed fixture. When a slightly larger construction area was needed, the cylinder was removed and the base was used on its own [18]. When using this vat, the automated elevator movement was overridden. Because of this, new polymer was added manually between each layer to raise the polymer level and allow for construction of a new layer on top of the existing one. Prior to building a part, it was necessary to test the volume of polymer needed to ensure good interlayer bonding.

1.2.2 Building Nerve Guidance Conduits by Stereolithography

Advances in photocrosslinkable biomaterials provide promising direction for the fabrication of conduits using SL. SL is a highly accurate technology. It can obtain one of the best surface finishes amongst additive manufacturing technologies [17]. Because SL systems work with CAD files, making modifications to the design of a conduit is simple. For example, the number of lumens, lumen diameter, conduit diameter, etc. can be changed within a brief period. The length of a conduit can also be changed to accommodate the need of a patient by increasing or decreasing the number of layers that are built. A CAD file can be changed to build several conduits at the same time. Critical exposure (E_C) and penetration depth (D_P) are properties of every photopolymer. E_C is the energy level required to change the photopolymer from a liquid to a solid state while D_P is the depth at which the irradiance becomes 1/e times that at the surface [19]. By modifying the E_C and D_P values on the system, the user can also modify the laser scan speed. It is important to use a speed appropriate to the type of photopolymer being used. As some require longer UV exposure to photocrosslink, a slower laser scan speed is required. The following equation, which gives the solidification shape along the laser-moving axis, shows the relationship amongst these parameters:

$$y = \frac{2}{W_0(z)^2}\sqrt{\ln\left(\sqrt{\frac{2}{\pi}}\frac{P_L}{W_0(z)^2 V_S E_C}\right) - \frac{z}{D_P}} \quad (1.2 - 1)\ [19]$$

where

$W_0(z)$ is Gaussian half-width of the laser beam,

P_L is laser power,

V_S is laser scan speed,

E_C is critical exposure,

D_P is penetration depth.

1.3 STEREOLITHOGRAPHY MATERIALS

1.3.1 Poly(ethylene glycol)

Poly(ethylene glycol) (PEG) is a biocompatible material, approved by the FDA for human use [20]. The material has been studied for use in numerous applications such as formation of PEG-protein conjugates for pharmaceutical purposes, formation of PEG tethers for synthesis of biomolecules and biological targeting, and surface modification to provide protein and cell rejecting properties. In hydrogel form PEG can be used for cell encapsulation, drug delivery, and wound covering [21]. It has been studied for a variety of tissue engineering applications including those for regeneration of bone, cartilage, and smooth muscle [22-24]. The safety of PEG for use in humans is dependent upon its molecular weight. At low molecular weights (< 1,000 Da) the material can be oxidized into toxic diacid and hydroxyl acid metabolites by liver enzymes, alcohol dehydrogenase and aldehyde dehydrogenase. High molecular weight PEG, on the other hand, is excreted through glomerular filtration of the kidney [25]. Typically, for tissue engineering purposes, molecular weights of 3,400 Da or 6,000 Da are used [23, 24, 26].

Previous work has shown it is possible to build nerve guidance conduits from high molecular weight PEG using SL [27]. Through acrylation or methacrylation of its endcaps, it can be chemically modified into a photocrosslinkable material. Such is the case of poly(ethylene glycol) diacrylate (PEGda). Crosslinking is achieved when there is free-radical polymerization of the acrylate groups. This takes place in the presence of a photoinitiator and UV light. The result is the formation of a

hydrogel that is stable over an extended period of time [28]. The chemical structures of PEG and PEGda can be seen in Figure 1.8 (A) and (B). PEGda is a good candidate for conduit construction because it possesses many of the previously mentioned properties required of a conduit material. Because of its hydrophilic nature, the hydrogel chains absorb and retain water in an effort to reach equilibrium [29]. When placed in liquid, PEGda scaffolds swell to a dimension that is 18 to 25% larger than the original [18, 27]. For this reason, PEGda mimics soft tissue well. Arcaute *et al.* showed that PEGda scaffolds can withstand the lyophilization and hydrogen peroxide sterilization processes; therefore, making conduits readily available and easy to transport [27]. In addition, PEGda exhibits low immunogenicity and antigenicity. It does not interfere with activities of enzymes or proteins [24, 26, 29]. Because of this, it can be made bioactive through addition of cell adhesion peptides or biodegradable through addition of peptides that are susceptible to enzymatic attack, chemical modification, or copolymerization [24, 26].

1.3.2 Irgacure 2959

Photoinitiators are light-sensitive compounds that can generate free radicals. Irgacure-2959 (I-2959) is a commercially available photoinitiator. Its chemical name is 2-hydroxy-1-[4-hydroxyethoxy)phenyl]-2-methyl-1-propanone [See Figure 1.8 (C)]. Photoinitiators commonly used in the formation of hydrogels, typically exhibit low cytotoxicity. This makes it possible to encapsulate viable cells within a hydrogel mesh, if desired [30].

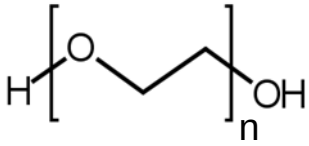

Poly(ethylene glycol)
(A)

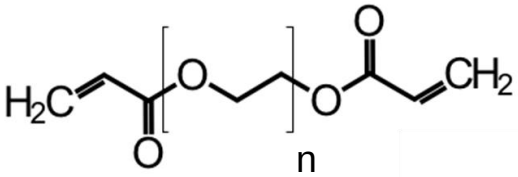

Poly(ethylene glycol) diacrylate
(B)

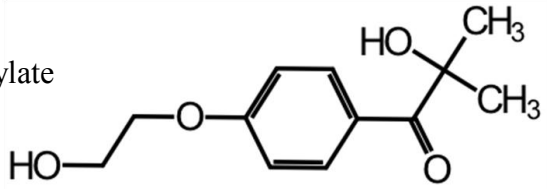

2-hydroxy-1-[4-hydroxyethoxy)phenyl]-2-methyl-1-propanone
(C)

Figure 1.8: Chemical structures; (A) PEG; (B) PEGda; (C) I-2959; [31].

Chapter 2: Controlling Release of Nerve Growth Factor by a Poly(ethylene glycol) Scaffold

2.1 INTRODUCTION

2.1.1 Nerve Growth Factor

Nerve growth factor (NGF) is a neurotrophin naturally produced by Schwann cells that is necessary for signaling in peripheral nerve regeneration [32]. NGF is a 140 kDa polypeptide composed of three protein subunits: α, β, and γ. The β subunit is the one responsible for the neurotrophin effects and is also known as 2.5S NGF. This subunit is a dimer with a molecular weight of 26 kDa [33]. The dimeric structure can be seen in Figure 2.1. NGF promotes cell survival, differentiation, and neurite extension [8]. A neurite is anything that sprouts from the cell body of a neuron: an axon or a dendrite. NGF also has the ability to protect neurons from death at sites of injury [34]. It has already been demonstrated that poly(ethylene glycol) (PEG) is a material that is receptive to addition of proteins and enzymes as it does not interfere with their activity [29]. NGF can therefore, be incorporated into PEG nerve guidance conduits, increasing their ability to guide complete nerve regeneration. Axonal regeneration in humans occurs at an approximate rate of 2 – 5 mm/day [8]. The time necessary for regeneration is dependent upon the length of the site of injury. This is because regeneration occurs from the proximal end to the distal end and is complete once axons reach the distal target. If the scaffold material releases the NGF too soon, before full regeneration takes place, there may not be enough left during the later stages of regeneration. Therefore NGF release by the polymer must occur in a controlled manner [35].

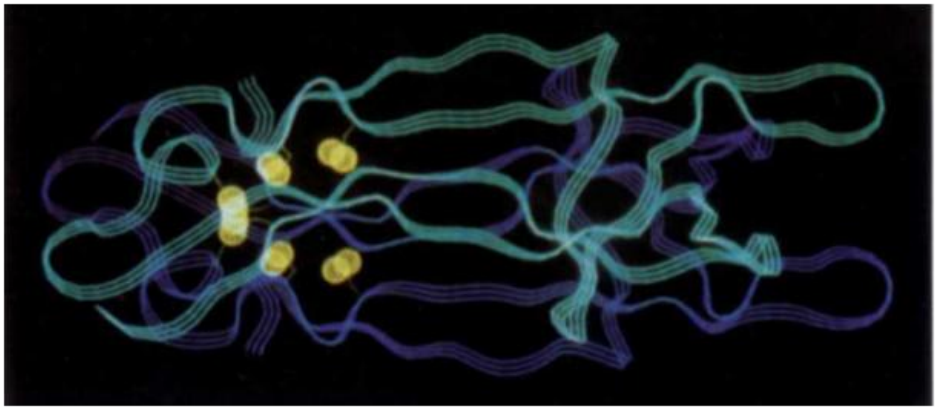

Figure 2.1: Structure of 2.5S NGF. Used with permission [36].

2.1.2 NGF in Tissue Engineering Scaffolds

Several methods have been tested for incorporating growth factors into a tissue engineering scaffolds. One method, as done by Evans *et al.*, incorporates Schwann cells into guidance conduits rather than adding the growth factors directly [37]. Others have tested the use of polymeric microspheres [38-40]. For example, Xu *et al.* used biodegradable poly(phosphoester) (PPE) microspheres to encapsulate NGF and achieve controlled delivery over a 10-week period of sciatic regeneration [41]. Lee *et al.*, on the other hand, tested regeneration along the sciatic nerve of a rat by using a fibrin-based matrix to control the delivery of NGF based on its affinity to interactions with heparin-binding sites [35].

2.1.3 PC-12 Cell Line

The rat pheochromocytoma cell line (PC-12) is derived from an embryonic adrenal tumor. These cells are commonly used in neuronal experiments because upon incubation with NGF they are differentiated from chromaffin-like cells to sympathetic neuron-like cells. As a result, they extend neurites and express neuron-specific proteins. Other morphological changes include elaboration of microtubule arrays in neurites and the appearance of synaptic vesicles [42].

2.1.4 Objective

This research utilized 2 methods of incorporating NGF into a poly(ethylene glycol) diacrylate (PEGda) disk-shaped scaffold, encapsulation of NGF within the hydrogel matrix and conjugation of NGF to the hydrogel molecules. This was achieved using 2 different molecular weights of PEGda, 3.4 kDa and 6 kDa. The objective was to test which method would best serve to obtain controlled release of NGF over a 30-day period. Prior to testing the rate of release, the protein's bioactivity was tested by seeding PC-12 cells with it and analyzing neurite extension.

2.2 MATERIALS AND METHODS

2.2.1 NGF Reconstitution

The NGF for these tests was obtained in dehydrated form from Promega (mNGF, 2.5S, Madison, WI). It was reconstituted at a concentration of 1 µg/µL with RPMI-1640 (Sigma-Aldrich, St. Louis,

MO) containing 1% Bovine Serum Albumin (BSA) and kept in microcentrifuge tubes at -20°C until further use.

2.2.2 NGF Bioactivity Test

PC-12 cells (ATCC, Manassas, VA) were maintained at 37°C, 90% relative humidity, and a 5% CO_2 environment. They were kept in complete RPMI-1640 media supplemented with 10% Horse Serum, 5% Fetal Bovine Serum, 1% glutamine-penicillin-streptomycin (GPS), 10 mM HEPES, and 1 mM sodium pyruvate. The cells were primed with NGF at 50 ng/mL 2 days before the start of the experiment. They were then transferred onto 24-well plates made of tissue-culture treated polystyrene at 10^3 cells/well. One mL of complete media containing either 50 ng/mL, 100 ng/mL, or 150 ng/mL of NGF was added per well. As a control, some cells were kept in media without NGF. The plates were incubated under the same conditions as before (37°C, 90% relative humidity, and 5% CO_2). The media was removed after 3 days and replaced with fresh media containing the same NGF concentrations. All of the steps were completed in a biosafety cabinet (Purifier Class II, Labconco, Kansas City, MO) to reduce the risk of contamination. Low (100x) and high (200x) magnification images were taken 7 days after the initial seeding using an inverted microscope (Leica DMIRB, Leica Microsystems, Germany) with a charge-coupled device camera (Retiga 2000S Fast 1394, QImaging Corp., Canada).

2.2.3 PEGda Preparation

All PEGda solutions were stored at -20°C and allowed to reach room temperature, approximately 1 hour before preparation. Two PEGda preparations were made using either 3.4 kDa or 6 kDa. At a molecular weight of 3.4 kDa, PEGda is commercially available through Laysan Bio Inc. (Arab, AL). At 6 kDa it was received from the University of Utah's Department of Bioengineering and synthesized via a process outlined in Gunn *et al.* [26]. Irgacure 2959 (I-2959, Ciba Specialty Chemicals, Tarrytown, NY) was used as the photoinitiator and 1X Phosphate Buffered Saline (PBS) as the solvent. The solutions were prepared by adding 1 g of PEGda and 0.0167 g of I-2959 to 2.33 mL of PBS. This yielded a 30 wt% concentration of PEGda and a 0.5 wt% concentration of I-2959. The solution was then placed on a shaker until the polymer and photoinitiator were completely dissolved (~2 hours). An

amber-colored glass vial was used for preparation of the solution to reduce the amount of ambient light exposure and prevent early photocrosslinking.

2.2.4 NGF Conjugation

To conjugate NGF to PEGda, a Michael-type addition reaction was conducted. In this reaction, a free thiol or primary amine on NGF reacts with an acrylate on PEGda under slightly basic conditions. For this, 4.4 μg of PEGda were dissolved in 2 mL PBS and syringe filtered to eliminate any clumps. This was done for both, the 3.4 kDa and 6 kDa, solutions. For the 3.4 kDa solution, 9 μL of the newly mixed PEGda solution and 26 μL of NGF were added to 65 μL of PBS (pH 7.4) in a new microcentrifuge tube. For 6 kDa, 5.27 μL of PEGda and 10 μL of NGF were added to 84.73 μL of PBS (pH 7.4) in another microcentrifuge tube. These quantities yielded a 1:5 ratio of NGF to PEGda for each respective molecular weight. Both tubes were covered with aluminum foil and left undisturbed for 2 hours at room temperature.

2.2.5 NGF Encapsulation

For encapsulated NGF, the protein was added to PEGda while the polymer was still in liquid form. This was done so that upon exposure to UV light, the PEGda molecules would crosslink forming a hydrogel mesh that encapsulated the NGF within. Calculations were made so each disk would contain 500 ng of NGF.

2.2.6 Disk Construction

Disk-shaped samples were designed using SolidWorks™ [See Figure 2.2]. They were built using the 3D Systems® model 250/50 (Valencia, CA). Prior to using the SL equipment, it was disinfected thoroughly with antibacterial wipes to prevent contamination during the construction process. The laser was allowed to reach maximum power (16-17 mW). The disks were built using 600 μL of PEGda at a laser scan speed of 8.085 in/s. Batches of 6 disks of each material were built and immediately suspended in 1 mL of RPMI-1640 media in ultra-low attachment microcentrifuge tubes. One disk was housed per tube. This media did not contain any of the supplements previously mentioned for cell culture. Unlike other PEGda samples, these disks were not rinsed in deionized water after

construction so as not lose any of the NGF within the scaffold. The tubes were incubated at 37˚C in a 5% CO_2 environment at 90% humidity [See Figure 2.3]. The media was collected and replaced with fresh RPMI-1640 at various time points following initial disk construction: 2 hours, 4 hours, 8 hours, 12 hours, 24 hours, 48 hours, 5 days, 7 days, 10 days, 15 days, and 30 days. The media collected at each time point was stored in microcentrifuge tubes at -20°C until ready for analysis with ELISA.

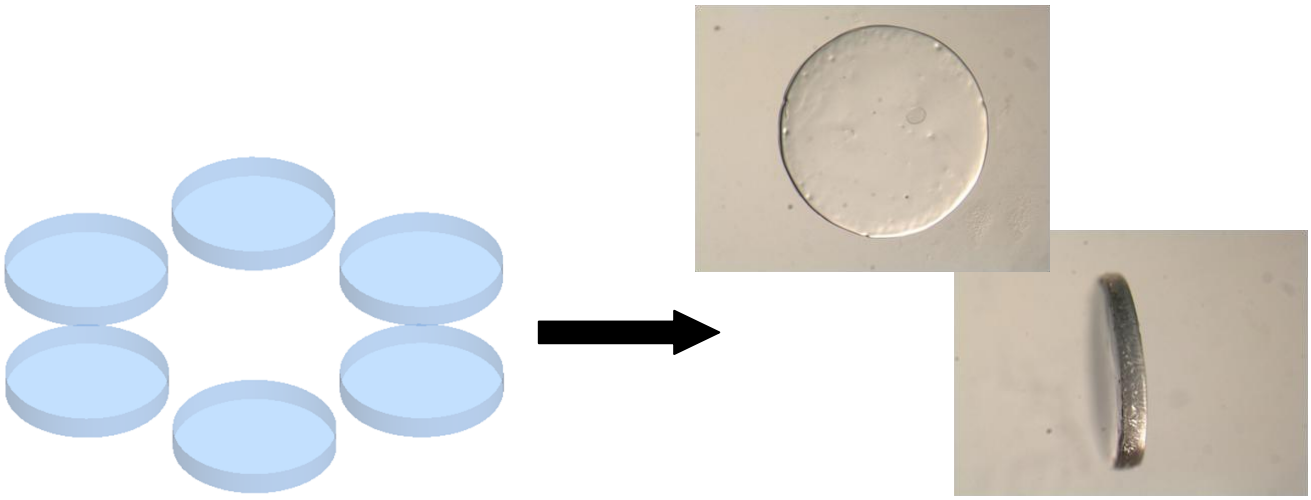

Figure 2.2: Disk design for NGF Release

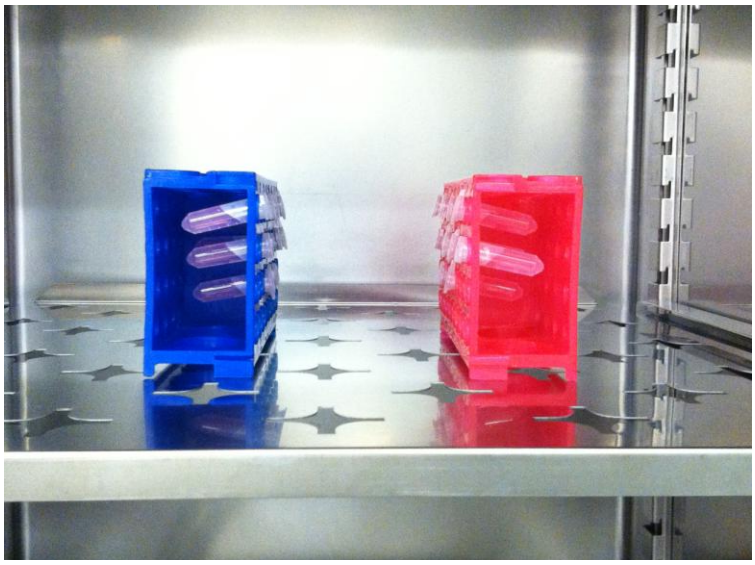

Figure 2.3: Disks incubated in microcentrifuge tubes

2.2.7 ELISA

The media collected at the various time points was analyzed using an enzyme-linked immunosorbent assay (ELISA), a 3-day procedure used to determine the NGF concentration. One ELISA was conducted for each of the 4 PEGda test groups: 3.4 kDa with encapsulated NGF, 3.4 kDa with conjugated NGF, 6 kDa with encapsulated NGF, and 6 kDa with conjugated NGF. The ELISA kit used was the Promega NGF E_{max}® ImmunoAssay System (Madison, WI) and the manufacturer's instructions were followed. All reagents used for this procedure were provided in the kit unless otherwise indicated. Each ELISA was carried out on a 96-well plate. First, a carbonate coating buffer was prepared consisting of 0.025M of both, sodium bicarbonate and sodium carbonate (Sigma-Aldrich, St. Louis, MO). The buffer was raised to a pH of 9.7 and was used to dilute Polyclonal Antibody (Anti-NGF-pAb). This solution was used to coat the surface of the plate [See Figure 2.4 (1)]. The plate was sealed using Parafilm Wrap and incubated overnight at 4°C. The plate was washed 3 times using a TBST wash buffer consisting of 20 mM tris-hydrochloride (Avantor, Performance Materials, Center Valley, PA), 150 mM sodium chloride (Avantor, Performance Materials, Center Valley, PA), and 0.05% (v/v) Tween® 20. Block & Sample 1X Buffer was used to block any surface of the plate where antibody did not bind [See Figure 2.4 (2)]. A 1-hour incubation period at room temperature was completed and the contents of the plate were washed once with TBST wash buffer. Two columns were designated for the NGF standard curve. NGF was diluted in Block & Sample Buffer at concentration of 250 pg/mL and placed in the top 2 wells of these columns. 1:2 dilutions were performed down the plate until the standard columns were full. The various samples were added to the remainder of the wells at 1:40, 1:80, and 1:160 dilutions. Only the 2-hour samples were diluted at 1:200, 1:400, and 1:800 as it was believed the NGF concentration would be much higher at this time point. The plate was sealed and incubated for 6 hours at room temperature on an orbital shaker (DS-500, VWR, Radnor, PA) at 500 rpm. This allowed for the binding of NGF to the Anti-NGF-pAb already bound to the surface [See Figure 2.4 (3)]. The wells were washed 5 times with TBST wash buffer. Monoclonal antibody (Anti-NGF mAb) was diluted in Block & Sample 1X Buffer and added to the plate to capture the NGF [See Figure 2.4 (4)]. The plate was sealed and incubated overnight at 4°C. The following day the wells were washed 5 times with TBST was buffer. A species specific antibody conjugated to horseradish peroxidase (Anti-

Rat IgG, HRP Conjugate) was diluted in Block & Sample Buffer and added to each well to detect the Anti-NGF mAb [See Figure 2.4 (5)]. The plate was incubated for 2.5 hours at room temperature with shaking at 500 rpm. The plate was washed 5 times with TBST wash buffer and TMB One Solution was added to each well [See Figure 2.4 (6)]. After 10 minutes, 1N hydrochloric acid (EMD Millipore, Billerica, MA) was added to each well to stop the reaction. The absorbance was recorded at 450 nm on a VersaMax Microplate Reader (Molecular Devices, Sunnyvale, CA) within 30 minutes of adding the acid. An NGF standard curve was prepared and the samples were read based on that curve as the amount of NGF is proportional to the color generated in the oxidation-reduction reaction.

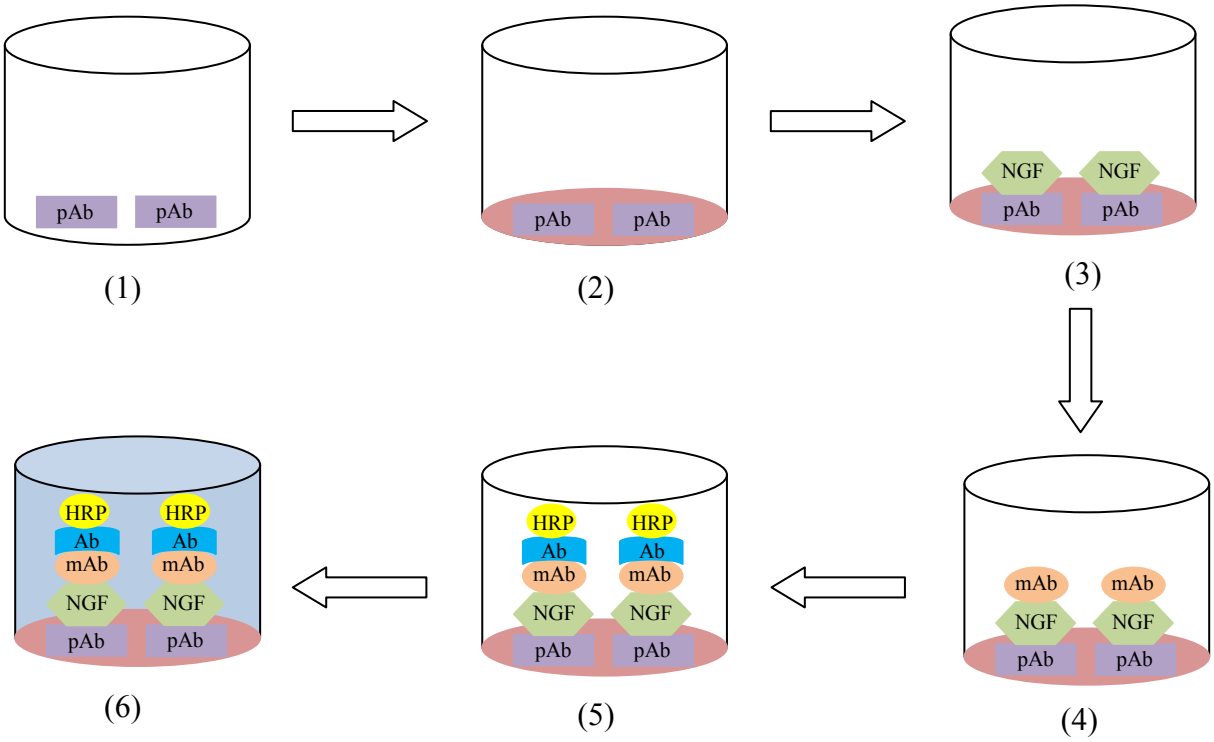

Figure 2.4: Order of steps in ELISA Procedure

2.2.8 ELISA Results Interpretation

Once the plate was read, the standard curve was graphed using the absorbance values obtained. An R^2 value closest to 1 was used to find the straightest possible line amongst the points. The equation for that line was then used to obtain the NGF concentration of the test samples using the known absorbance values. This was done by solving for the value *x*. This value was then multiplied by the dilution factor and averaged with the other dilutions of that sample to obtain the final amount of NGF released for that specific time point. Figure 2.5 shows an example of one of the standard curves used for these tests.

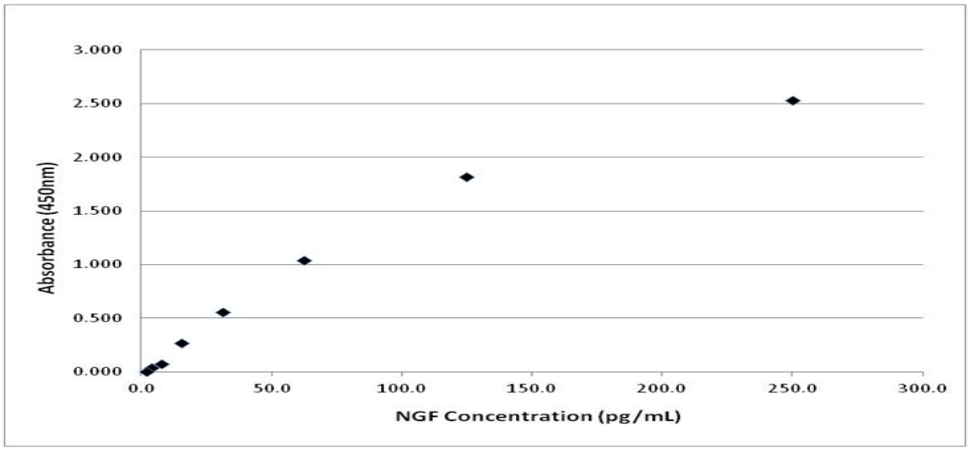

(A)

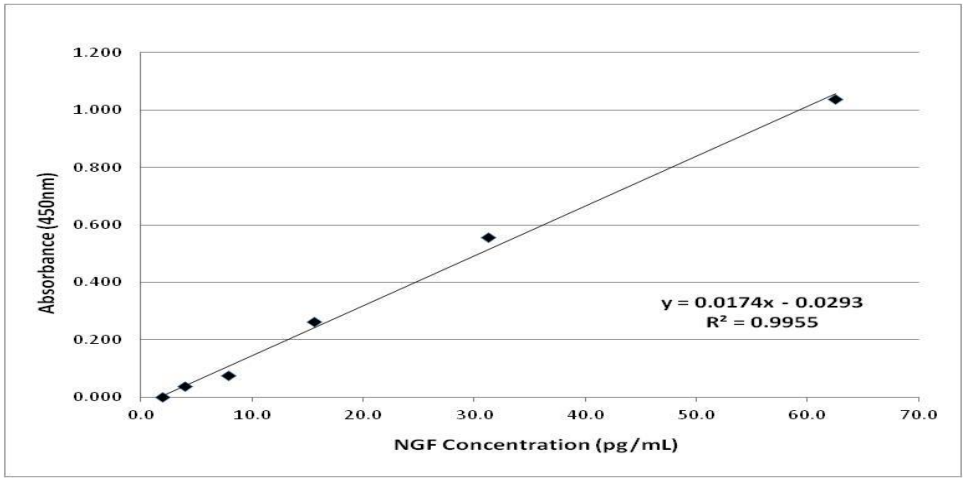

(B)

Figure 2.5: Example of an NGF standard curve (A) Curve displayed using all 8 values; (B) Lower 6 values used to obtain a formula for the straightest possible line (R^2 value closest to 1)

2.3 RESULTS

2.3.1 NGF Bioactivity

The results obtained from seeding cells without any NGF can be seen in Figure 2.6. These images show minimal to no neurite extension. On the other hand, cells seeded with NGF did, in fact, promote neurite extension in the cells after 7 days. Therefore, its bioactivity was proven. Although cells were seeded with 3 different NGF concentrations, this did not have great effect on the number of cells extending neurites nor on the length of such neurites. Therefore, a concentration of 50 ng/mL of NGF is enough to achieve good, overall, extension.

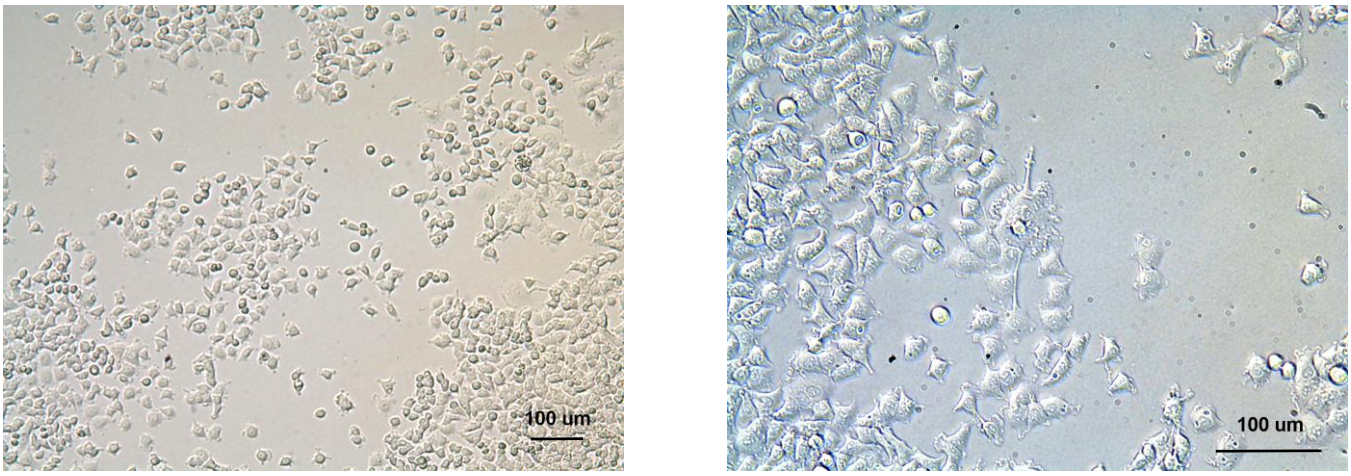

Figure 2.6: Low and high magnification images of PC-12 cells after 7 days without NGF exposure

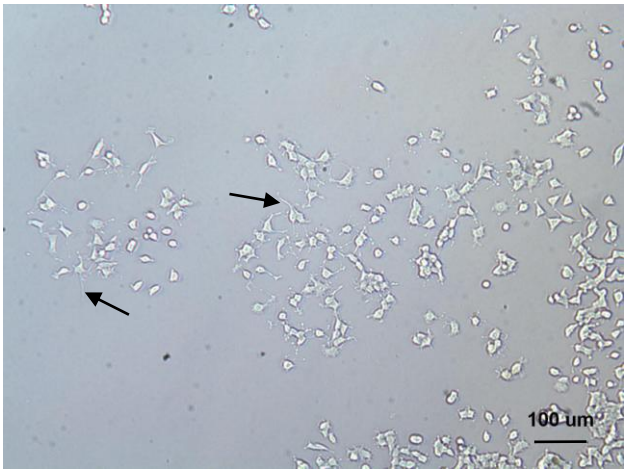

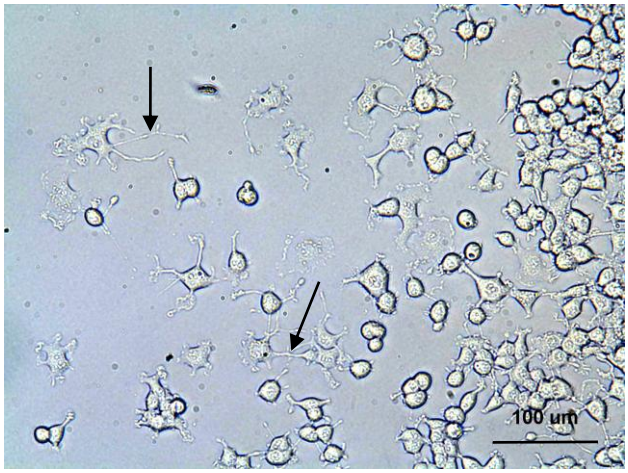

50 ng/mL of NGF

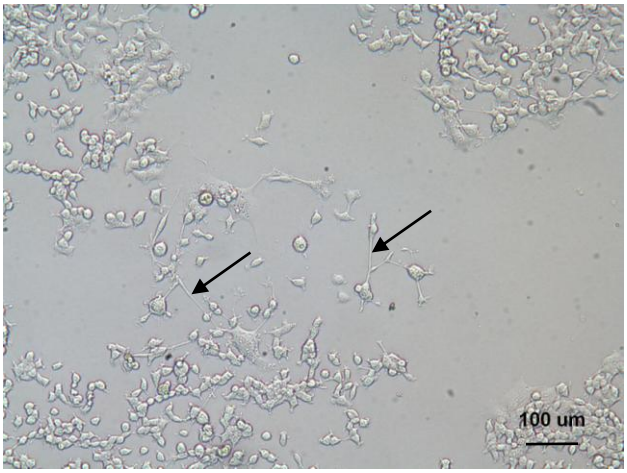

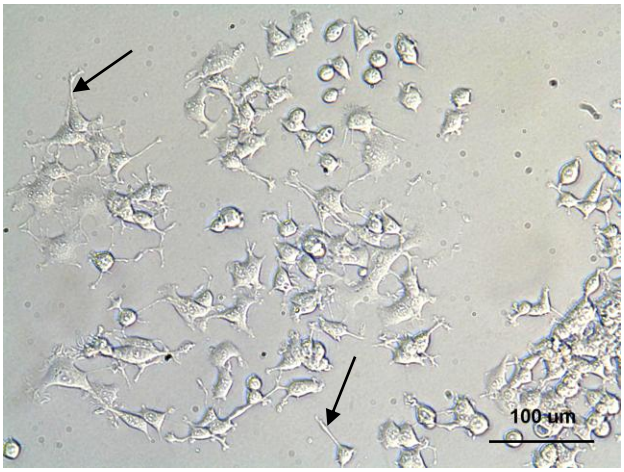

100 ng/mL of NGF

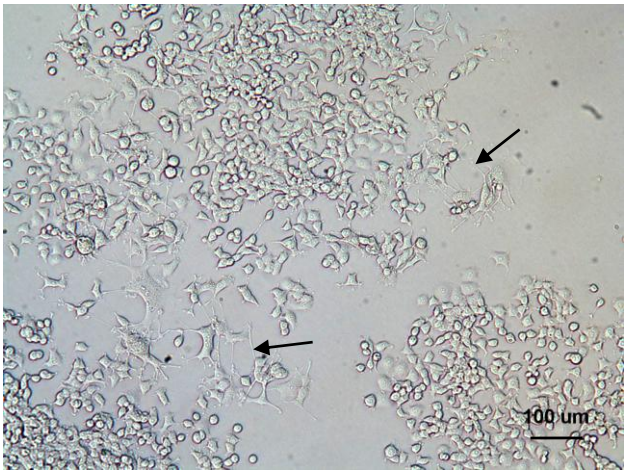

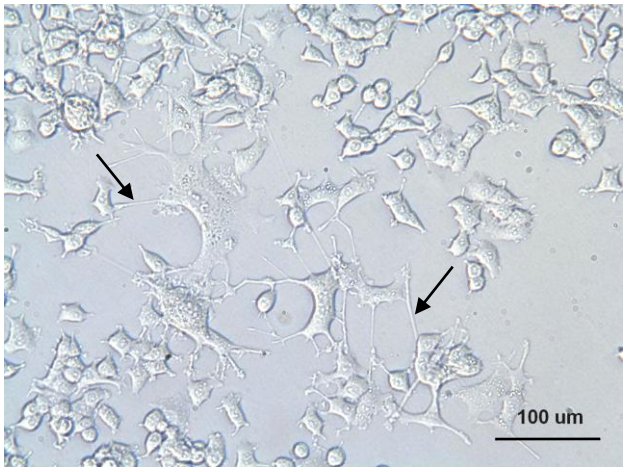

150 ng/mL of NGF

Figure 2.7: Low and high magnification images of PC-12 cells after 7 days of NGF exposure at various concentrations: 50 ng/mL, 100 ng/mL, and 150 ng/mL. Neurites are indicated by arrows.

2.3.2 NGF Release

Upon addition to the plate, TMB One Solution turned each well blue. The intensity of the color correlated with the concentration of NGF within that well. As shown in image (A) of Figure 2.8, the darkest blue was seen in the first and last 2 columns. The first 2 columns contained the media collected at the 2 hour mark, where the highest release of NGF was expected. The last 2 columns housed the NGF standard values used to make the standard curve. The NGF concentration in the standard was highest in the top wells. As HCl was added, the wells turned yellow immediately. The intensity of the yellow color is what was read by the plate reader to yield the absorbance of the solution in every well.

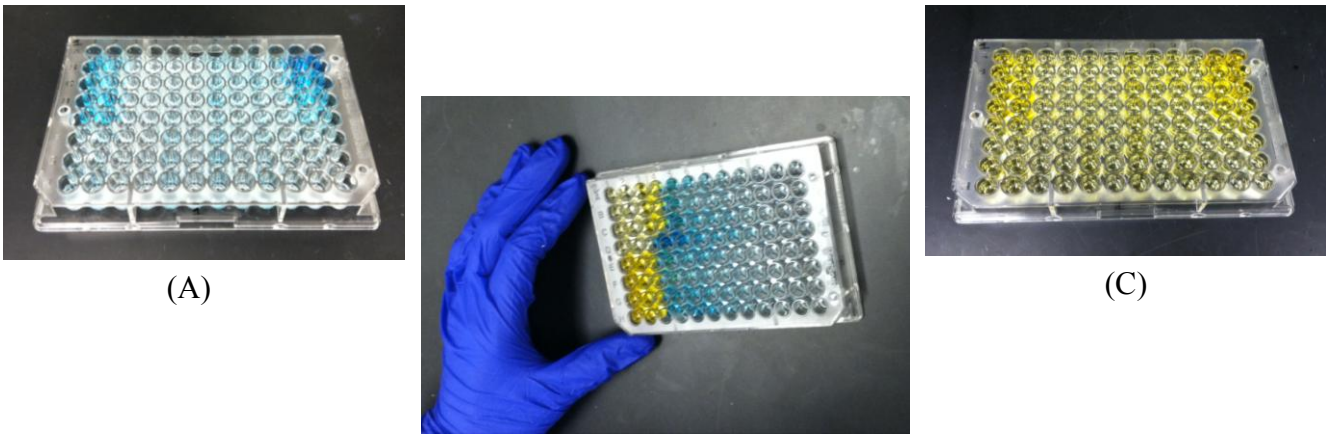

(A) (B) (C)

Figure 2.8: ELISA Plate; (A) After addition of TMB Solution; (B) During addition of HCl to stop reaction; (C) After addition of HCl

The total NGF release over a 30-day period is illustrated in Figure 2.9. All of the disks built contained 500 ng of NGF at the start of the experiment. The highest release was seen by PEGda at 3.4 kDa with conjugated NGF at 154.2 ng (30.8% of the total). This was then followed closely by the 6 kDa samples with encapsulated NGF at 150.2 ng (30.0%). Far behind was the 6 kDa with conjugated NGF at 58.2 ng (11.6%). The lowest cumulative release was seen by 3.4 kDa with encapsulated NGF at 22.8 ng (4.6%). All four formulations showed a similar initial burst with the greatest release occurring within the first 24 hours. After about 7 days, very small quantities of NGF were released. The initial 24-hour burst is illustrated more clearly in Figure 2.10. For example, in the samples with the highest release, 72.2% of that release occurred during the initial 2 hours. In the lower 2 samples, 6 kDa with conjugated NGF and 3.4 kDa with encapsulated NGF, there is not much release after that 2-hour marker.

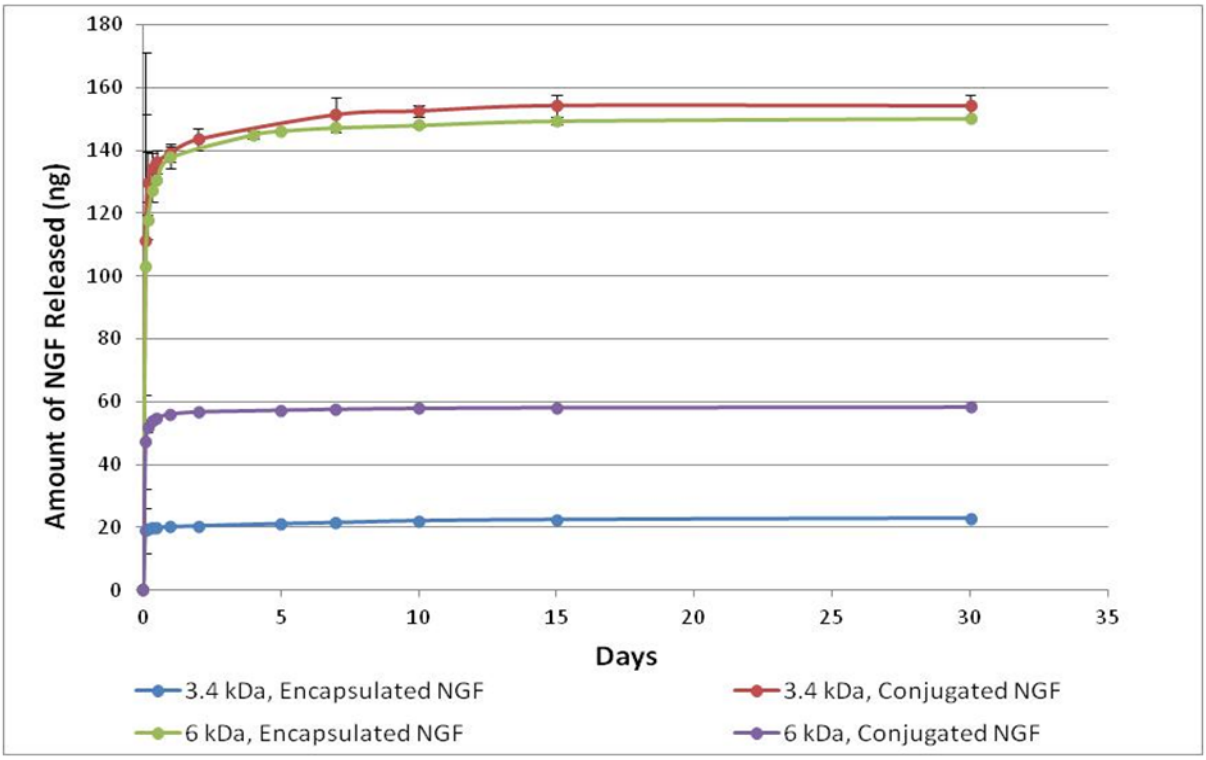

Figure 2.9: Cumulative NGF release over a 30-day period

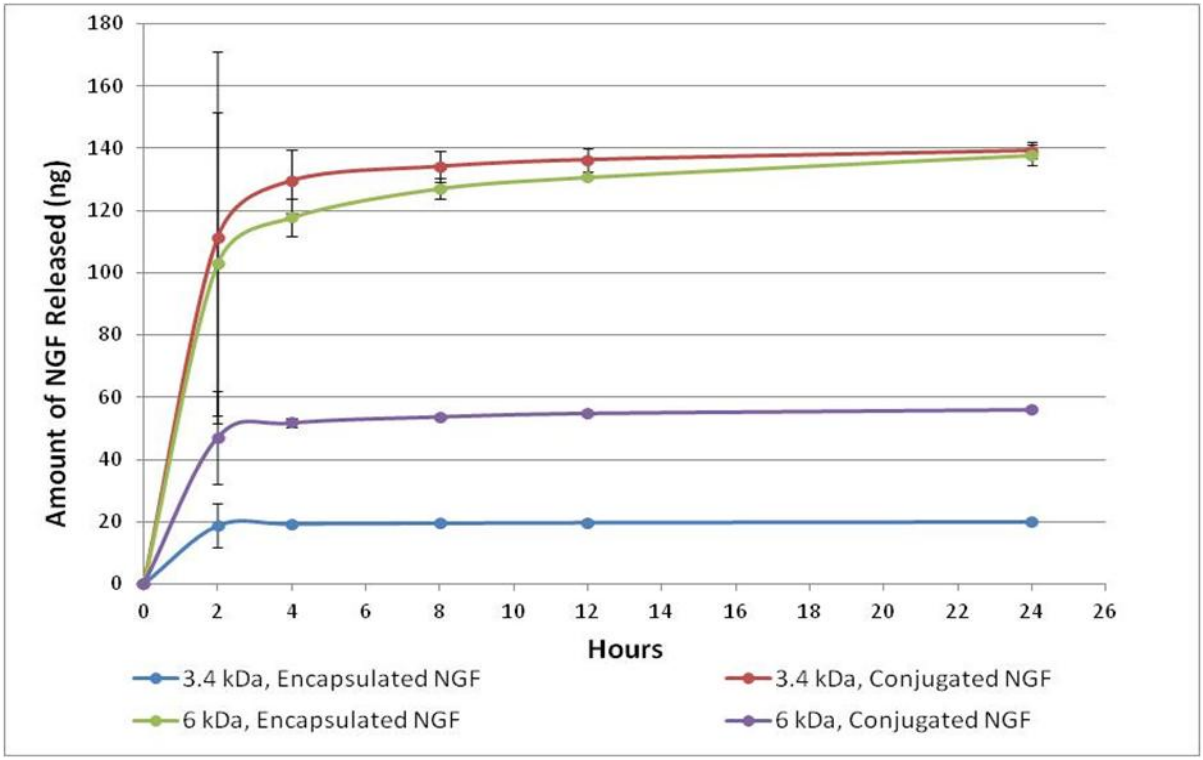

Figure 2.10: Cumulative NGF release during initial 24 hours

2.4 DISCUSSION

PEG has been studied for use in nerve regeneration techniques for its versatility in regards to addition of growth factors and other peptides. NGF is a growth factor that may improve regeneration because it promotes neurite extension in cells. The protein must be integrated into the nerve regeneration scaffold in a way that release of the protein occurs in a controlled manner. A controlled release is best because it provides sufficient NGF for the duration of recovery. Two methods of incorporating NGF into a PEGda scaffold were tested here, encapsulated NGF and conjugated NGF, using 2 molecular weights of the polymer, 3.4 kDa and 6 kDa.

NGF which was encapsulated during photocrosslinking is released by simple diffusion. A higher overall amount was released from the higher of the 2 molecular weights. This is due to the number of acryl groups in each one. PEGda at 3.4 at 30 wt% has an acryl group molarity of 0.25 while 6 kDa at the same concentration has an acryl group molarity of 0.10. The higher the molarity of acryl groups, the more crosslinking that occurs during UV exposure. This yields a more complex hydrogel mesh which in turn, blocks the diffusion of NGF. Encapsulated NGF may be useful when the injury gap is short and an initial burst of protein is desired. As an alternative, NGF was covalently conjugated to each of the 2 molecular weights by producing a hydrolytically degradable ester bond between NGF and PEGda. This was done in hope that this may slow down the release due to the extra time it takes to break that bond. Once the bond is broken, NGF is free to diffuse as with its encapsulated counterpart. Therefore, the release would rely on the rate of diffusion as well as the rate of hydrolysis. This was not the case, however. The highest release from all of the samples was seen in the 3.4 kDa, conjugated, preparation. This also contradicted the previous argument which stated that lower molecular weights yield less diffusion. It is possible that not all of the NGF conjugated to PEGda during the addition reaction. This would allow a high initial burst of unconjugated NGF. It may also mean that the rate of hydrolysis was not slow enough to endure past the 2-hour time point, especially in NGF conjugated near the surface.

None of the samples released the total 500 ng of NGF. The sample with the greatest release only released 30.8% of the total. It is possible that the NGF is so trapped within the hydrogel network that it may take much longer than 30 days for the total amount to be released. Previous work incorporated the protein BSA into PEGda microspheres at a high polymer molecular weight (575 kDa). Only about 20%

of the total amount of protein was released by day 30. It took 280 days for the total amount of BSA to be released [43]. On the other hand, when using a lower molecular weight (10 kDa), as was done in West *et al.,* 100% of the BSA was released in 5 days [44]. As a reference, BSA is a 66 kDa protein while NGF is 26 kDa. NGF should, therefore, be diffused with greater ease.

Several modifications can be made to acquire better results if the experiment is to be repeated. Running the experiment for a much longer amount of time (~ 9 months) may make 100% release of the protein possible. However, this may not be plausible given that nerve regeneration occurs at 2 - 5 mm/day and it may not take that long for full regeneration. On the hand, including biodegradation factors in the PEGda scaffold may allow total release of the protein over a shorter period of time. That is, the amount of time necessary for degradation of PEGda. Future tests are also necessary to determine how much of the protein actually does conjugate to the PEGda molecules.

2.5 CONCLUSIONS

PEGda provides much promise for construction of nerve guidance conduits. It is a nonreactive, biocompatible, material to which NGF may be incorporated. It is clear that NGF promotes cellular neurite extension in addition to some of its other functions. Therefore, it is important to achieve controlled release of NGF so that the protein will be available for the entire duration of nerve regeneration. For encapsulated NGF, a greater release was seen using a higher molecular weight of PEGda. On the other hand, for conjugated NGF, a greater release was seen from lower molecular weight. A quick initial burst was present in all of the samples. This may only be desirable when working with short injury gaps as the time of regeneration is dependent upon the length of the injury. For longer gaps, conjugated NGF may yield better results once it is determined how to best conjugate all of the protein.

Chapter 3: Testing Cell Attachment to a Poly(ethylene glycol) Surface Using RGDS as a Cell Adhesion Peptide

3.1 Introduction

3.1.1 RGDS

Poly(ethylene glycol) (PEG) is an excellent material for tissue engineering purposes because it is essentially a blank canvas. By nature, PEG is a nonadhesive property [45]. However, it can be made bioactive through covalent attachment of cell adhesion peptides. Cell adhesion peptides allow for the attachment of a cell to a polymer by binding to integrins or other transmembrane receptors, located along the surface of the cell membrane. This is illustrated in Figure 3.1. A peptide commonly conjugated to PEG is RGDS, which consists of the following amino acid sequence: Arginine - Glycine - Aspartic acid - Serine [See Figure 3.2]. RGDS is the binding site of fibronectin. Small peptide sequences are preferred to entire proteins because they are easier to manufacture and can withstand harsher processing conditions [26]. Aside from its use in neural regeneration techniques, RGDS has been used in a variety of tissue engineering applications such as regeneration of smooth muscle, bone, and cartilage, as well as wound healing [24, 46-48]. In addition to PEG, RGDS has been tested as a cell adhesion peptide for other scaffold materials including, but not limited to, polyvinyl alcohol (PVA), poly(propylene fumarate-*co*-ethylene glycol) (P(PF-co-EG)), polycaprolactone (PCL), and silk scaffolds, [47, 49-51].

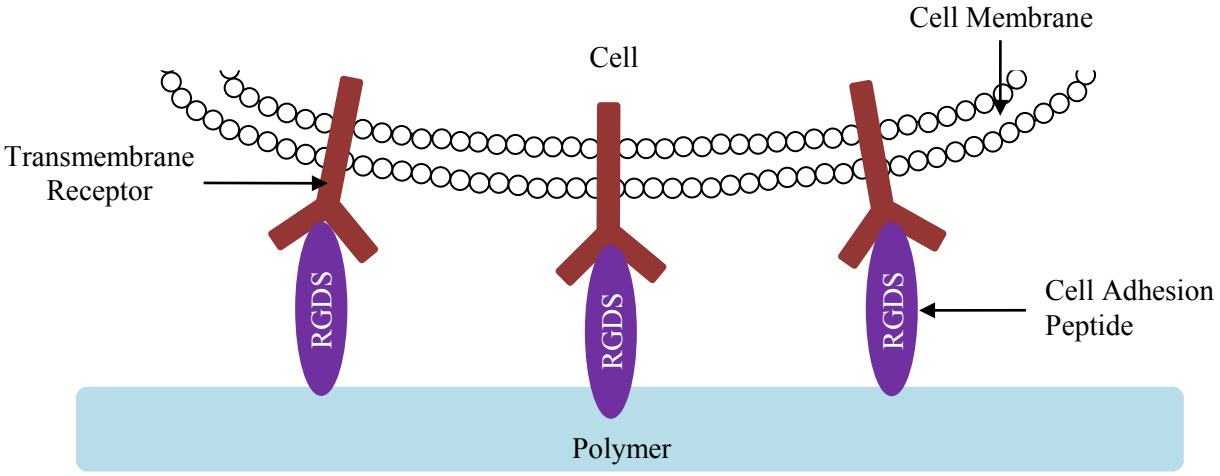

Figure 3.1: Polymer-cell adhesion using cell-adhesion peptides

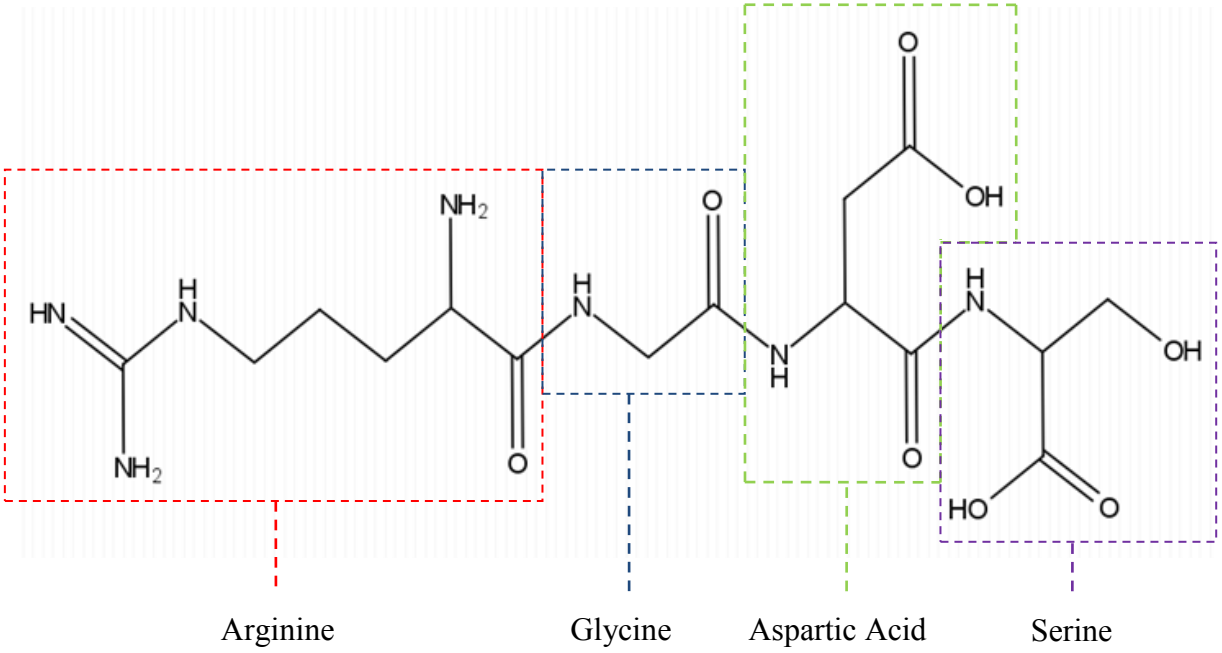

Figure 3.2: Chemical structure of RGDS [52]

3.1.2 Nerve Growth Factor

Nerve growth factor (NGF) is a neurotrophin naturally produced by Schwann cells that can be incorporated into poly(ethylene glycol) diacrylate (PEGda) nerve guidance conduits, increasing their ability to guide complete nerve regeneration. NGF promotes neurite extension. A neurite is anything that sprouts from the cell body of a neuron, such as an axon or a dendrite. Neurite extension has previously been achieved on hydrogels [26]. Upon interaction with NGF, PC-12 cells, like the ones used here, differentiate. This means that they show neuron-like behaviors, including neurite extension [42]. Aside from being able to attach cells to a hydrogel surface, it is important that such cells have the capacity to extend neurites. This increases the prospect of full regeneration.

3.1.3 Tissue Culture-Treated Polystyrene

Vessels and plates used for cell culture can be treated to improve cell attachment. One of 2 processes can be used, corona discharge or gas-plasma, to generate highly energetic oxygen ions. These ions then attach to the polystyrene chains on the surface making them hydrophilic and negatively

charged upon addition of cell culture media. The higher the oxygen content on the surface, the more hydrophilic, the better it is for cell attachment and cell spreading [53].

3.1.3 Objective

The objective of the experiments outlined in this chapter was to test the cell attachment properties of RGDS on a PEGda surface. For this, RGDS was covalently bound to PEGda and disk-shaped scaffolds were photocrosslinked by stereolithography (SL). Cells were seeded on the surface of these scaffolds in 24-well plates to evaluate cell attachment and viability. Additional cells were seed directly onto the polystyrene surface of the plates and used as a control. NGF was added to test if neurite extension could be achieved by cells seeded on a PEGda surface.

3.2 Materials and Methods

3.2.1. PEGda Solution Preparation

A solution of commercially available 3.4 kDa PEGda (Laysan Bio Inc., Arab, AL) was prepared at a 30 wt% concentration. I-2959 (Ciba Specialty Chemicals, Tarrytown, NY) was used as a photoinitiator at 0.5 wt% concentration. Prior to preparing the solution, PEGda was stored at -20°C. It was taken out of storage and allowed to reach room temperature, approximately 1 hour before solution preparation. An amber-colored glass vial was always used for preparation of the solution to reduce the amount of ambient light exposure and prevent photocrosslinking. The solution was then placed on a shaker until the polymer and photoinitiator were completely dissolved.

3.2.2 RGDS-PEG Conjugation

RGDS (Sigma-Aldrich, St. Louis, MO) was conjugated to 3.4 kDa Acryloyl-PEG-*N*-hydroxysuccinimide (ACRL-PEG-NHS, Laysan Bio, Arab, AL) at a 2:1 peptide to polymer ratio. This was done by first preparing a 50 mM sodium bicarbonate ($NaHCO_3$) buffer and raising it to a pH of 8.5. Buffer (230 μL) was added to each of 7 vials containing 10 mg of RGDS. The contents of all vials were combined into a single 15 mL microcentrifuge tube and vortexed. An additional 230 μL of buffer were used to collect any remaining RGDS from the vials. Buffer (3.22 mL) was then used to dilute 1.095 g of ACR-PEG-NHS and the solution was vortexed. The polymer was added to the peptide in a dropwise fashion, adding 1 or 2 drops and swirling. Once the polymer solution was consumed, the mixture was

transferred to a 50 mL microcentrifuge tube in case of expansion of the contents in the freezer. An additional 500 µL of buffer were used to collect any solution remaining in the previous vial. The solution was placed on an orbital shaker for 2 hours at room temperature and frozen overnight at -80 °C. The cap was removed and a Kim wipe was secured at the mouth with a rubber band. The contents were lyophilized until dry. Any clumps were broken up with a spatula and the tube was placed in the freezer at -20 °C until further use. Prior to sample fabrication, the concentration of RGDS was stabilized to 25 mg/mL with additional PEGda.

3.2.3 PEGda Disk Fabrication

The disk-shaped PEG samples were designed using SolidWorks™. The diameter of each well in a 24-well plate is 15.6 mm. By using a Dimensional Swelling Factor of 1.20, it was calculated that the disks needed to be fabricated at a diameter of 13 mm so they would swell to 15.6 mm and fit tightly within the wells. All disks were built using the 3D Systems® model 250/50 (3D Systems, Valencia, CA). Prior to using the equipment, it was cleaned thoroughly with antibacterial wipes to prevent contamination during the construction process. The laser of the SL system was allowed to reach maximum power (~16-17 mW). The disks were built using 600 µL of PEGda solution at a previously established laser scan speed of 8.085 in/s. Each newly polymerized disk was immediately placed in deionized water in an ultra low attachment 24-well plate to remove any unreacted material and allow the disks to reach equilibrium swelling. One disk was built at a time, totaling 6 disks.

3.2.4 Cell Seeding

PC-12 cells for this experiment were obtained from ATCC (Manassas, VA). Prior to seeding, cells were maintained in a 37°C, 90% relative humidity, and 5% CO_2 environment. All of the following steps were completed in a biosafety cabinet to reduce the risk of contamination. Two hours after fabrication, the 6 disks were moved from deionized water to Phosphate Buffered Saline (PBS). Because PBS is a buffer, there is less risk for pH changes. After 48 hours, these 6 disks were moved to an ultra low attachment 24-well polystyrene plate and placed in complete RPMI-1640 media (Sigma-Aldrich, St. Louis, MO) supplemented with 10% Horse Serum, 5% Fetal Bovine Serum, 1% glutamine-penicillin-streptomycin (GPS), 10 mM HEPES, and 1 mM sodium pyruvate. These were incubated under the

same conditions for 4 days. The media was removed and rubber o-rings, sterilized in 10% ethanol, were placed on top of each disk. This was necessary to create a seal that would prevent the cells from attaching to the floor of the well instead of the disk. A concentration of 10^4 cells was seeded on each of the 6 disks. As a control, 10^4 cells were also seeded in 6 wells of a tissue culture treated 24-well plate made of polystyrene. Both plates were incubated as before. The cell seeding process can be seen in Figure 3.3 (A).

3.2.5 Addition of NGF

After 3 days, the media was removed from each of the 12 wells. Of the 6 wells containing PEG disks, 3 were given complete RPMI-1640 containing 220 ng/mL of NGF. The other 3 were given complete media without NGF. The same was done for the cells growing on tissue culture-treated plastic. After an additional 2 days, the media was replaced and the NGF concentration was increased to 638 ng/mL in the same 6 wells. Addition of NGF is illustrated in Figure 3.3 (B).

3.2.6 Histomorphological Analysis

Seven days after the initial cell seeding, the cells were viewed using an inverted microscope (DMIRB, Leica Microsystems, Germany) and images were taken with a charge-coupled device camera (Retiga 2000S Fast 1394, QImaging Corp., Canada). Three images were taken of each well containing NGF at 100x magnification, totaling 9 images for analysis on each of the 2 surfaces. Cell counts were conducted to determine the number of cells attached to the PEGda surface versus the plastic surface. In addition, the number of cells showing neurite extension was recorded. Only neurites longer than the cell body they had extended from were considered in these counts. A two-sample t-test was used to compare results of single-lumen samples. Equal variances were assumed. A p value lower than 0.05 was considered statistically significant. Data are presented as mean ± standard deviation.

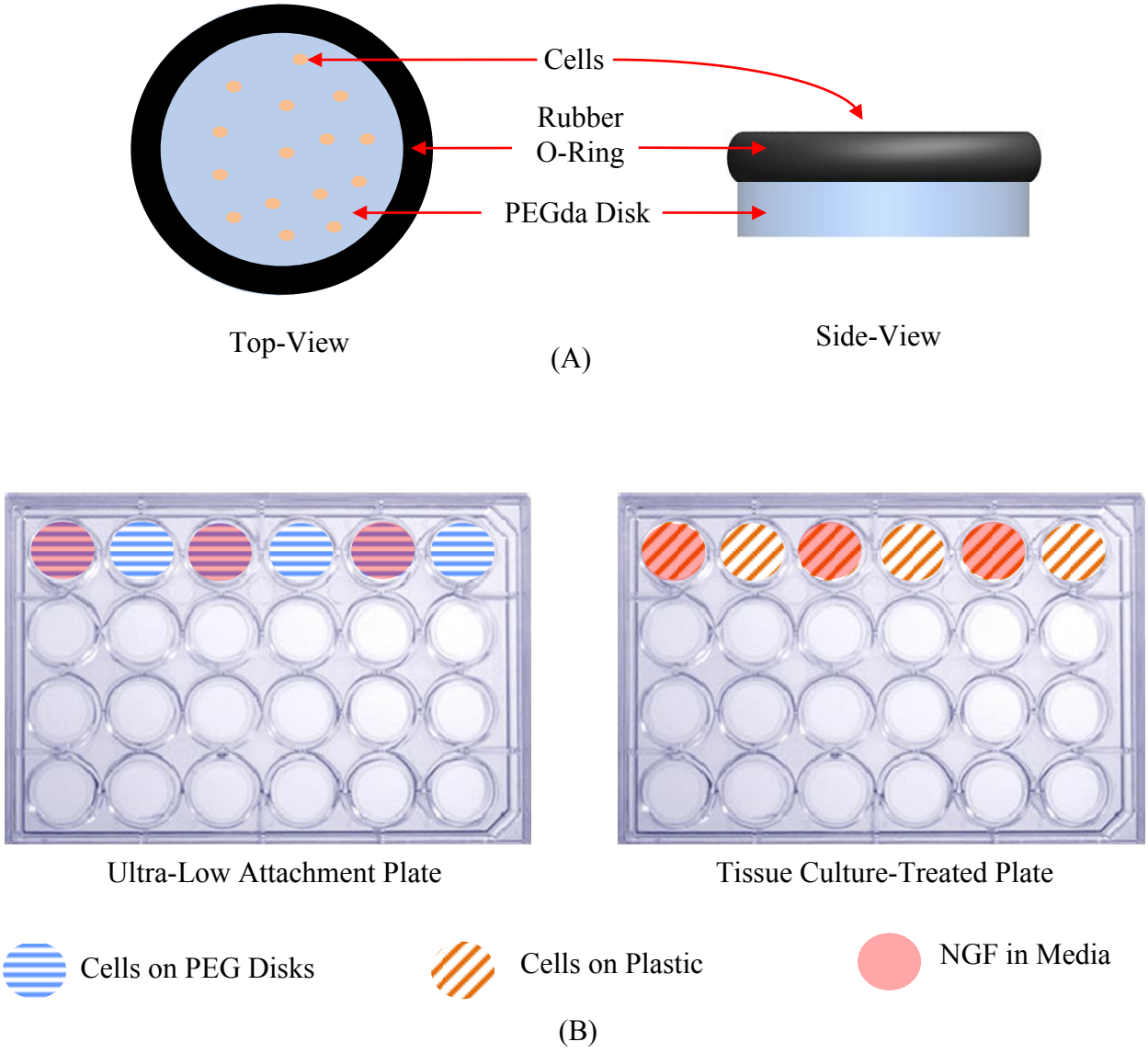

Figure 3.3: Cell adhesion procedure; (A) Cell seeding on 24-well plates; (B) Addition of NGF

3.3 RESULTS

3.3.1 Cell Attachment and Neurite Extension

Cell attachment to the PEGda surface after 7 days was good. Cells were still alive and reproducing on both surfaces. This is visible in the images in Figure 3.4 at 200x. There were, however, what appeared to be large floating particles (encircled in red) surrounding cells seeded on the polymer. Cells in wells containing NGF appeared to be better attached. There was also better neurite extension on the PEGda surface as compared to the plastic surface. The neurites were longer and there were several

cells with 3 or more extensions. Of the total cells counted, 11 cells on the PEGda surface had 3 or more neurite extensions compared to only 5 on the plastic surface.

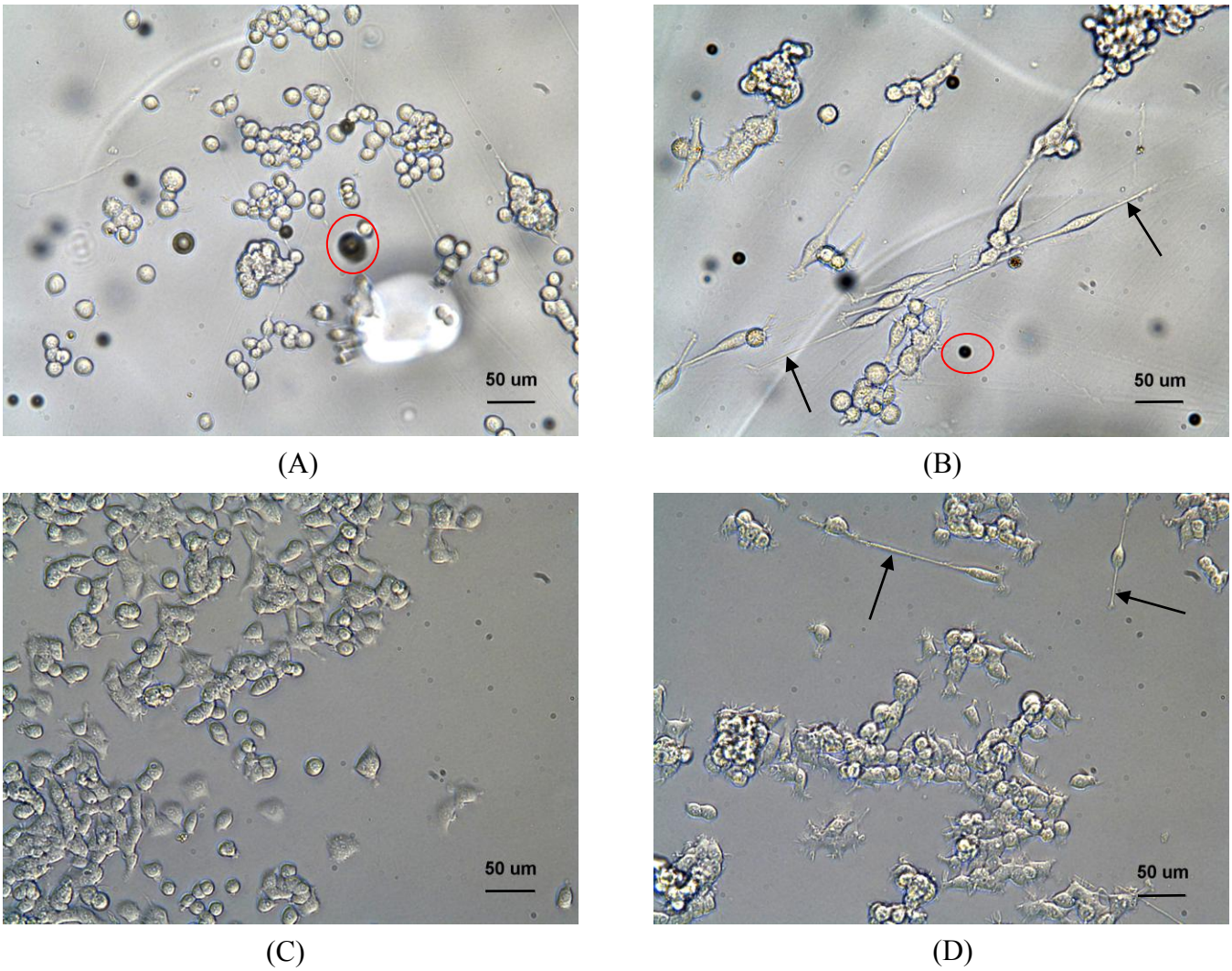

Figure 3.4: Cell growth after 7 days (200x); (A) Cells on PEG surface; (B) Cells with 4-day NGF exposure on a PEG surface; (C) Cells on tissue culture-treated plastic; (D) Cells with 4- day NGF exposure on tissue culture-treated plastic; (black arrows indicate neurite extensions and red circles indicate paticles)

Figure 3.5 compares the cell attachment on a PEGda surface versus tissue culture-treated plastic. Overall, cell attachment was greater on plastic than on PEGda. The average number of cells on a PEGda surface was 5,778 ± 2,571 per cm^2 whereas on plastic it was 8,808 ± 2,653 per cm^2. Both sets of samples contained NGF; therefore, this was not a factor. There was a statistically significant difference amongst the results.

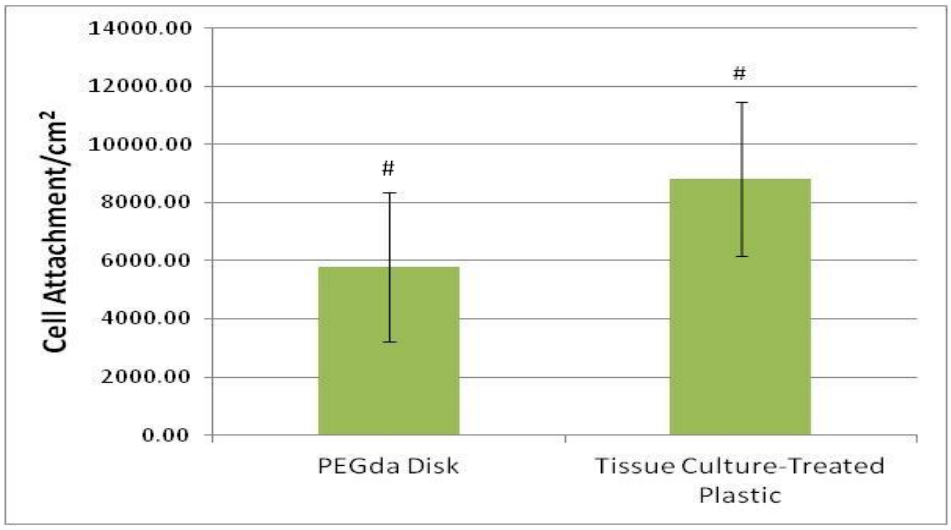

Figure 3.5: Average cell attachment on PEGda disk vs. tissue culture-treated plastic with NGF present in both cases; #: Difference is statistically significant, $p<0.05$

Figure 3.6 compares the neurite extension present on either surface. Only samples with NGF present in the media were considered. Image (A) shows the percentage of cells extending at least 1 neurite. A greater percentage of cells were extending neurites on the PEGda surface, 22% ± 6.0%, than the plastic surface, 10% ± 5.5%. Image (B) illustrates the average density of cells extending neurites per cm^2. The PEGda disks had an average density of 1,160 ± 382 cells with neurites per cm^2. The tissue culture-treated plastic only had an average density of 737 ± 160 cells with neurites per cm^2. There was a statistically significant difference amongst the results in both graphs.

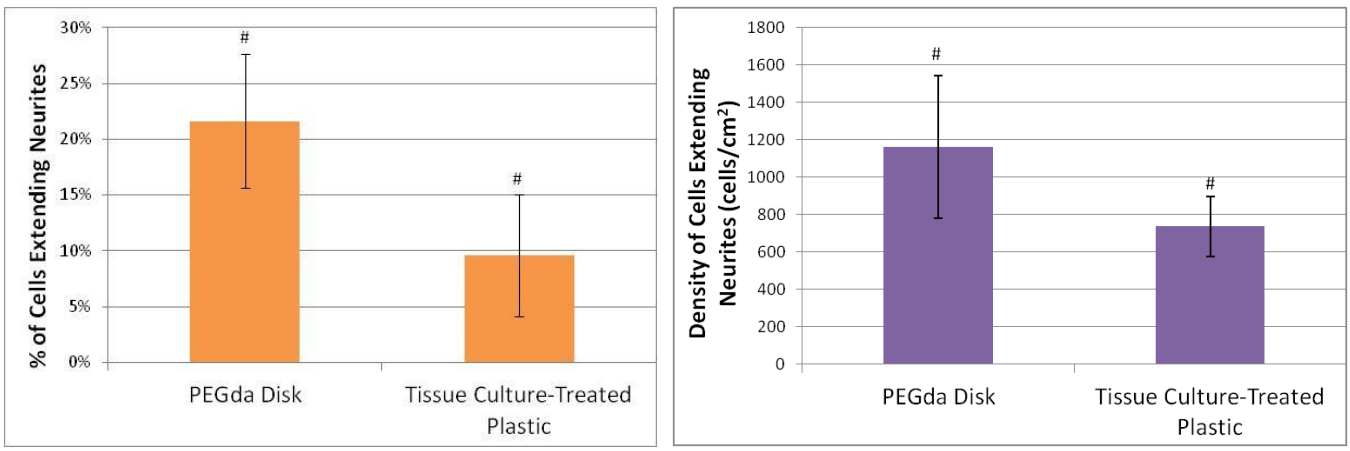

(A) (B)

Figure 3.6: Neurite extension; (A) Percentage of cells extending neurites; (B) Density of cells extending neurites per image area; #: Difference is statistically significant, $p<0.05$

3.4 DISCUSSION

The decision to use RGDS as the cell adhesion peptide for this research was due in part to previous work conducted by Gunn *et al.* They evaluated 3 different peptides to determine which worked best for nerve regeneration purposes using a PEG scaffold. Aside from RGDS, they tested Tyr-Ile-Gly-Ser-Arg (YIGSR) and Ile-Lys-Val-Ala-Val (IKVAV). While RGDS is found in fibronectin, YIGSR and IKVAV are both found in laminin. They too incorporated growth factors to evaluate which peptide showed greater sprouting of neurites from cells. Although all 3 peptides demonstrated good cell attachment, the greatest amount of neurite extension was seen using RGDS [26]. The cell attachment tests presented here yielded helpful results. Good cell attachment was seen on both surfaces, meaning the RGDS peptide was working. Cell growth was greater on tissue culture-treated plastic than on the PEGda surface. However, in the samples containing NGF, PEGda provided a better surface for neurite extension as a higher percentage of cells extended neurites. Yet, neurite extension was low considering the concentration of NGF in each well was very high. Gunn *et al.*, tested PEG surfaces at different concentrations. They noticed that the number of neurites increased as the flexibility of the material increased [26]. Although cells for the present research were only seeded on one PEGda concentration, they were also seeded on polystyrene, a stronger, less flexible, material. Like them, the cells showed greater neurite extension on the more flexible of the two materials, the hydrogel. Stronger, less elastic, materials, like the plastic surface of a 24-well plate, may require the neurites to exert more tension when they move. On the other hand, a material that is too elastic may not be strong enough to support attachment and extension. A PEGda surface at the 30 wt% concentration used, mimics soft tissue well, allowing for good neurite extension.

Dark particles were seen surrounding cells in the media. The original hypothesis was that these particles were cell waste products. Replacing the culture media every 2-3 days is necessary to remove waste products, replenish nutrients, and keep the correct pH. However, through further observation, it was determined these were gas bubbles. Therefore, a gas release occurred as the result of the interaction between the PEG, the PC12 cells, and the RGDS used to bind the two. These bubbles are seen in much higher number on the cells seeded on the PEGda surface. Only a few very small bubbles were seen in

wells of cells seeded on plastic. NGF was not the cause of the gas exchange because bubbles were seen in wells without NGF as well. Further studies are necessary to evaluate the meaning of these bubbles and their effect on cell attachment and neurite extension.

3.5 CONCLUSIONS

Based on the results, it can be concluded that PEGda does provide a suitable surface for cell attachment. RGDS provided an anchor for cells to attach the polymer and grow. Although neurite extension was low considering the concentration, it is highly likely that this is a consequence of mistreated NGF and human error. If the experiment is repeated, it is best to use fresh NGF to ensure neurite extension. Yet, the same NGF was used for growth on both surfaces and better neurite extension was seen on PEGda. For this reason, PEGda would provide an excellent material for construction of scaffolds that could be used for tissue engineering purposes.

Chapter 4: Implantable Poly(ethylene glycol) Nerve Conduits Built by Stereolithography for Peripheral Nerve Regeneration *In Vivo*

4.1 INTRODUCTION

Peripheral nerve injuries can occur as a result of automobile accidents, work accidents, falls, athletic injuries, etc. They are a significant source of morbidity in trauma patients. Recent technology has allowed for many advances in the repair of nerve injuries; two forms being direct repair and autograft repair [10]. Neurorrhaphy, a type of direct repair, consists of direct surgical reconnection of the proximal and distal nerve ends [See Figure 1.4 (A)]. Such repair can only be performed when the defect is less than 5 mm [11]. Autograft repair, on the other hand, uses a nerve graft taken from a donor site [10]. Autografts are more likely to be biocompatible than synthetic materials and they therefore, the current standard of care for peripheral nerve injuries too large to be treated by direct repair. However, there are several limitations to autograft repair including donor site morbidity and limited supply of donor tissue [11]. Such deficiencies in direct and autograft repair have led researchers to look for other methods to treat peripheral nerve injuries. A nerve guidance conduit can provide a promising alternative to the previously mentioned methods [10, 11, 13].

Several biomaterials, both natural and synthetic, have been studied for construction of nerve guidance conduits. Only a few have been approved by the US Food and Drug Administration (FDA) for use in peripheral nerve repair: type I collagen, polyglycolic acid (PGA), poly(α-lactide-ε-caprolactone) (PCL), porcine small intestine submucosa (SIS), and polyvinyl alcohol (PVA) [16]. Of these materials, results obtained with PCL conduits more closely resemble those obtained with autografts [54]. Animal studies are an essential part of the testing process of medical devices intended for human use. This is because it is necessary to see how the devices interact with and react to the physiological environment. Animal studies are also a critical part of the FDA's application process. The FDA will not allow a product to go to human trials until it has been proven through animal studies that the product does not harm the organism.

4.1.2 Objective

A study was conducted to assess the ability of nerve guidance conduits in promoting nerve regeneration *in vivo*. A rat sciatic nerve injury model was used. Stereolithography (SL) was used to build both, single and multi-lumen, conduits out of Poly(ethylene glycol) diacrylate (PEGda) to see which type of conduit would better serve axon regrowth following injury.

4.2 MATERIALS AND METHODS

4.2.1 PEGda Solution Preparation

A solution of commercially available 3.4 kDa PEGda (Laysan Bio Inc., Arab, AL) was prepared at a 30 wt% concentration. Irgacure-2959 (I-2959, Ciba Specialty Chemicals, Tarrytown, NY) was used as a photoinitiator at 0.5 wt% concentration. An RGDS-PEG conjugate was synthesized via a previously outlined process [24] and added to the PEGda solution at 25 mg/mL.

4.2.2 Conduit Fabrication

The conduits were designed using SolidWorks™ software. With the material's hydrophilic properties in mind, the NCs were designed so they would reach a size appropriate to the animal model at the equilibrium swollen state. The lumens were designed so that both single and multi-lumen conduits would have the same cross-sectional area available for regeneration, 1.45 mm^2 [See Figure 4.1]. The SL equipment used for conduit fabrication was a 3D Systems® model 250/50 (3D Systems, Valencia, CA). Conduits were built in batches of four using a laser scan speed of 8.085 in/s at a laser power of approximately 19 mW. They were rinsed with deionized water to remove any unreacted PEGda and photoinitiator and left to swell overnight. They were then lyophilized at -55°C using a freeze-dry system (FreeZone 6, Labconco Corp., Kansas City, MO) and sterilized via low-temperature hydrogen peroxide gas plasma (STERRAD® 100S, Advanced Sterilization Products, Irvine, CA).

4.2.3 Conduit Implantation

Eight Sprague Dawley rats were used for this procedure. Four were randomly chosen to receive single-lumen conduits while the others were chosen to receive multi-lumen conduits. Ketamine and xylazine were used as anesthetics. The sciatic nerve of one leg was sharply transected while the contralateral sciatic nerve was preserved as a control. The conduits were reconstituted in saline and the nerve ends were sutured into the cap portion on each end. A 10 mm gap was left between nerve ends

but no segments of nerve were removed. The animals were fed sterilized standard rat chow and water *ad libitum* and were housed individually. The rats were sacrificed with carbon dioxide after 5 weeks and the sciatic nerves and conduits were harvested. The contralateral healthy sciatic nerve was also harvested as a control. Surgeries were conducted at the University of California, Irvine and approved by the University of California, Irvine Institutional Animal Care and Use Committee (IACUC) (protocol can be seen in Appendix 3). They were performed in accordance with guidelines from the Association for Assessment and Accreditation of Laboratory and Animal Care (AAALAC) and the National Institutes of Health (NIH).

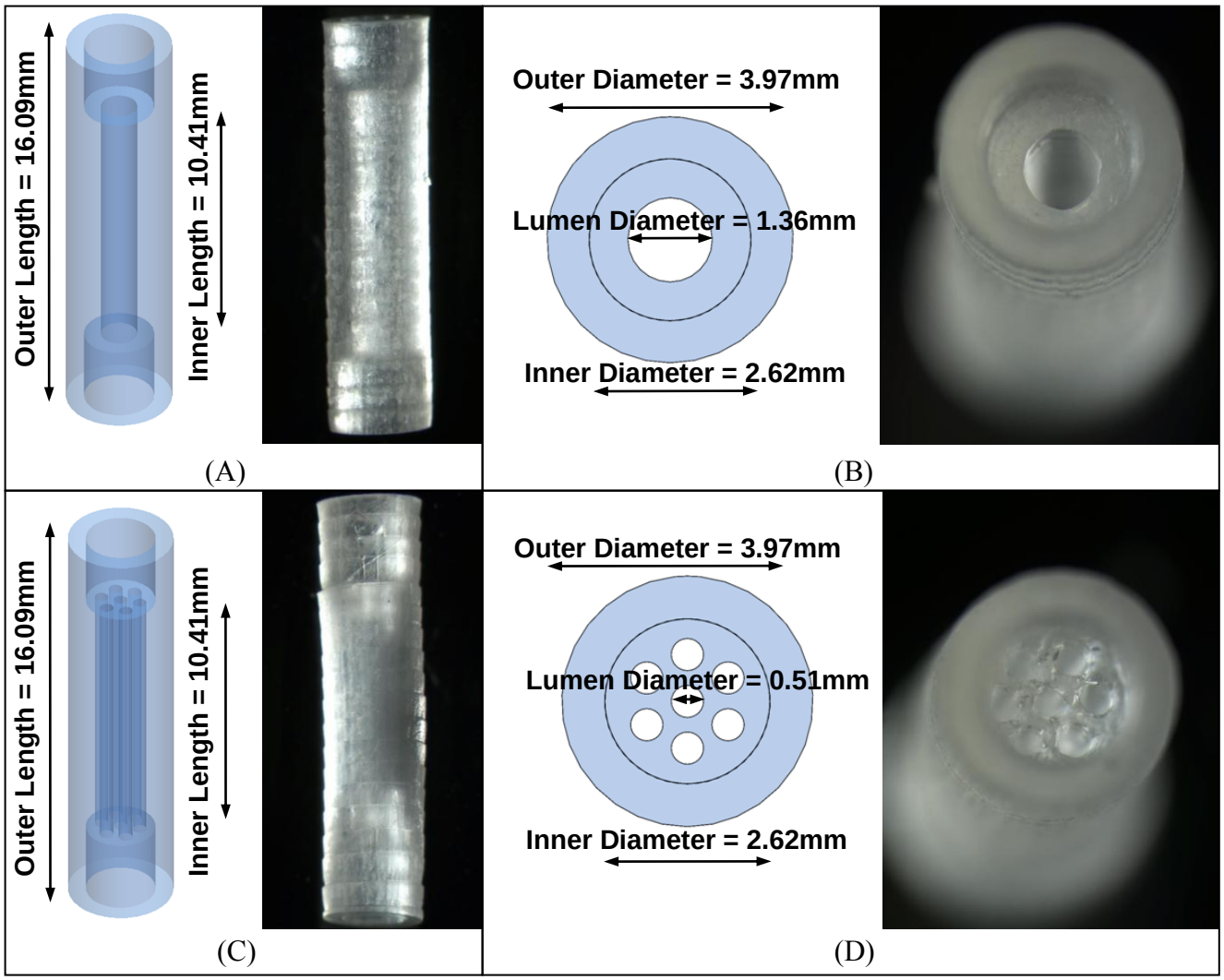

Figure 4.1: Conduit dimensions after being reconstituted; (A) Side view of single-lumen conduit; (B) Top view of single-lumen conduit; (C) Side view of multi-lumen conduit; (D) Top view of multi-lumen conduit

4.2.4 Histomorphological Analysis

The resected nerves were fixed with a 3% glutaraldehyde solution and embedded in epoxy resin. They were then stained with toluidine blue. It was decided to analyze the conduits at the proximal, middle, and distal sections. Therefore, 3 slices were taken about 2 mm from the proximal section of the nerve, 3 slices from the middle section, and 3 slices about 2 mm away from the distal section. From the control samples, 3 slices were taken from the middle section only. An inverted microscope (Leica DMIRB, Leica Microsystems, Germany) was used to digitize images with a charge-coupled device camera (Retiga 2000S Fast 1394, QImaging Corp., Canada). High magnification (400x) images were taken per slice for manual analysis. This included counting and measuring the number of small fibers (axon < 6 μm), number of large fibers (axon > 6 μm), fiber diameter, axon diameter, and myelin thickness. From these, g-ratio (axon diameter divided by fiber diameter) and the ratio of myelin thickness to axon diameter were derived. Statistical differences between groups were analyzed using analysis of variance (ANOVA). A two-sample t-test was used to compare results of single-lumen samples. Equal variances were assumed and a p value lower than 0.05 was considered statistically significant. Data are presented as mean ± standard deviation. Figure 4.2 shows a schematic of a myelinated axon illustrating how the measurements were taken.

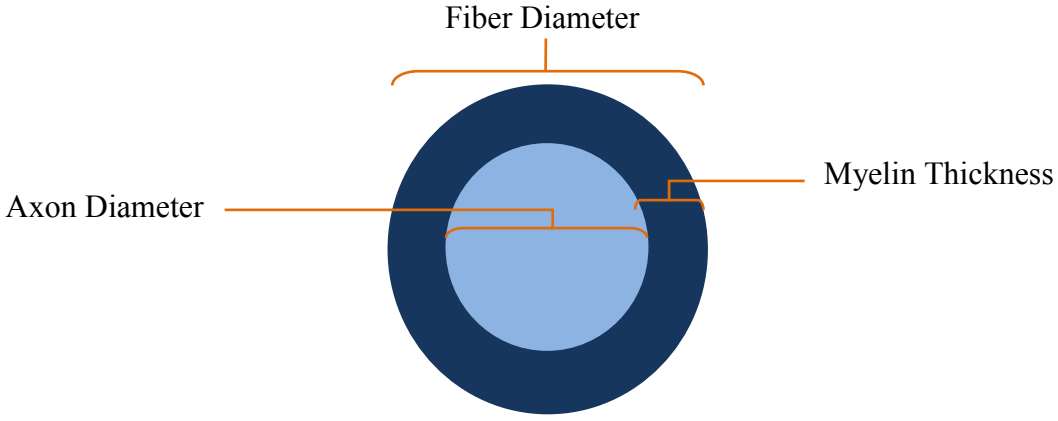

Figure 4.2: Schematic of a myelinated axon showing how measurements were taken.

4.3 RESULTS

4.3.1 Single-Lumen Conduits

In 2 of the 4 single-lumen conduits that were implanted, the conduit material was no longer present at harvest. One conduit remained intact and regenerated tissue was visible within the lumen. The last of the 4 conduits was surrounded by a large amount of tissue, possibly a neuroma. Images of the single-lumen conduits during the harvest surgery can be seen in Figure 4.3.

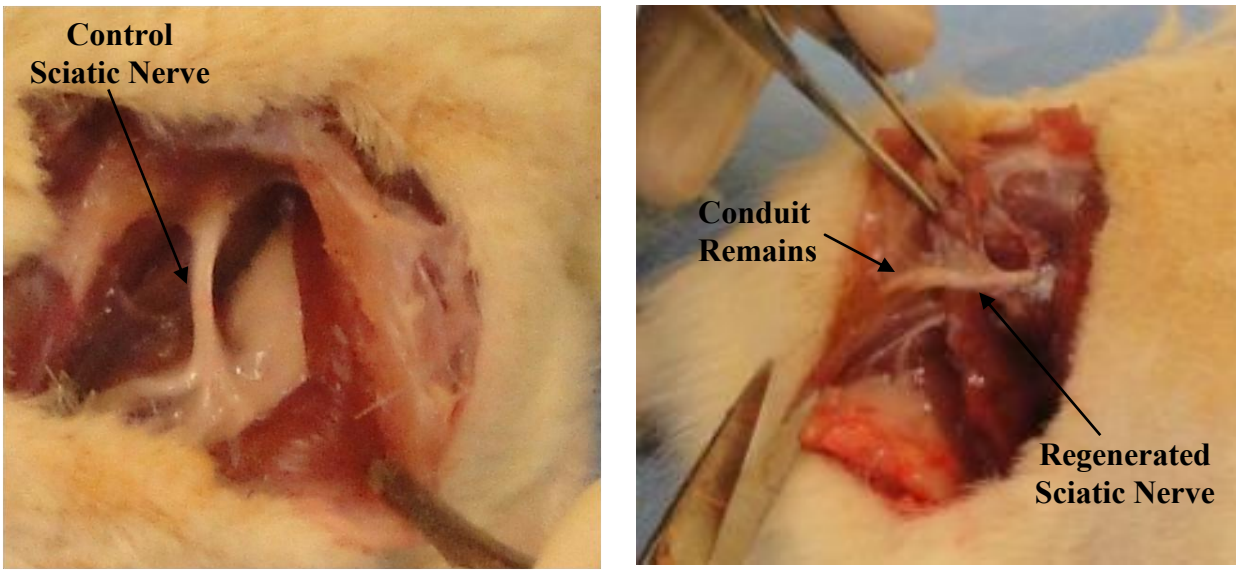

(A) (B)

Figure 4.3: Resection of single-lumen samples after 5 week period; (A) Control sciatic nerve on opposite leg; (B) Implanted single-lumen conduit, sample was absorbed but some remains were still present

From histological examination, 3 of the 4 rats given single-lumen conduits showed partial regeneration. The tissue surrounding the remaining sample was a neuroma. Therefore, it was not possible to analyze this sample. Figure 4.4 shows some of the high magnification (400x) images obtained. The control (A) shows consistency and symmetry in axon diameter and myelin thickness. The proximal section (B) resembles the control the most. However, small axons appear to be more abundant. The middle section (C) is an example of the unrestrained growth nature of nerves. This results in the presence of both transverse and longitudinal fibers within the same section. Finally, the

distal section (D) shows many Schwann cell nuclei (illustrated by red circles). An increase in Schwann cells is a common occurrence in regenerating fibers [55].

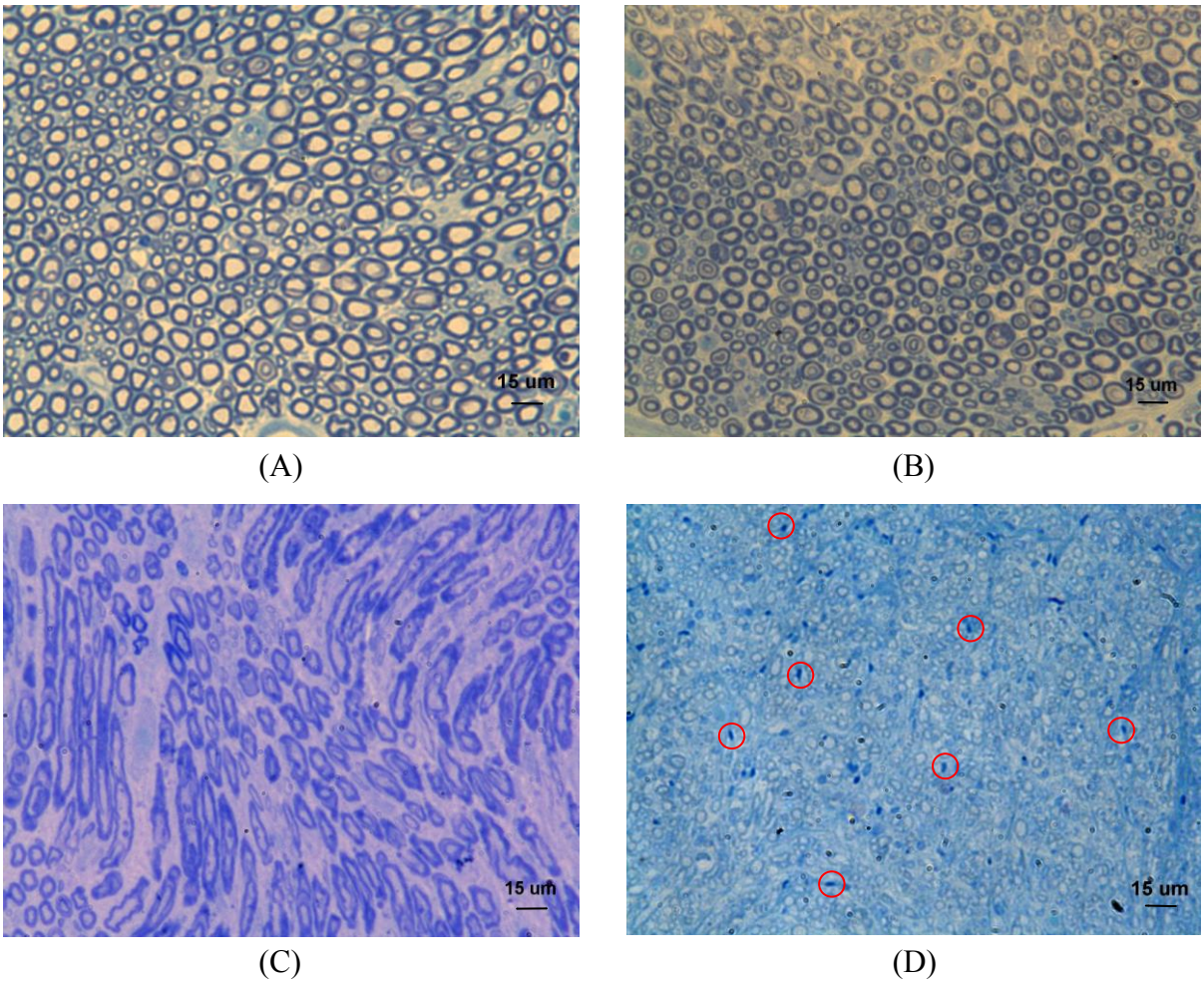

(A) (B)

(C) (D)

Figure 4.4: Cross-sectional images of single-lumen samples; (A) Control; (B) Proximal section; (C) Middle section; (D) Distal section

As illustrated in Figure 4.5, the controls consistently showed a greater number of axons than the test samples. The middle portion of the controls averaged 6080 ± 628 fibers/mm^2 while the middle section of the samples averaged 4490 ± 2810 fibers/mm^2. There was also a visible decrease in total number of fibers between the proximal and distal sections of the single-lumen samples. This was expected being that regenerating fibers sprout from the proximal stump of an injured nerve. There was no statistically significant difference between the samples and the control. Fiber composition was analyzed by classifying any fibers with an axon diameter smaller than 6 μm as "small fibers." Fibers

with axons larger than 6 μm were labeled "large fibers." The test samples all demonstrated a greater number of small axons, averaging 71.3 ± 44.0% with the highest proportion seen in the distal section. On the other hand, in the control group, small fibers represented only 41.9 ± 6.6%.

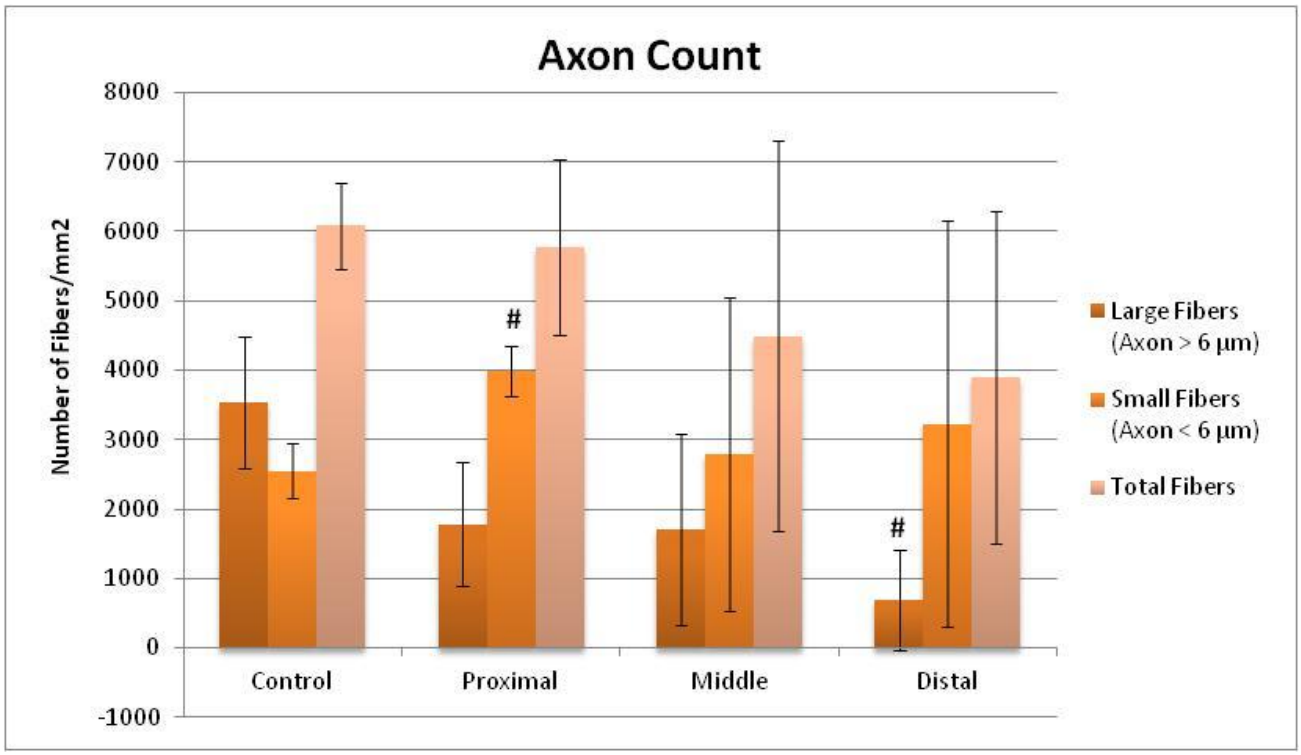

Figure 4.5: Large, small, and total number of fibers per mm^2 in single-lumen samples; #: Difference from the control is statistically significant, $p<0.05$

The total fiber diameter can be seen in Figure 4.6. It was calculated as the sum of axon diameter and myelin thickness [See Figure 4.2]. In this case, the average myelin thickness was doubled to represent the total thickness across both sides of the axon. The control showed a larger fiber diameter than the test samples. However, the decrease was not consistent as the middle section had a larger fiber diameter than the proximal section. This was due to a larger axon diameter. All differences from the control were statistically significant. Myelin thickness too was lower in the test samples as compared to the control. This is illustrated in Figure 4.7. Myelination thinned from the proximal to distal direction. In the middle, myelin thickness was 2.53 ± 0.87 μm compared to 3.00 ± 1.02 μm in the control. This is a decrease of 15.8%. The difference between all of the sections and the corresponding controls was statistically significant.

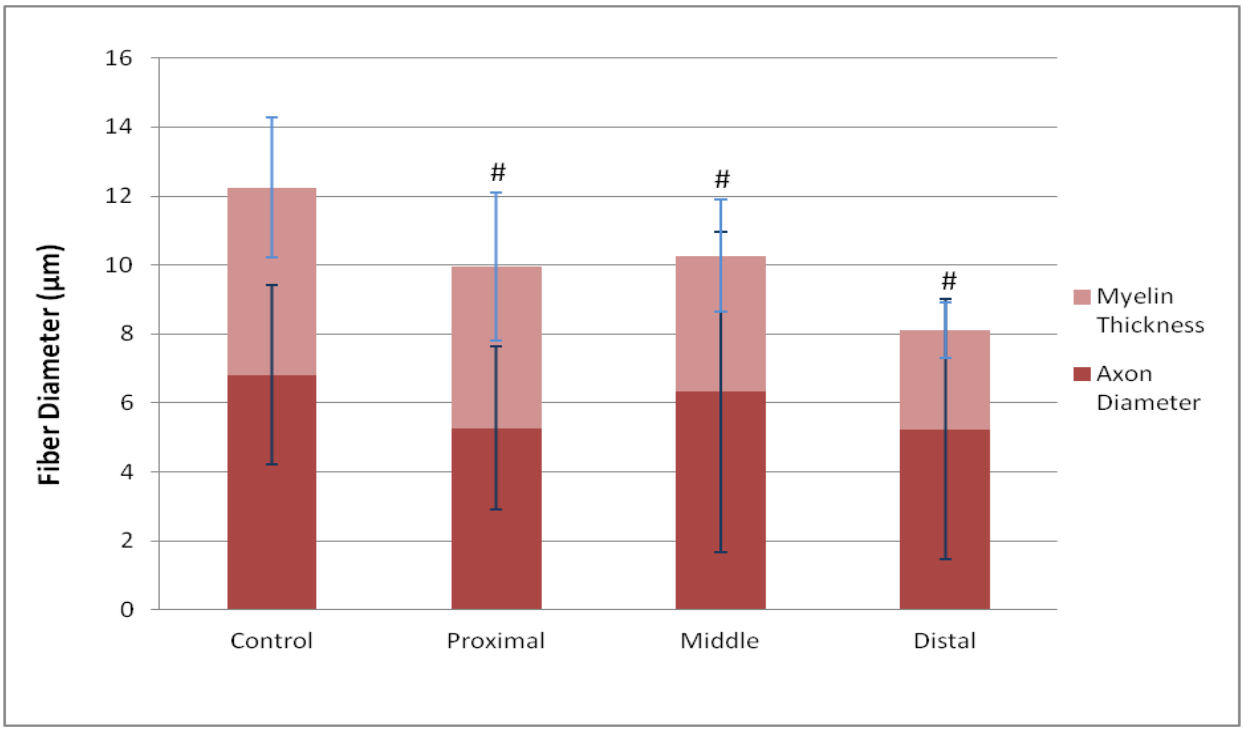

Figure 4.6: Average fiber diameter according to axon diameter and myelin thickness, average myelin thickness was doubled to represent total thickness across both sides of the axon. #: All differences from the control are statistically significant, $p<0.05$

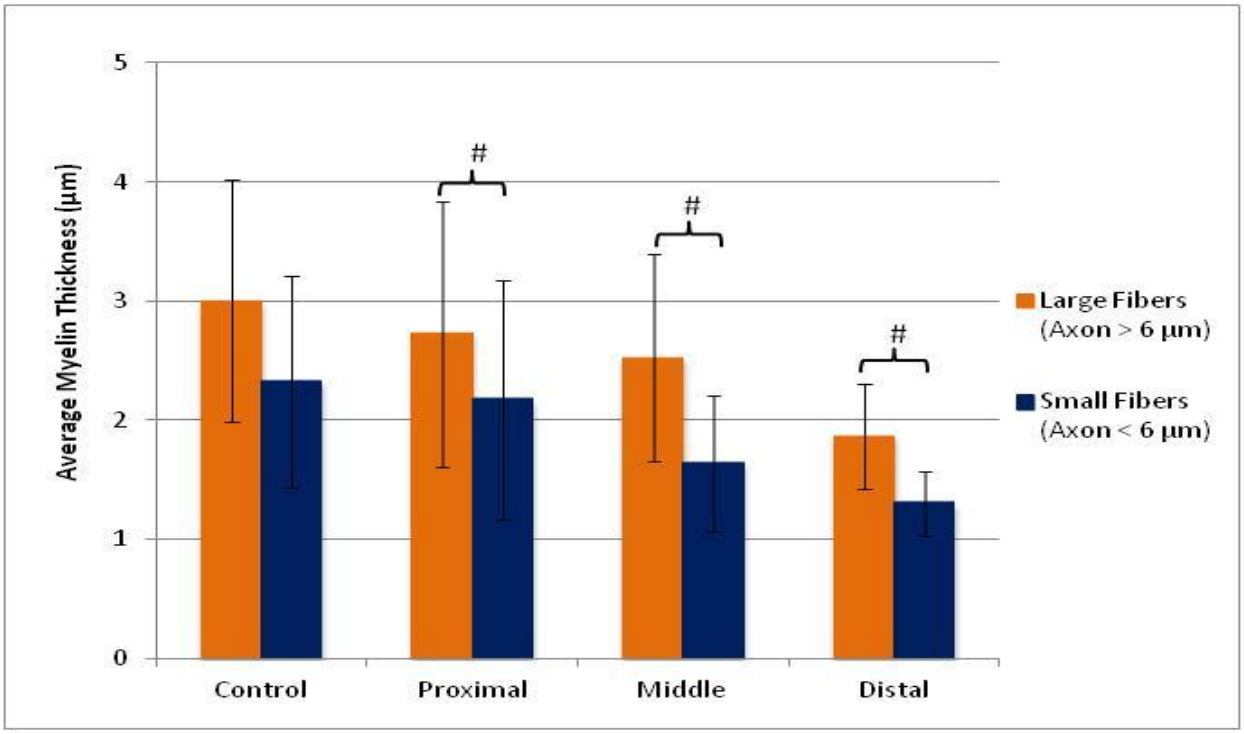

Figure 4.7: Average myelin thickness separated between small and large nerve fibers. #: All differences from the control are statistically significant, $p<0.05$

Table 4.1 represents the myelin thickness to axon diameter ratio. It too was smaller in the test samples than the control and showed a trend of decrease from proximal to distal. The g-ratio, a ratio of axon diameter to total fiber diameter, was actually greater in the middle and distal sections when compared to the control group. This can be seen in Table 4.2.

Table 4.1: Ratio of Myelin Thickness to Axon Diameter

	Large Fibers		Small Fibers	
	Average Ratio	Standard Deviation	Average Ratio	Standard Deviation
Control	0.77	0.14	1.07	0.13
Proximal	0.67	0.18	1.01	0.16
Middle	0.49	0.13	0.86	0.12
Distal	0.35	0.01	0.75	0.04

Table 4.2: g-Ratio

	Average Ratio	Standard Deviation
Control	0.54	0.05
Proximal	0.45	0.05
Middle	0.63	0.08
Distal	0.63	0.08

4.3.2 Multi-Lumen Conduits

Upon harvest, 2 of the multi-lumen conduits remained intact. Regenerated tissue was visible within some of the lumens. The other 2 conduits appeared to be encapsulated in fibrous tissue. Images of the multi-lumen conduits during the harvest surgery can be seen in Figure 4.8. Histolomorphological examination revealed severe paucity of axon regrowth within the multi-lumen conduits. Partial regeneration was seen in only 1 of 4 conduits. Therefore, it was not possible to calculate the various parameters calculated for single-lumen conduits. Examples of images obtained from the multi-lumen group are seen in Figure 4.9. Image (A) shows a low magnification (25x) image of the middle portion of a test sample. The lumens are visible and regenerated tissue is present in 6 of the 7 lumens. Image

(B) is a high magnification (400x) image of a distal section. Some axonal and myelin formation is present. However, there is little consistency in size and shape.

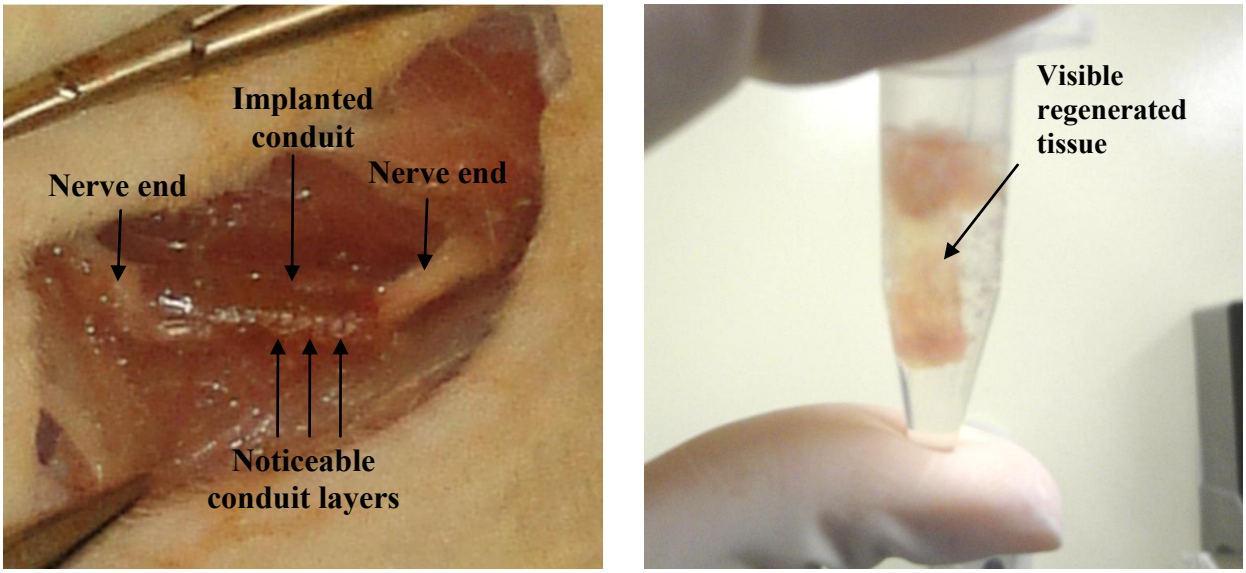

(A) (B)

Figure 4.8: Resection of multi-lumen samples after 5 week period; (A) Nerve sutured to NGC; (B) Resected NGC in preservation fluid.

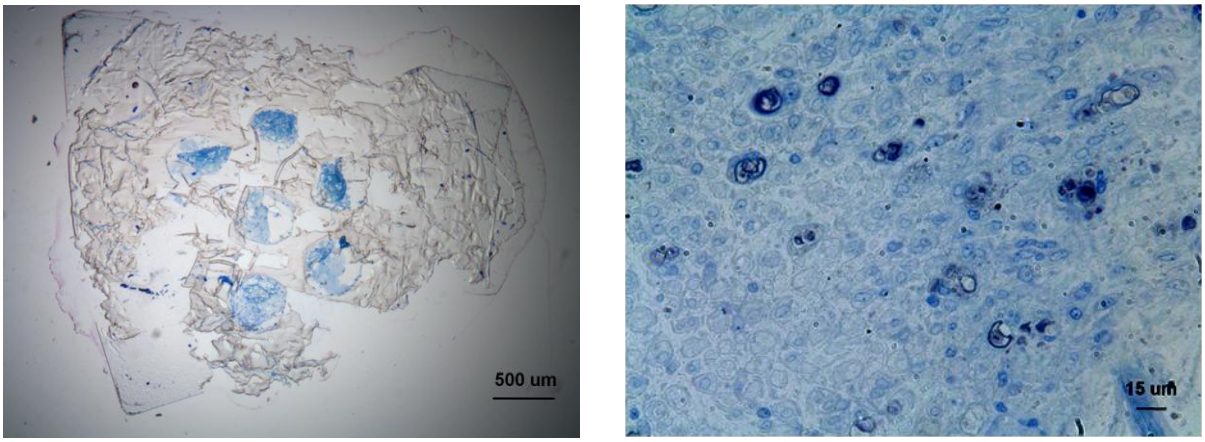

(A) (B)

Figure 4.9: Cross-sectional images of multi-lumen samples; (A) Low magnification image of middle section; (B) High magnification image of distal section

4.4 DISCUSSION

The purpose of this study was to explore the use of single and multi-lumen conduits as an alternative to the current nerve repair techniques. It also attempted to study the axonal growth and myelination at proximal, middle, and distal segments of a sciatic nerve injury. Two of the 4 single-lumen conduits that were implanted were no longer present upon harvest. Despite the fact that no degradation sequences were used in this PEG solution, others have shown that PEG-RGDS is susceptible to oxidative degradation. Lynn *et al.* demonstrated that PEG-RGDS can degrade faster than PEG-only solutions [56]. This is likely due to the negatively-charged Arginine in RGDS, which has a higher equilibrium swelling ratio, leading to faster degradation times. Histomorphological analysis revealed partial regeneration in 3 of 4 single-lumen conduits. It also revealed that morphology within single-lumen conduits was approaching that found in the controls. There were a greater percentage of fibers of small diameter within the single-lumen conduits than in the controls, indicating the presence of new, regenerating axons. Previous work by Sanders *et al.* showed there is a decrease in axon diameter and an increase in myelin thickness commonly seen in regenerating axons [57]. The axons in this study did, in fact, present a decrease in axon diameter within single-lumen samples. However, there was not a similar increase in myelin thickness. This can also be seen in the myelin thickness to axon diameter ratio. When a decrease in axon diameter and an increase in myelin thickness are present, a higher value would be expected in regenerating axons versus the controls. In this case, the ratio values were lower when compared to the controls. The main difference between this study and that conducted by Sander *et al.* is that their samples were analyzed after 60 days while these were harvested after 35 days. It may have been too early to allow the expected increase in myelin thickness to take place. Another study also saw peripheral nerve regeneration occurring at approximately the 2 month time point [58]. The g-ratio, or the ratio of axon diameter to fiber diameter, was calculated as it is used to assess nerve maturity. For a nerve to have optimum conduction velocity, a g-ratio of about 0.50, as seen in the controls, is necessary. The g-ratio of the middle and distal sections in single-lumen samples was slightly higher (~0.60), implying that considerable myelination had still not taken place.

The purpose of building multi-lumen conduits was increased the surface area available for Schwann cell adherence and delivery of growth stimulating proteins without decreased cross-sectional

area. Hadlock *et al.* used poly(lactic-co-glycolic acid) (PLGA) conduits to demonstrate improved regeneration in multi-lumen conduits and proposed that additional lumens lead to better regeneration [59]. On the hand, De Ruiter *et al.* found no difference amongst single- and multi-lumen PLGA conduits even tissue regenerated tissue was seen in only 3 of 7 lumens. It should also be noted that their conduits differed in cross-sectional area (0.8 mm^2 in multi-lumen conduits and 2 mm^2 in single-lumen conduits) while those of the present work did not (1.45 mm^2 for both types). PEGda and PLGA also differ in hydrophilicity, stiffness, and degradability. These are physical properties that can have an influence on an organism's response to a material. Regenerated tissue was visible within 2 of the 4 multi-lumen samples, as was seen in the cross-sectional view where regeneration was present in 6 of the 7 lumens [Figure 4.8 (A)]. There may have also been some regenerated tissue within the other 2 conduits that were encapsulated in fibrous tissue. However, the multi-lumen architecture made these more difficult to section and stain, complicating analysis. The PEGda conduits used for this research were not degradable nor contained any growth factors, other than a cell adhesion peptide. Both are features that can significantly affect the biological response to multi-lumen conduits; therefore, improving nerve regeneration.

Several factors made this analysis difficult to conduct. Due to an unrestrained growth nature of nerves, some sections had fibers cut longitudinally rather than transversely, affecting axon counts and diameters. Neuroma formation on 1 of the single-lumen conduits prevented regeneration within that conduit. There were also complications from sectioning and staining of multi-lumen samples. Therefore, nerve regeneration was visible in only 1 sample within the multi-lumen group. It was not possible to calculate the various histomorphological parameters of the nerve fibers in this group. As a result, only parameters in the single-lumen and control groups were compared. This, in conjunction with low sample size and short experimental duration, limited the ability to draw conclusions with statistical significance. Future studies, using other methods for fixation, staining, and sectioning of tissue, may provide better histomorphological results. These should also use larger sample sizes and longer time points. Functional and behavioral investigation would better characterize the therapeutic

potential of these conduits such as gastrocnemius and soleus muscle weight, sciatic functional index, and extensor postural thrust.

4.5 CONCLUSIONS

Peripheral nerve injuries are a significant issue amongst trauma patients. Nerve guidance conduits provide a potential solution. Although some conduits are available on the market today, they can only be utilized for bridging small gaps and do not work as well as autografts. Conduits built via SL may provide a more successful alternative to the current methods. This study demonstrates the ability of single-lumen PEGda conduits built using SL to facilitate nerve regeneration. Initially, it was hypothesized that multi-lumen conduits would outperform their single-lumen counterparts due to the fact that they provide a greater surface area for regeneration. However, better axon regrowth was seen in single-lumen conduits. This does not suggest multi-lumen conduits are inefficient in aiding regeneration. It simply means that other methods of tissue preparation for microscopic analysis should be explored.

Chapter 5: Using a Small Beam Stereolithography System for Increased Surface Area in Nerve Guidance Conduits

5.1 INTRODUCTION

5.1.1 Background

One of the topics being studied in the field of nerve tissue engineering is whether an increase in the surface area of a conduit will result in improved regeneration. This is because it is believed that increasing surface area increases the area for Schwann cell adherence as well as the area for delivery of growth stimulating proteins [59]. Attachment is necessary to Schwann cell survival and proliferation. When axons are not yet present, the cells need a surface to adhere to [60]. Several techniques for increasing surface area within nerve guidance conduits have been investigated including, electrospinning and polymer foam processing [59, 61, 62]. Similarly, stereolithography (SL) can be used to achieve these results. *In vivo* tests performed in Chapter 4 of this thesis focused on studying conduits which were designed to have either 1 large lumen (530 μm diameter) or 7 medium lumens (400 μm diameter). The SL machine used to build those conduits (SLA 250/50) used a HeCd UV laser with a beam diameter of 250 μm. This laser limits the line widths and wall thickness to 250 μm; which in turn, limits the amount of lumens that can be incorporated into a conduit. By reducing the laser diameter, more lumens of smaller size can be incorporated into conduits, increasing the surface area available for cell attachment.

5.1.2 HeCd Laser Specifications

The HeCd laser found in an SLA 250/40 has a wavelength of 325 nm and a beam diameter of 1.40 mm. The U-shaped structure of the laser can be seen in Figure 5.1. A glass plasma discharge tube is filled with He gas and is connected to a reservoir containing solid Cd. The reservoir is attached to a heating element which heats the Cd to vaporize. It then mixes with the He gas. Two electrodes, attached to the ends of the U-shaped tube, provide a high voltage potential creating an electric field across the tube. This field ionizes the He-Cd gas mixture, emitting photons as the result of excessive energy. A percentage of these photons are used by the SL system in the photopolymerization process. The rest of the photons are resonated back into the tube by two parallel mirrors, located on either side of

the tube, and collide with excited Cd atoms. This causes the release of another photon. The process is repeated creating photons of equal wavelength, phase, and traveling direction which are bounced back and forth between the mirrors. This is how a constant laser beam is produced [63].

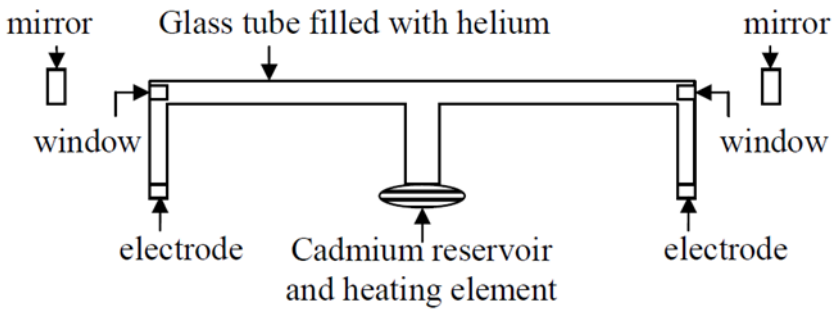

Figure 5.1: Structure of the HeCd Laser [64]

As mentioned in Chapter 1, the critical exposure (E_C) and penetration depth (D_P) are modifiable parameters on an SL system. In addition to these, another parameter was analyzed, line width compensation. Line width compensation is intended to compensate for the diameter of the laser and is typically half of the laser beam diameter [65]. For example, the original laser diameter on an SLA 250/40 is 250 μm. As a result, the default line width compensation is .005 in (125 μm). Figure 5.2 illustrates this concept. The laser beam diameter can cause a slight increase in the dimensions of the design. Line width compensation prevents this from happening so parts can have accurate dimensions. It is a value that can be changed on the Build Style of the design in 3D Lightyear, prior to importing the file into the SL system.

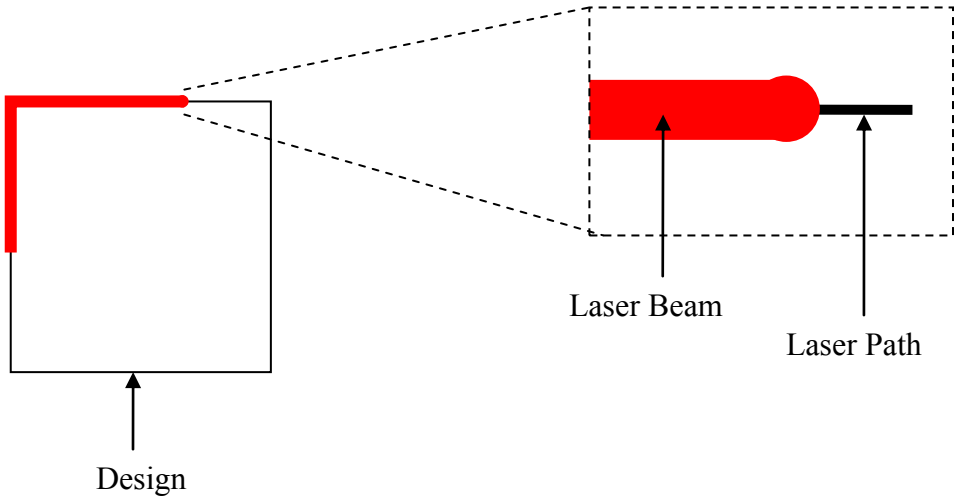

Figure 5.2 Line width compensation

5.1.3 Objective

For this research, a commercial SLA 250/40 (3D Systems, Rock Hill, SC) was retrofitted inside a laminar flow hood. This action served two objectives: to produce a laser beam of smaller diameter than that found in a commercial SL system and to design an aseptic SL system in which clean, particulate-free scaffolds could be built. The laser diameter was reduced by modifying the location of the optics as well as elevating the build stage and decrease the distance between the stage and the scanning mirror system. A reduction in diameter should improve microfabrication capabilities by allowing construction of smaller more complex features. It should also allow for construction of conduits with a greater surface area for cell attachment while not sacrificing the cross-sectional area through which nerves can regenerate.

5.2 Materials and Methods

5.2.1 SL System Modification

The modification of the SL system was performed by Espalin *et al.* and can be seen in Figure 5.3 (A). To do this, they determined at which stage height and optical configuration the smallest beam diameter could be achieved. As a beam of light travels, it spreads. Therefore, the beam is smaller closest to the light source. A commercial SLA 250/40 already uses a computer controlled elevator to move the stage vertically. However, the maximum height reached by the elevator was insufficient. Therefore, adjustable metal rods were used to place a secondary, smaller stage closer to the optical

window [See Figure 5.3 (B)]. Four rods were used in total, 2 for the stage and 1 for each of the beam aligning sensors. By fastening the rods directly onto the original stage, the secondary stage could still be controlled by movement of the elevator. An optical train was placed on the roof of the laminar flow hood to which the lenses and mirrors could be attached. The components were placed on the train in a way that they could slide back and forth along the rails, allowing for testing of the beam diameter at several distances from each other. Using MATLAB (MathWorks, Natwick, MA), a Cooke triplet optical system was chosen for placement of the lenses. This system uses a convex-concave-convex lens configuration with symmetrical spacing between the 3 components. Five mirrors were placed throughout to guide the beam toward the computer controlled optical scanning mirror directly above the stage. Fine tuners on the lenses and mirrors were used to ensure the beam maintained a circular shape [64]. In the end, the laser beam diameter was reduced to as small as 139.3 ± 14.5 μm. The Cooke triplet set-up can be seen in Figure 5.4.

5.2.2 PEGda Solution Preparation

For these tests, a solution of commercially available 3.4 kDa PEGda (Laysan Bio Inc., Arab, AL) was prepared at a 30 wt% concentration. Irgacure-2959 (Ciba Specialty Chemicals, Tarrytown, NY) was used as a photoinitiator at 0.5 wt% concentration. Sterile 1X phosphate buffered saline (PBS) was used as the solvent. All solutions were prepared in a biosafety cabinet (Purifier Class II, Labconco, Kansas City, MO).

5.2.3 SL System Calibration

The first step in attempting to build parts using the retrofitted SL system was calibration. Initial attempts at building yielded samples approximately one quarter the size of the CAD file. A calibration file provided by 3D Systems (Rock Hill, SC) was used to calibrate the system. For this, a simple 25.4 mm x 25.4 mm (1 in x 1 in) square design was built to acquire x and y dimensions. The dimensions were saved into the calibration file and the file was imported into the retrofitted SL system's control center. The square was re-built to confirm success of the calibration. All samples were analyzed using a Leica MZ16 Stereomicroscope (Leica Microsystems, Germany). Images were taken with a charge-coupled device camera (Retiga 2000S Fast 1394, QImaging Corp., Canada).

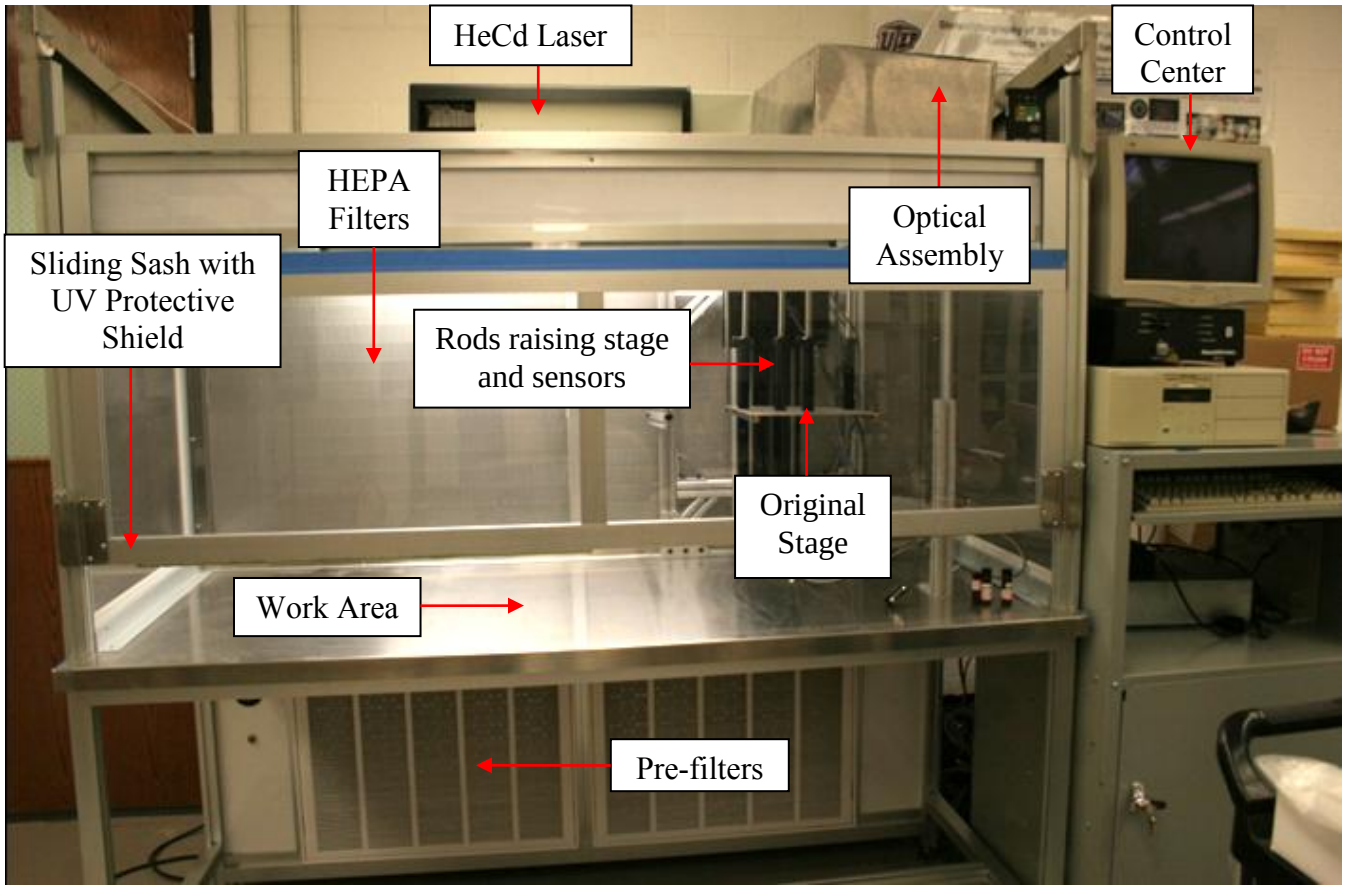

(A)

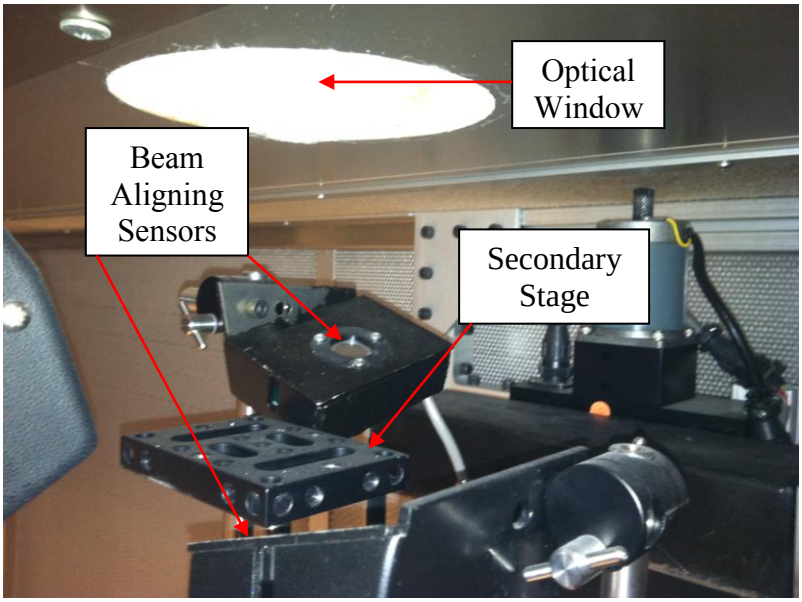

(B)

Figure 5.3: (A) Retrofitted SL system, (B) View of elevated build stage

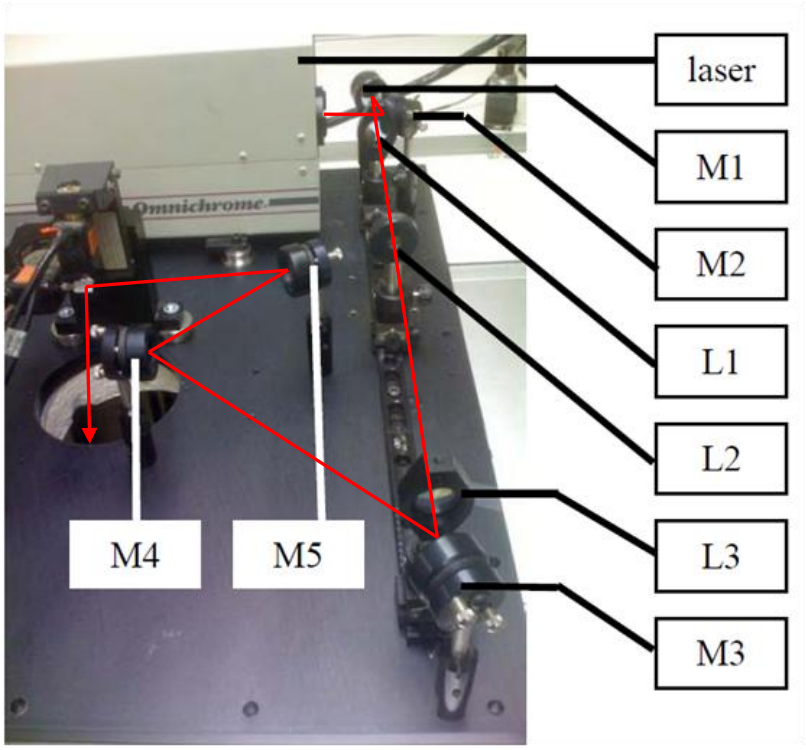

Figure 5.4: Cooke triplet optical assembly of lenses and mirrors; red line indicates laser path. Adapted from [63]

Various conduit configurations were designed using Solidworks™. All conduit designs had an outer diameter of 2.94 mm and an inner diameter of 1.97 mm. A single-lumen conduit was designed to have a 530 µm lumen. A 7-lumen conduit with lumen diameter of 400 µm was also made. Finally, three more conduits were designed to have 14, 16, and 18 lumens of a 240 µm diameter. These CAD files can be seen in Figure 5.5. The 7-lumen design was chosen to determine the best build parameters to use with this laser. This was done by building a single layer of a 7-lumen sample at various D_P and line width compensation values. All of the samples were built with an EC value of 12 mJ/cm^2 as it had proven to work well in the past. Once the best parameters were chosen, single layer samples of the other 3 designs were built to verify dimensions. Two-layer samples were also built to note if the various lumens remained open when a new layer was built above an existing one. Partial conduits of each were built consisting of 4 lumenal layers and 2 cap layers. Finally, a whole layer 14-lumen conduit was built with 2 cap portions.

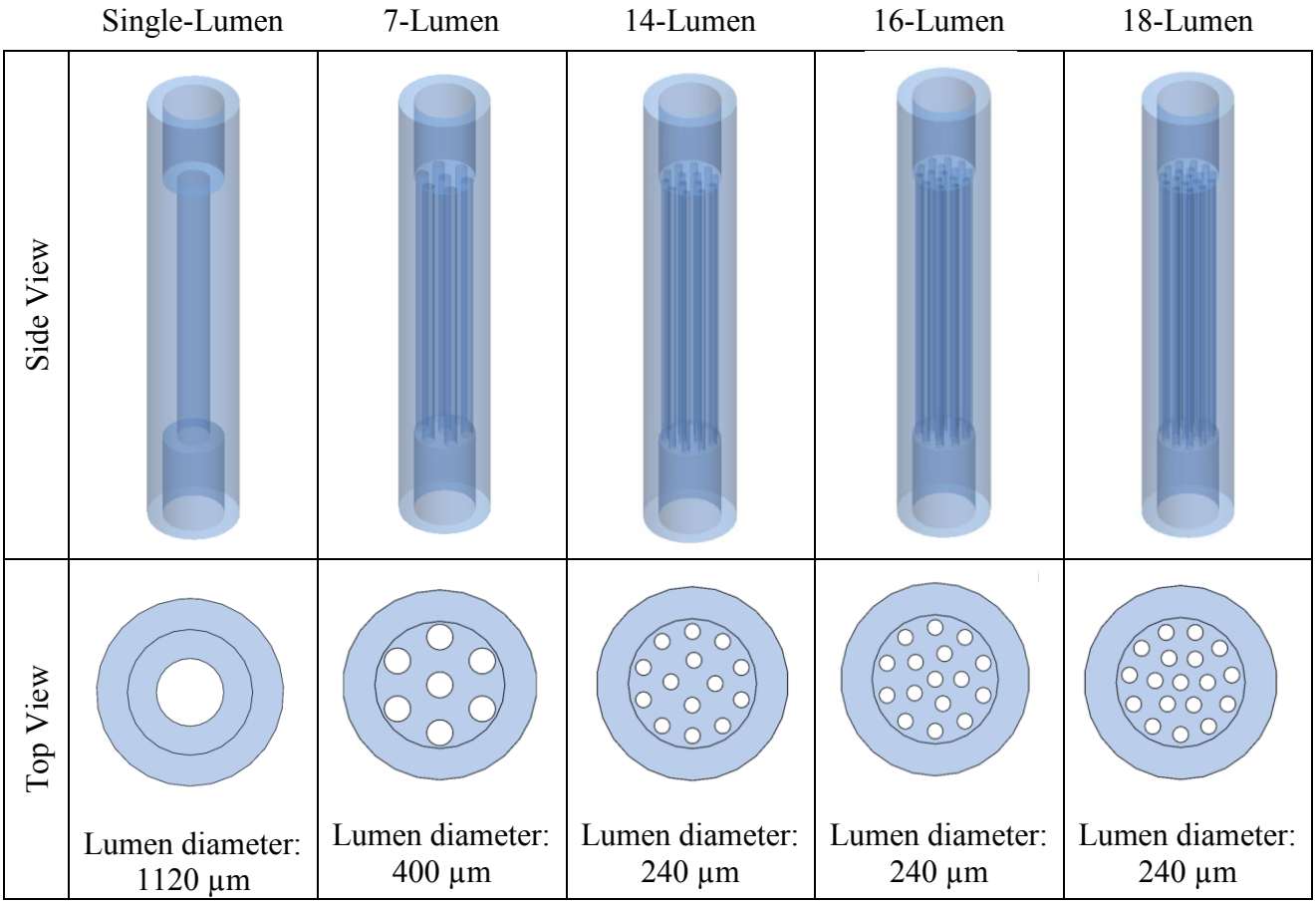

Figure 5.5: Side and top views of conduit CAD models. All had the following dimensions: inner diameter = 1.97 mm, outer diameter = 2.94 mm, total length = 16 mm, length of lumen portion = 10 mm

5.2.5 Comparing Cross-sectional and Surface Areas

Cross-sectional and surface areas of the various lumen diameters were calculated for both the CAD dimensions and swollen dimensions. A length of 10 mm was used for the lumen portion of the conduits. However, it should be noted that conduit length can be adapted to fit the length of the injury. The following equation was used to calculate cross-sectional area:

$$A = \pi r^2 n \qquad (5.2 - 1)$$

where

A is cross-sectional area,

r is radius of the lumens,

n is number of lumens.

Surface area was calculated using the following equation:

$$SA = 2\pi rhn \quad (5.2 - 2)$$

where

SA is surface area,

r is radius of the lumens,

h is height of the lumen portion of conduit,

n is number of lumens.

To calculate cross-sectional and surface areas when the sample is in a swollen state, the Dimensional Swelling Factor was used. The values for this material (PEGda 3.4 kDa at 30 wt%) were previously calculated by Arcaute *et al.*: 1.18 ± 0.008 for conduit length and 1.21 ± 0.039 for lumen diameter [27]. The following equation was used:

$$Dimensional\ Swelling\ Factor = \frac{Swollen\ Dimension}{Design\ Dimension} \quad (5.2 - 3)\ [27]$$

5.3 RESULTS

The results of the various build parameters that were tested can be seen in Figure 5.6. As previously mentioned, all samples were built with an E_C value of 12 mJ/cm^2. For Sample A, a D_P value of 8 mil was used which yielded a speed of 2.994 in/s. This sample used a line width compensation of 0.005 in. The diameter of the lumens (~509 μm) was too large. Therefore, for Sample B, the line width compensation was decreased by half, at .0025 in. Without modifying E_C or D_P values, the speed decreased slightly to 2.837 in/s. The diameter of the lumens was better than the previous (~397 μm). However, the outer edges on this sample were rather rough. On the bottom surface of the sample, the lumens did not have a nice circular shape. In Sample C the laser speed was reduced to 2.343 in/s by reducing the D_P to 7 mil. This made the lumens slightly smaller (~390 μm) but they had a more consistent round shape on the top and bottom surfaces. The edges on this sample were smoother than the previous two. Finally, in Sample D the D_P was lowered to 6 mil, lowering the speed to 1.739 in/s. Although the surface finish was smooth, the decrease in speed caused a decrease in the size of the

lumens (~361 μm). Therefore, the parameters set in Sample C were considered the best option for construction of additional samples.

	Build Parameters	Outer Diameter	Lumen Diameter
(A)	E_C = 12 mJ/cm^2 D_P = 8 mil V_S = 2.994 in/s LWC = 0.005 in		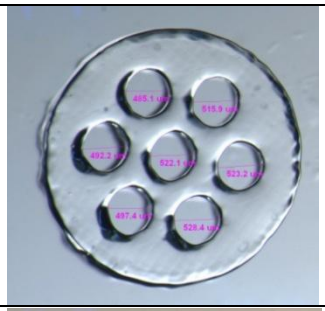
(B)	E_C = 12 mJ/cm^2 D_P = 8 mil V_S = 2.837 in/s LWC = 0.0025 in	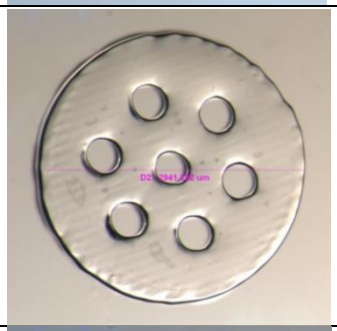	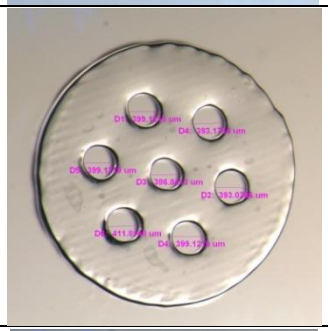
(C)	E_C = 12 mJ/cm^2 D_P = 7 mil V_S = 2.343 in/s LWC = 0.0025 in		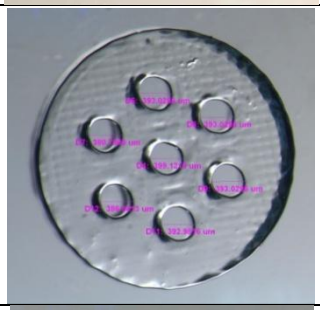
(D)	E_C = 12 mJ/cm^2 D_P = 6 mil V_S = 1.739 in/s LWC = 0.0025 in	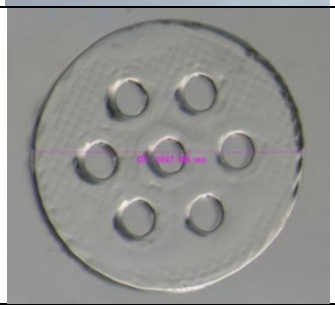	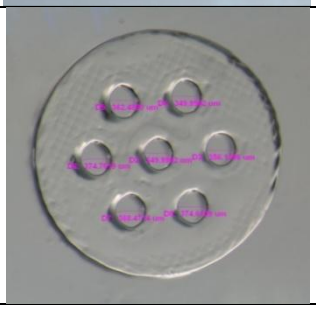

Figure 5.6: Testing build parameters on a 7-lumen sample; E_C = critical exposure, D_P = penetration depth, V_S = laser scan speed, LWC = line width compensation

Successful construction of 14, 16, and 18-lumen samples was achieved. The best results of these can be seen in Figure 5.7. Initially only a single layer of each design was built to ensure proper lumen shape and dimensions. The 2-layer samples showed good attachment between the layers. The bottom layer (first layer built) became thinner once the top layer was added. There was some decrease in diameter by the lumens when compared to the single layer samples. However, both top and side views show the lumens remained open. Like the single layer samples, the lumens have a uniform circular shape. The 6 layer samples (4 lumen layers + 2 cap layers) also showed consistent shape and diameter of the lumens. The lumens still remained open. The 14-lumen sample was built with the cap portion first and the lumen portion on top. However, like the 2-layer sample the first layer decreases in size with addition of a second layer. It was decided to build the 16 and 18-lumen samples with the lumen portion first and the cap portion on top. This way, the length of the cap portion would not be affected. The surface finish was somewhat rough as there was clear definition amongst the individual layers. The 14-lumen design was chosen for construction of a full conduit. Four layers were used for the bottom cap, 8 for the lumen section, and 3 for the top cap. This sample can be seen in Figure 5.8. Image (A) shows how the sample looked immediately after fabrication. Unlike the 6 layer samples previously built, this sample had a cleaner surface finish. It also appeared more symmetrical. Suture thread was used to show the lumens remained open despite the layers being built on top of one another [See Figure 5.8 (B)]. Although the single-lumen conduit was designed, it was not built. This was decided because the large lumen can be built with a commercial SL system. The CAD file, though, did help in calculating surface and cross-sectional areas.

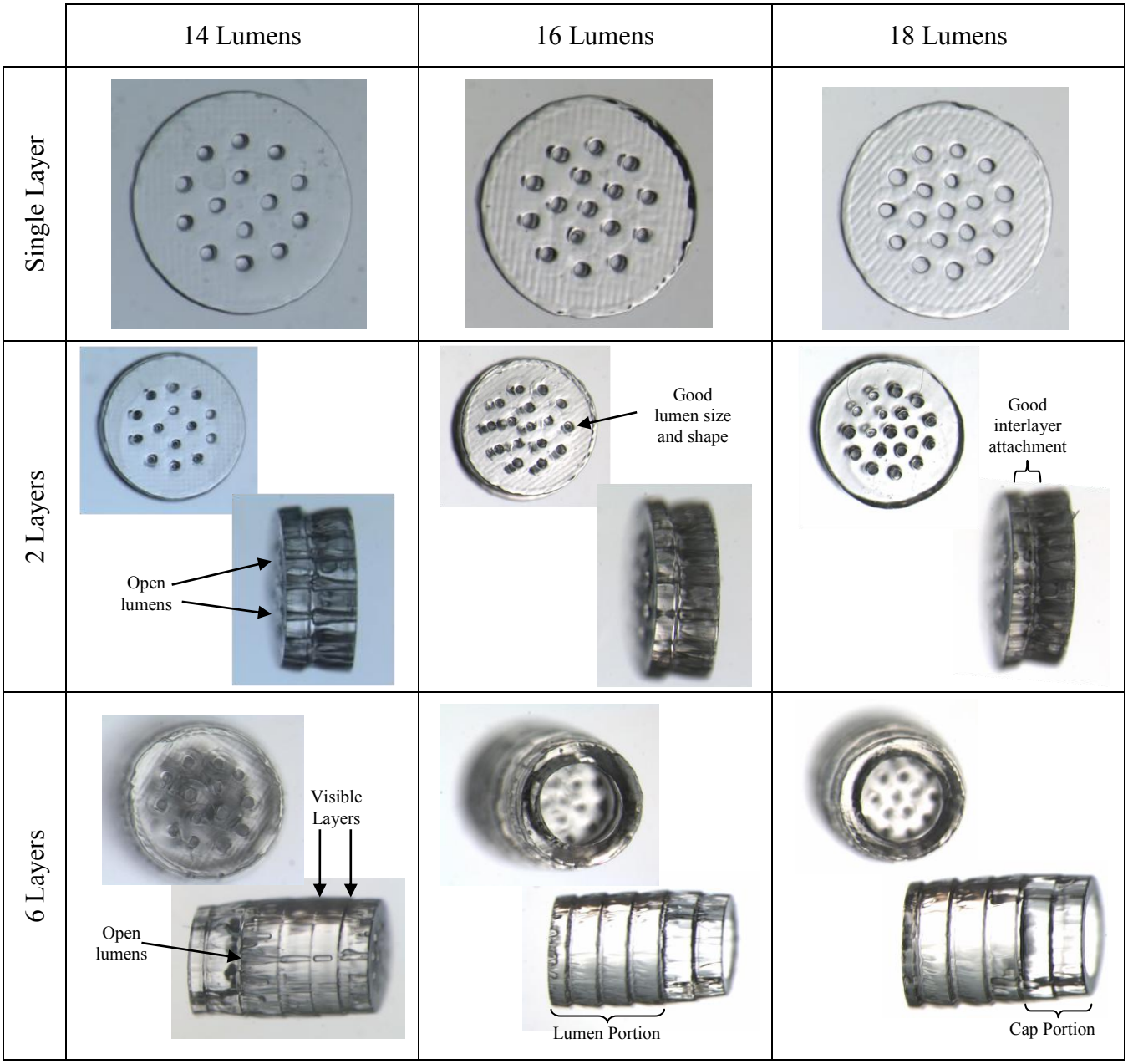

Figure 5.7: Top and side views of 14, 16, and 18-lumen samples

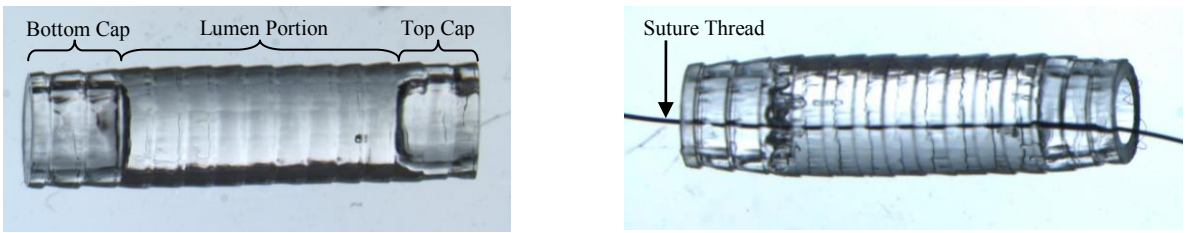

(A) (B)

Figure 5.8: Full size 14-lumen conduit; (A) As fabricated; (B) Suture thread used to show open lumens

Using the equation for Dimensional Swelling Factor (5.2-3), swollen values were obtained for the length of the lumen portion of the conduit as well as the lumen diameters. Both, swollen and as-fabricated, dimensions can be seen in Table 5.1. These were used to calculate the cross-sectional and lumenal surface areas. The dimensions of the single and 7-lumen conduits were previously calculated so they would both have the same cross-sectional area. In this case, the cross-sectional area is larger for both than it is for the samples with the smallest lumen size. However, the 18-lumen sample has cross-sectional areas of 0.81 mm^2 and 1.19 mm^2 for as-fabricated and swollen dimensions, respectively. These differ by only 0.07 mm^2 and 0.1 mm^2 from the single and 7-lumen samples. On the other hand, the lumenal surface area increases as the number of lumens increases. The surface area found in 18-lumen samples was greater than 4 times that found in single-lumen samples. This is seen in both as-fabricated and swollen conduit dimensions.

Table 5.1: As-Fabricated and Swollen Conduit Dimensions

	As-Fabricated			**Swollen**		
	Single-lumen	**7-lumen**	**14, 16, 18-lumen**	**Single-lumen**	**7-lumen**	**14, 16, 18-lumen**
Length of Lumen Portion	10 mm	10 mm	10 mm	11.8 mm	11.8 mm	11.8 mm
Lumen Diameter	1.06 mm	0.40 mm	0.24 mm	1.28 mm	0.484 mm	0.29 mm

Table 5.2: Area Comparisons

	As-Fabricated		**Swollen**	
	Cross-Sectional Area	**Lumenal Surface Area**	**Cross-Sectional Area**	**Lumenal Surface Area**
Single-Lumen	0.88 mm^2	33.30 mm^2	1.29 mm^2	47.45 mm^2
7-Lumen	0.88 mm^2	87.96 mm^2	1.29 mm^2	125.60 mm^2
14-Lumen	0.63 mm^2	105.56 mm^2	0.92 mm^2	150.51 mm^2
16-Lumen	0.72 mm^2	120.64 mm^2	1.06 mm^2	172.01 mm^2
18-Lumen	0.81 mm^2	135.72 mm^2	1.19 mm^2	193.51 mm^2

5.4 DISCUSSION

Various methods have been studied for increased surface area within nerve guidance conduits. This is because it is believed that increasing surface area increases the area for Schwann cell adherence as well as the area for delivery of growth stimulating proteins [59]. One method that has been studied for construction of conduits is electrospinning [61, 62]. Electrospinning is a technique that creates fibrous scaffolds when high voltage is applied to a photopolymer solution [66]. The fibrous nature of these scaffolds is of interest to researchers because it provides a large surface area for regeneration. For example, Chew *et al.* used electrospinning to build a conduit made from a caprolactone and ethyl ethylene phosphate (PCLEEP) copolymer. The electrospun conduits outperformed non-electrospun control conduits by 50% [62]. Another technique that has been studied to increase conduit surface area is polymer foam processing. This is done by injecting a polymer solution under low pressure into a stainless steel mold and cooling the solution. Hadlock *et al.* used stainless steel wire molds to create conduits of over 100 lumens. Cross-sectional images revealed neural tissue regeneration that was comparable to autograft controls [59].

Similar results can be obtained using SL. *In vivo* tests performed in Chapter 4 of this thesis focused on studying conduits which were designed to have either 1 large lumen (530 μm diameter) or 7 medium lumens (400 μm diameter). The SL machine used to build those conduits (SLA 250/50) used a HeCd UV laser with a beam diameter of 250 μm. This laser limits the line widths and wall thickness to 250 μm; which in turn, limits the amount of lumens that can be incorporated into a conduit. By reducing the laser diameter, more lumens of smaller size can be incorporated into conduits, increasing the surface area available for cell attachment.

Construction of a retrofitted SL system with a reduced laser beam diameter, allowed for construction of conduits with increased number of lumens. Testing various parameters using a 7-lumen design was necessary to determine E_C, D_P, laser scan speed, and line with compensation values to achieve the best samples. By reducing the lumen diameter from 400 μm to 240 μm, it was possible to incorporate over twice the number of lumens as that found in a 7-lumen conduit. Successful construction of 1, 2, and 6 layer samples was achieved to verify lumen diameter and shape consistency. Building a full 14-lumen conduit proved that lumens remain open despite layer stacking. Although

cross-sectional area is decreased the difference in samples with a high number of lumens is comparable to that of larger lumens. On the other hand, surface area is significantly increased as lumen diameter is reduced and number of lumens is increased.

5.5 CONCLUSIONS

Researchers in nerve regeneration methods believe that increasing surface area on a conduit increases the surface available for cell attachment and delivery and nerve stimulating proteins. Construction of a retrofitted SL system with a reduced laser beam diameter, allowed for construction of conduits with increased number of lumens. Testing various parameters using a 7-lumen design was necessary to determine E_C, D_P, laser scan speed, and line with compensation values to achieve the best samples. By reducing the lumen diameter from 400 μm to 240 μm, it was possible to incorporate over twice the number of lumens as that found in a 7-lumen conduit. Successful construction of 1, 2, and 6 layer samples was achieved to verify lumen diameter and shape consistency. Building a full 14-lumen conduit proved that lumens remain open despite layer stacking. Although cross-sectional area is decreased, the difference in samples with a high number of lumens is comparable to that of larger lumens. On the other hand, surface area is significantly increased as lumen diameter is reduced and number of lumens is increased.

References

[1] K. L. Moore, A. M. R. Agur and A. F. Dalley, Essential Clinical Anatomy, 4th ed., Baltimore , MD: Lippincott Williams & Wilkins, 2011.

[2] D. Randall, W. Burggren and K. French, Animal Physiology: Mechanisms and Adaptations, 5th ed., New York, NY: W. H. Freeman and Company, 2002.

[3] "neuron. Art.," Encyclopaedia Britannica, [Online]. Available: http://www.britannica.com/EBchecked/media/66776/Anatomy-of-a-nerve-cell-Structural-features-of-a-motor. [Accessed 2 December 2013].

[4] M. Siemionow and G. Brzezicki, "Chapter 8 Current techniques and concepts in peripheral nerve repair," *International Review of Neurobiology,* vol. 87, pp. 141-172, 2009.

[5] J. Noble, C. Munro, V. Prasad and R. Midha, "Analysis of upper and lower extremity peripheral nerve injuries in a population of patients with multiple injuries," *The Journal of Trauma: Injury, Infection, and Critical Care,* vol. 45, no. 1, pp. 116-122, July 1998.

[6] J. L. Kelsey, A. Praemer, L. Nelson, A. Felberg and D. Rice, Upper extremity disorder: frequency, impact, and cost, New York: Churchill Livingstone, 1997.

[7] G. Lundborg, "A 25-year perspective of peripheral nerve surgery: evolving neuroscientific concepts and clinical significance," *The Journal of Hand Surgery,* vol. 25A, no. 3, pp. 391-414, 3 May 2000.

[8] C. E. Schmidt and J. Baier Leach, "Neural tissue engineering: strategies for repair and regeneration," *Annual Review of Biomedical Engineering,* vol. 5, pp. 293-347, 2003.

[9] G. Stoll, J. W. Griffin, C. Y. Li and B. D. Trapp, "Wallerian degeneration in the peripheral nervous system: participation of both Schwann cells and macrophages in myelin degradation," *Journal of Neurocytology,* vol. 18, pp. 671-683, 1989.

[10] J. S. Belkas, M. S. Shoichet and R. Midha, "Peripheral nerve regeneration through guidance tubes," *Neurological Research,* vol. 26, March 2004.

[11] X. Jiang, S. H. Lim, H.-Q. Mao and S. Y. Chew, "Current applications and future perspectives of artificial nerve conduits," *Experimental Neurology,* vol. 223, no. 1, pp. 86-101, 2010.

[12] E. J. Wall, J. B. Massie, M. K. Kwan, B. L. Rydevik, R. R. Myers and S. R. Garfin, "Experimental stretch neuropathy: changes in nerve conduction under tension," *The Journal of Bone and Joint Surgery,* Vols. 74-B, no. 1, 1992.

[13] R. A. Weber, W. C. Breidenbach, R. E. Brown, M. E. Jabaley and D. P. Mass, "A randomized prospective study of polyglycolic acid conduits for digital nerve reconstruction in humans," *Plastic and Reconstructive Surgery,* vol. 106, no. 5, pp. 1036-1045, October 2000.

[14] T. H. Nijhuis, C. W. Bodar, J. W. van Neck, E. T. Walbeehm, M. Siemionow, M. Madajka, J. Cwykiel, J. H. Blok and S. E. Hovius, "Natural conduits for bridging a 15-mm nerve defect: Comparison of the vein supported by muscle and bone marrow stromal cells with a nerve autograft," *Journal of Plastic, Reconstructive & Aesthetic Surgery,* vol. 66, no. 2, pp. 251-259, 2013.

[15] T. W. Hudson, G. R. Evans and C. E. Schmidt, "Engineering strategies for peripheral nerve repair," *Orthopedic Clinics of North America,* vol. 31, no. 3, pp. 485-497, 1 July 2000.

[16] S. Kehoe, X. F. Zhang and D. Boyd, "FDA approved guidance conduits and wraps for peripheral nerve injury: a review of materials and efficacy," *Injury,* vol. 43, no. 5, pp. 553-572, 2012.

[17] C. K. Chua, K. F. Leong and C. S. Lim, Rapid prototyping: principles and applications, 2nd ed.,

Singapore: World Scientific Publishing Co. Pte. Ltd., 2003, pp. 35-52.

[18] K. Arcaute, B. Mann and R. Wicker, "Stereolithography of spatially controlled multi-material bioactive poly(ethylene glycol) scaffolds," *Acta Biomaterialia,* vol. 6, no. 3, pp. 1047-1054, March 2010.

[19] I. H. Lee and D. W. Cho, "Micro-stereolithography photopolymer solification patterns for various laser beam exposure conditions," *International Journal of Advanced Manufacturing Technology,* vol. 22, no. 5/6, pp. 410-416, 2003.

[20] "Polyethylene Glycol," U.S. Food and Drug Administration, [Online]. Available: http://www.accessdata.fda.gov/scripts/cder/drugsatfda/index.cfm?fuseaction=Search.Overview&DrugName=POLYETHYLENE%20GLYCOL%203350. [Accessed 2013].

[21] S. Zalipsky and J. M. Harris, "Chapter 1: Introduction to Chemistry and Biological Applications of Poly(ethylene glycol)," in *Poly(ethylene glycol) Chemistry and Biologial Applications*, J. M. Harris and S. Zalipsky, Eds., Washington D.C., American Chemical Society, 1997, pp. 1-13.

[22] J. A. Burdick and K. S. Anseth, "Photoencapsulation of osteoblasts in injectable RGD-modified PEG hydrogels for bone tissue engineering," *Biomaterials,* vol. 23, no. 22, pp. 4315-4323, 2002.

[23] S. J. Bryant and K. S. Anseth, "The effects of scaffold thickness on tissue engineered cartilage in photocrosslinked poly(ethylen oxide) hydrogels," *Biomaterials,* vol. 22, no. 6, pp. 619-626, 2001.

[24] B. K. Mann, A. S. Gobin, A. T. Tsai, R. H. Schmedlen and J. L. West, "Smooth muscle cell growth in photopolymerized hydrogels with cell adhesive proteolytically degradable domains: synthetic ECM analogs for tissue engineering," *Biomaterials,* vol. 22, no. 22, pp. 3045-3051, 2001.

[25] P. K. Working, M. S. Newman, J. Johnson and J. B. Cornacoff, "Chapter 4: Safety of Poly(ethylene glycol) and Poly(ethylene glycol) Derivatives," in *Poly(ethylene Glycol) Chemistry and Biological Applications*, J. M. Harris and S. Zalipsky, Eds., Washington D.C., 1997, pp. 45-57.

[26] J. W. Gunn, S. D. Turner and B. K. Mann, "Adhesive and mechanical properties of hydrogels influence neurite extension," *Journal of Biomedical Materials Research Part A,* vol. 72, no. 1, pp. 91-97, 2004.

[27] K. Arcaute, B. K. Mann and R. B. Wicker, "Fabrication of off-the-shelf multilumen poly(ethylene glycol) nerve guidance condutis using stereolithography," *Tissue Engineering: Part C,* vol. 17, no. 1, pp. 27-38, 2011.

[28] A. T. Metters and C.-C. Lin, "Biodegradable Hydrogels: Tailoring Properties and Function through Chemistry and Structure," in *Biomaterials*, Boca Raton, FL, Taylor & Francis Group, 2007, pp. 5.27-5.28 .

[29] S. Zalipsky, "Chemistry of Polyethylene Glycol Conjugates with Biologically Active Molecules," *Advanced Drug Delivery Reviews ,* vol. 16 , pp. 157-182, 13 April 1995.

[30] J. S. Miller and J. L. West, "Rapid Prototyping of Hydrogels to Guide Tissue Formation," in *Bio-Materials and Prototyping Applications in Medicine*, 2008, Springer, New York, NY, pp. 49-65.

[31] 2013. [Online]. Available: http://www.sigmaaldrich.com/catalog/product/aldrich/437441?lang=en&region=US.

[32] M. Yamamoto, G. Sobue, M. Li, Y. Arakawa, T. Mitsuma and K. Kimata, "Nerve growth factor (NGF), brain-derived neurotrophic factor (BDNF) and low-affinity nerve growth factor receptor (LNGFR) mRNA levels in cultured rat Schwann cells; differential time- and dose-dependent regulation by cAMP," *Neuroscience Letters,* vol. 152, pp. 37-40, 1993.

[33] H. Kerkhoff and F. G. I. Jennekens, "Peripheral nerve lessions: the neuropharmacological outlook," *Clinical Neurology and Neurosurgery,* vol. 95, pp. 103-108, 1993.

[34] D. Otto, K. Unsicker and C. Grothe, "Pharmacological effects of nerve growth factor and fibroblast growth factor applied to the transectioned sciatic nerve on neuron death in adult rat dorsal root ganglia," *Neuroscience Letters,* vol. 83, no. 1-2, pp. 156-160, 1987.

[35] A. C. Lee, V. M. Yu, J. B. Lowe III, M. J. Brenner, D. A. Hunter, S. E. Mackinnon and S. E. Sakiyama-Elbert, "Controlled Release of Nerve Growth Factor Enhances Sciatic Nerve Regeneration," *Experimental Neurology,* vol. 184, pp. 295-303, 2003.

[36] N. Q. McDonald, R. Lapatto, J. Murray-Rust, J. Gunning, A. Wlodawer and T. L. Blundell, "New protein fold revealed by a 2.3-Å resolution crystal structure of nerve growth factor," *Letters to Nature,* vol. 354, pp. 411-414, 1991.

[37] G. R. D. Evans, K. Brandt, S. Katz, P. Chauvin, L. Otto, M. Bogle, B. Wang, R. K. Meszlenyi, L. Lu, A. G. Mikos and C. W. Patrick, "Bioactive poly(L-lactic acid) conduits seeded with Schwann cells for peripheral nerve regeneration," *Biomaterials,* vol. 23, no. 2, pp. 841-848, 2002.

[38] P. J. Camarata, R. Suryanarayanan, D. A. Turner, R. G. Parker and T. J. Ebner, "Sustained release of nerve growth factor from biodegradable polymer microspheres," *Neurosurgery,* vol. 30, no. 3, pp. 313-319, 1992.

[39] X. Cao and M. S. Shoichet, "Delivering neuroactive molecules from biodegradable microspheres for application in central nervous system disorders," *Biomaterials,* vol. 20, pp. 329-339, 1999.

[40] X. M. Lam, E. T. Duenas and J. L. Cleland, "Encapsulation and stabilization of nerve growth factor into poly(lactic-co-glycolic) acid microspheres," *Journal of Pharmaceutical Sciences,* vol. 90, no. 9, pp. 1356-1365, 2001.

[41] X. Xu, W.-C. Yee, P. Y. K. Hwang, H. Yu, A. C. A. Wan, S. Gao, K.-L. Boon, H.-Q. Mao, K. W. Leong and S. Wang, "Peripheral nerve regeneration with sustained release of poly(phosphoester) microencapsulated nerve growth factor within nerve guide conduits," *Biomaterials,* vol. 24, pp. 2405-2412, 2003.

[42] N. Ratner, L. Glaser and R. P. Bunge, "PC12 cells as a source of neurite-derived cell surface mitogen, which stimulates schwann cell division," *The Journal of Cell Biology,* vol. 98, pp. 1150-1155, 1984.

[43] M. B. Mellott, K. Searcy and M. V. Pishko, "Release of protein from highly cross-linked hydrogels of poly(ethylene glycol) diacrylate fabricated by UV polymerization," *Biomaterials,* vol. 22, no. 9, pp. 929-941, 2001.

[44] J. L. West and J. A. Hubbel, "Photopolymerized hydrogel materials for drug delivery applications," *Reactive Polymers,* vol. 25, no. 2-3, pp. 139-147, 1995.

[45] W. R. Gombotz, W. Guanghui, T. A. Horbett and A. S. Hoffman, "Protein adsorption to poly(ethylene oxide) surfaces," *Journal of Biomedical Materials Research,* vol. 25, pp. 1547-1562, 1991.

[46] X. Liu and P. X. Ma, "Polymeric scaffolds for bone tissue engineering," *Annals of Biomedical Engineering,* vol. 32, no. 3, pp. 477-486, 2004.

[47] Y. Wang, U.-J. Kim, D. J. Blasioli, H.-J. Kim and D. L. Kaplan, "In vitro cartilage tissue engineering with 3D porous aqueous-derived silk scaffolds and mesenchymal stem cells," *Biomaterials,* vol. 26, no. 34, pp. 7082-7094, 2005.

[48] M. D. Pierschbacher, J. W. Polarek, W. S. Craig, J. F. Tschopp, N. J. Sipes and J. R. Harper, "Manipulation of cellular interactions with biomaterials toward a therapeutic outcome: a perspective," *Journal of Cellular Biochemistry,* vol. 56, no. 2, pp. 150-154, 1994.

[49] R. H. Schmedlen, K. S. Masters and J. L. West, "Photocrosslinkable polyvinyl alcohol hydrogels that can be modified with cell adhesion peptides for use in tissue engineering," *Biomaterials,* vol. 23, pp. 4325-4332, 2002.

[50] E. Behravesh, K. Zygourakis and A. G. Mikos, "Adhesion and migration of marrow-derived osteoblasts on injectable in situ crosslinkable poly(propylene fumarate-co-ethylene glycol)-based hydrogels with a covalently linked RGDS peptide," *Journal of Biomedical Materials Research Part A,* vol. 65A, no. 2, pp. 260-270, 2003.

[51] F. J. Xu, Z. H. Wang and W. T. Yang, "Surface functionalization of polycaprolactone films via surface-initiated atom transfer radial polymerization of covalently coupling cell-adhesive biomolecules," *Biomaterials,* vol. 31, no. 2, pp. 3139-3147, 2010.

[52] "Arg-Gly-Asp-Ser," 2013. [Online]. Available: http://www.sigmaaldrich.com/catalog/product/sigma/a9041?lang=en&region=US.

[53] "Corning® Cell Culture Surfaces: Standard Tissue Culture Treated Surface," Corning, 1994-2013. [Online]. Available: http://www.corning.com/lifesciences/us_canada/en/technical_resources/surfaces/culture/stc_treated_polystyrene.aspx.

[54] N. D. Deal, J. W. Griffin and M. V. Hogan, "Nerve conduits for nerve repair or reconstruction," *Journal of the American Academy of Orthopaedic Surgeons,* vol. 20, no. 2, pp. 63-68, 2012.

[55] A. J. Windebank and J. F. Poduslo, "Neuronal growth factors produced by adult peripheral nerve after injury," *Brain Research,* vol. 385, pp. 197-200, 1986.

[56] A. D. Lynn, T. R. Kyriakides and S. J. Bryant, "Characterization of the in vitro macrophage response and in vivo hose response to poly(ethylene glycol)-based hydrogels," *Journal of Biomedical Materials Research Part A,* vol. 93A, no. 3, pp. 941-953, 2010.

[57] F. K. Sanders and D. Whitteridge, "Conduction velocity and myelin thickness in regenerating nerve fibres," *The Journal of Physiology,* vol. 105, no. 2, pp. 152-174, 1946.

[58] T. Scholz, J. M. Rogers, A. Krichevsky, S. Dhar and G. R. D. Evans, "Inducible nerve growth factor delivery for peripheral nerve regeneration in vivo," *Plastic and Reconstructive Surgery,* vol. 126, no. 6, p. 1874, 2010.

[59] T. Hadlock, C. Sundback, D. Hunter, M. Cheney and J. P. Vacanti, "A polymer foam conduit seeded with Schwann cells promotes guided peripheral nerve regeneration," *Tissue Engineering,* vol. 6, 2000.

[60] C. L. A.-M. Vleggeert-Lankamp, A. P. Pêgo, E. A. Lakke, M. Deenen, E. Marani and R. T. Thomeer, "Adhesion and proliferation of human Schwann cells on adhesive coatings," *Biomaterials,* vol. 25, pp. 2741-2751, 2004.

[61] W. Yu, W. Zhao, C. Zhu, X. Zhang, D. Ye, W. Zhang, Y. Zhoy, X. Jiang and Z. Zhang, "Sciatic nerve regeneration in rats by a promising electrospun collagen/poly(ε-caprolactone) nerve conduit with tailored degradation rate," *BME Neuroscience,* vol. 12, p. 68, 2011.

[62] S. Y. Chew, R. Mi, A. Hoke and K. W. Leong, "Aligned protein-polymer composite fibers enhance nerve regeneration: a potential tissue-engineering platform," *Advanced Functional Materials,* vol. 17, no. 8, pp. 1288-1296, 2007.

[63] *SLA User Guide,* Valencia, CA: 3D Systems, Inc., 1995.

[64] D. Espalin and E. Morales, "Development of a High Resolution Stereolithography Apparatus," El Paso, TX, 2010.

[65] P. F. Jacobs, Rapid Prototying & Manufacturing: Fundamentals of Stereolithography, Society of Manufacturing Engineers, 1992, p. 181.

[66] D. Li and Y. Xia, "Electrospinning of nanofibers: reinventing the wheel?," *Advanced Materials,* vol. 16, no. 14, pp. 1151-1170, 2004.

Appendix 1: Glossary of Abbreviations

3D	Three-dimensional
ACRL-PEG-NHS	Acryloyl-PEG-*N*-hydroxysuccinimide
Anti-NGF mAb	Monoclonal antibody
Anti-NGF pAb	Polyclonal antibody
Anti-Rat IgG, HRP Conjugate	Antibody conjugated to horseradish peroxidase
BSA	Bovine Serum Albumin
CAD	Computer-aided design
CNS	Central nervous system
D_P	Penetration depth
E_C	Critical exposure
ELISA	Enzyme-linked immunosorbent assay
GPS	Glutamine-penicillin-streptomycin
IKVAV	Isoleucine-Lysine-Valine-Alanine-Valine
NGF	Nerve growth factor
PBS	Phosphate buffered saline
PC-12	Rat pheochromocytoma cell line
PCL	Poly(α-lactide-ε-caprolactone)
PCLEEP	Caprolactone and ethyl ethylene phosphate copolymer
PEG	Poly(ethylene glycol)
PEGda	Poly(ethylene glycol) diacrylate
PGA	Polyglycolic acid
PLGA	Poly(lactic-co-glycolic acid)
PNS	Peripheral nervous system
PPE	Poly(phosphoester)
P(PF-*co*-EG)	Poly(propylene fumarate-*co*-ethylene glycol)
PVA	Polyvinyl alcohol
RGDS	Arginine-Glycine-Aspartic acid-Serine
SIS	Porcine small intestine submucosa
SL	Stereolithography
UV	Ultraviolet
YIGSR	Tyrosine-Isoleucine-Glycine-Serine-Arginine

Appendix 2: Calculations

Calculating solutes for a PEGda solution at 30 wt% concentration:

$$\% \text{ by mass solute} = \frac{\text{mass of solute}}{\text{mass of solution}} \times 100\%$$

Mass of PEGda = 1 g
Mass of PBS = x
Mass of I-2959 = y

To calculate Mass of PBS, starting with 1 g PEGda:

$$30\% = \frac{1}{1+x} \times 100\%$$

$0.3\ (1+x) = 1$

$0.3 + 0.3x = 1$

$0.3x = 0.7$

$$x = \frac{0.7}{0.3} = 2.33$$

Density of PBS = 1 g/mL

2.33 mL of PBS

To calculate Mass of I-2959:

$$0.5\% = \frac{y}{1+2.33+y} \times 100\%$$

$0.005\ (3.33 + y) = y$

$0.01665 + 0.005y = y$

$0.01665 = 0.995y$

$y = 0.0167$

0.0167 g of I-2959

Totals: 1 g PEGda
2.33 mL PBS
0.0167 g I-2959

Calculating solutes for a PEGda solution at 20 wt% concentration:

$$\% \text{ by mass solute} = \frac{\text{mass of solute}}{\text{mass of solution}} \times 100\%$$

Mass of PEGda = 1 g
Mass of PBS = x
Mass of I-2959 = y

To calculate Mass of PBS, starting with 1 g PEGda:

$$20\% = \frac{1}{1+x} \times 100\%$$

$$0.2\,(1+x) = 1$$

$$0.2 + 0.2x = 1$$

$$0.2x = 0.8$$

$$x = \frac{0.8}{0.2} = 4$$

Density of PBS = 1 g/mL

4 mL of PBS

To calculate Mass of I-2959:

$$0.5\% = \frac{y}{1+4+y} \times 100\%$$

$$0.005\,(5+y) = y$$

$$0.025 + 0.005y = y$$

$$0.025 = 0.995y$$

$$y = 0.0167$$

0.0251 g of I-2959

Totals: 1 g PEGda 4 mL PBS 0.0251 g I-2959

Calculating cross-sectional area of nerve guidance conduits, <u>as-fabricated</u>:

$CA = \pi r^2 n$

where

CA is cross-sectional area
r is radius of the lumens
n is number of lumens

1 Lumen: r = 0.53 mm, n = 1
$CA = \pi(0.53mm)^2 \times 1 = 0.88\ mm^2$

7 Lumen: r = 0.20 mm, n = 7
$CA = \pi(0.2\ mm)^2 \times 7 = 0.88\ mm^2$

14 Lumen: r = 0.12 mm, n = 14
$CA = \pi(0.12\ mm)^2 \times 14 = 0.63\ mm^2$

16 Lumen: r = 0.12 mm, n = 16
$CA = \pi(0.12\ mm)^2 \times 16 = 0.72\ mm^2$

18 Lumen: r = 0.12 mm, n = 18
$CA = \pi(0.12\ mm)^2 \times 18 = 0.81\ mm^2$

Calculating cross-sectional area of nerve guidance conduits, <u>swollen</u>:

$CA = \pi r^2 n$

where

CA is cross-sectional area
r is radius of the lumens
n is number of lumens

1 Lumen: r = 0.64 mm, n = 1
$CA = \pi(0.64\ mm)^2 \times 1 = 1.29\ mm^2$

7 Lumen: r = 0.242 mm, n = 7
$CA = \pi(0.242\ mm)^2 \times 7 = 1.29\ mm^2$

14 Lumen: r = 0.145 mm, n = 14
$CA = \pi(0.145\ mm)^2 \times 14 = 0.92\ mm^2$

16 Lumen: r = 0.145 mm, n = 16
$CA = \pi(0.145\ mm)^2 \times 16 = 1.06\ mm^2$

18 Lumen: r = 0.145 mm, n = 18
$CA = \pi(0.145\ mm)^2 \times 18 = 1.19\ mm^2$

Calculating surface area of nerve guidance conduits, <u>as-fabricated</u>:

$SA = 2\pi rhn$

where

SA is surface area
r is radius of the lumens
h is height of the lumen portion of conduit
n is number of lumens

1 Lumen: r = 0.53 mm, h = 10 mm, n = 1
SA = 2л (0.53 mm) (10 mm) x 1 = 33.30 mm^2

7 Lumen: r = 0.20 mm, h = 10 mm, n = 7
SA = 2л (0.20 mm) (10 mm) x 7 = 87.96 mm^2

14 Lumen: r = 0.12 mm, h = 10 mm, n = 14
SA = 2л (0.12 mm) (10 mm) x 14 = 105.56 mm^2

16 Lumen: r = 0.12 mm, h = 10 mm, n = 16
SA = 2л (0.12 mm) (10 mm) x 16 = 120.64 mm^2

18 Lumen: r = 0.12 mm, h = 10 mm, n = 18
SA = 2л (0.12 mm) (10 mm) x 18 = 135.72 mm^2

Calculating surface area of nerve guidance conduits, <u>swollen</u>:

$SA = 2\pi rhn$

where

SA is surface area
r is radius of the lumens
h is height of the lumen portion of conduit
n is number of lumens

1 Lumen: r = 0.64 mm, h = 11.8 mm, n = 1
SA = 2л (0.64 mm) (11.8 mm) x 1 lumens = 47.45 mm^2

7 Lumen: r = 0.242 mm, h = 11.8 mm, n = 7
SA = 2л (0.242 mm) (11.8 mm) x 7 lumens = 125.60 mm^2

14 Lumen: r = 0.145 mm, h = 11.8 mm, n = 14
SA = 2л (0.145 mm) (11.8 mm) x 14 lumens = 150.51 mm^2

16 Lumen: r = 0.145 mm, h = 11.8 mm, n = 16
SA = 2л (0.145 mm) (11.8 mm) x 16 lumens = 172.01 mm^2

18 Lumen: r = 0.145 mm, h = 11.8 mm, n = 18
SA = 2л (0.145 mm) (11.8 mm) x 18 lumens = 193.51 mm^2

Appendix 3: UC Irvine's IACUC Protocol

PROTOCOL NARRATIVE

University of California, Irvine
Institutional Animal Care and Use Committee
Version: May 2007

IACUC#:_____
For IACUC Office Use Only

Lead Researcher Name: Gregory R. D. Evans, M.D., F.A.C.S.
Title: Inducible Nerve Growth Factor Delivery for Peripheral Nerve Regeneration

Important: Save this form before filling it out.
Review of the Protocol Instructions is strongly recommended. Click on each section heading for a direct link to the corresponding section of the application instructions.

SECTION 1: PROJECT OVERVIEW

Provide a non-technical, lay language summary of the proposed project that can be understood by IACUC members with varied research backgrounds, non-scientists and community members. Discuss the potential relevance (e.g., benefits) of findings to human or animal health, advancement of knowledge, and/or the good of society. ***This summary should not exceed 250 words.***

Notes:
- Avoid using scientific terminology, jargon or unexplained abbreviations; where use of such language is unavoidable, provide definitions of all terms.
- Do not cut and paste from a grant application, journal article or abstract.

The ultimate goal of this proposal is to develop a clinically translatable tissue engineered strategy for peripheral nerve repair and replacement that avoids the limitations associated with the current standard of care, which is the use of autologous nerve transplants harvested from uninjured regions of the patient's body. Peripheral nerve injuries can result from mechanical, thermal, chemical, congenital or pathological causes. To date surgical approaches for nerve repair are limited due to various reasons. The availability of normal donor nerves from an uninjured body location for surgical nerve repair is limited, and it may be associated with an increase in deformities, differences in structure and size and surgical complications such as bleeding, infections and pain. Furthermore, the use of nerves from other human beings or even animals for nerve replacement has shown poor outcomes. One possible alternative is the development of engineered constructs to replace those elements necessary for regeneration of the injured nerve and include a structural lead for the nerve growth to bridge the nerve gap, support cells, growth factors, and substances that fill the space between the cells of the nerve. Despite advances and contributions in the field of tissue engineering, results have failed to equal nerve regeneration realized when surgical repair was done with a nerve from a different body location.

The objective of this proposal is to develop a strategy to deliver nerve growth factor (NGF) to improve peripheral nerve regeneration. Nerve growth factor (NGF) is one of the most important regulatory substances to stimulate nerve regeneration. Creating an inducible system which allows the production of NGF to boost and stop would make peripheral nerve regeneration controllable.

SECTION 2: JUSTIFICATION FOR THE USE OF ANIMALS

A. Rationale for the Use of Animals

Federal regulations require that all investigators provide a narrative describing the rationale for using animals, the appropriateness of the species and the methods and specific sources used to determine

that alternatives (e.g. replacement, reduction, refinement) to the use of animals and to the procedures have been considered.

Please answer all of the subsections below:

1. Explain **why animals are required** for these studies, and why non-animal model replacements, such as cell culture or computer modeling, cannot fully replace animals:

Animals are utilized to measure the efficacy of the NGF delivery system on peripheral nerve regeneration and functional restoration.

In-vitro analysis is employed within this study to evaluate the early transfection efficacy. However, the ultimate test of nerve proliferation is in-vivo analysis. This combines the complex process of axonal migration and cell interaction. Nerve injury and a novel approach to nerve repair injury repair is proposed. An intact and injured nerve responding in it's natural physiological milieu is essential in order to assess functional nerve recovery. This can only be achieved using a live vertebrate animal model.

2. Explain **why the proposed species** are the most appropriate:

The Nude rat is being chosen to eliminate immunologic reactions between the human NGF protein and the HEK-293 cells. Further, the use of Nude rats better equates to the use of autografts when nerve is harvested from donor animals and placed within a recipient's defect (isografts). Additionally, functional analysis, electrical conduction studies and histochemical markers have been well-established for the Nude rat. Although larger nerve gaps will entail the use of larger animals (i.e. rabbits), the nerve gaps within the rat will prove adequate to determine the feasibility of this delivery system.

B. Alternatives to the Use of Animals

The United States Department of Agriculture (USDA) requires that you specify at least two sources or databases used to determine that the model and methods described in this protocol do not:

- Unnecessarily duplicate previous experiments,
- Unnecessarily use animals, or
- Unjustifiably expose animals to potentially painful, uncomfortable or distressful procedures.

1. Database Searches
   Indicate with an "**X**" in the bracket **[ ]** which databases (at least 2) were used to search for alternatives:

[X] National Agricultural Library (AGRICOLA)		**[ ]** AltWeb
[ ] BIOSIS Previews	**[ ]** CORDIS	**[ ]** CRIS
[ ] CRISP	**[ ]** NORINA	**[ ]** PsycINFO
[ ] TBASE	**[ ]** TOXLINE	**[X]** MEDLINE via PubMed
[ ] Web of Science		

2. Date(s) the database search was performed:
Note: *the search must be within the last 3 months*

09/11/2009

3. Years (e.g., 1985 to present) covered by the search:

1989 to present

4. Keywords used in the search:

- Peripheral nerve regeneration
- Nerve regeneration
- Sciatic nerve exposure
- Animal alternatives
- Computer-based nerve regeneration
- Nerve growth factor/NGF
- Regulation of growth factor/NGF
- Cell kill by HSV-TK
- Ponasterone A

Note: In general the more "keywords" you use the more specific your search will be; however, it is possible to be so specific that nothing will be found. In that case you should reduce the number of terms used. Click here for search tips.

5. If a **consultant** was used for considering alternatives, provide the following information:

[X] Not applicable – Two databases in #1 were the primary means for considering alternatives.

Expert consultant's name:	Type here
Consultant's qualifications/expertise:	Type here
Content of the consultation:	Type here
Date(s) of the consultation:	Type here

6. Narrative Description - Reduction, Refinement and Replacement

Discuss the results and findings of search—be specific. Describe the steps you have taken to **replace** the use of animals with *in vitro* procedures, **reduce** the number of animals used, **refine** the experimental design, and **refine** procedural techniques. If similar experiments are found, describe the aspects of your research project that are novel (i.e., not unnecessarily duplicative of other published work.) If alternative methods or procedures representing refinements to your procedures were found, please discuss **why** those alternatives cannot be used:

No alternatives to animal-based nerve regeneration studies was identified. This proposed procedure does not duplicate any current or previously published work.

Because of our experience in the previous studies with this topic we were able to reduce the total number of animals 50% (n=270).

Because of our results from this study during the last 3 years there is no need to repeat the same amount of experiments. We think if we combine the new with our previous results we are still able to get significant data. So we reduced the number of needed animals in the current protocol 50%. We did not change any procedures and techniques.

SECTION 3: EXPERIMENTAL DESIGN

Provide a **concise description** of the experimental design below, describing all experiments to be performed. For **each experiment**, provide the following information:

1. Briefly describe the **rationale** behind the experiment or the hypothesis being tested (i.e., the reason for performing the procedure).

2. Define the **groups and number of animals per group** needed for the experiment, including both experimental and control animals, and list the **procedures to be performed** on each group. A table or block design may be an effective way to present this information.

3. Explain **how the number of animals for the experiment was determined** to be adequate for the generation of statistically significant data (i.e., power analysis, previous publications).

4. Describe the **sequence and timing** of all live animal procedures to be performed, according to the groups defined in #2 above. Provide a timeline, diagram or flowchart if appropriate.

5. Define the **procedural endpoints** for each group of animals defined in #2 above (i.e., what determines when the live animal portion of the experiment is complete and animals are euthanized.)

Notes:

- Do not cut and paste from a grant application, journal article or abstract.
- Do not provide a detailed description of the procedures here. These details should be provided in Sections 5 and 6 of the protocol narrative.
- Do not provide detailed descriptions of analytical methods or procedures that do not involve the use of animals.

HEK-293 cells are ubiquitous and easily transfected. The HEK-293 cells offer advantages over our previous fibroblast cell line in that the HEK-293 cells are 1) Commercially available, 2) Easily transfected, 3) Well studied, 4) Virtually no cellular output (i.e collagen). Although we have been able to transfect HEK-293 cells with NGF and have demonstrated inducible NGF secretion and its biological activity, questions regarding potential alterations to cellular function remain. It is the purpose of this Specific Aim to answer these questions and complete our evaluation of the regulatory system.

Specific Aim #1: No animals used. HEK-293 cell culturing, sorting and preparing for transfection.

Specific Aim #2: No animals used. Transfection of the cells with our NGF- and HSV-TK-codons and preparation for the conduits.

Specific Aim #3:

The following groups will be utilized:

Group 1 hNGF-EcR-293 induced Pon (+) [via infusion catheter]
(N=10)

Group 2 hNGF-EcR-293 induced Pon (+) [intraveneously]
(N=10)

Group 3 hNGF-EcR-293 noninduced Pon (-)
(N=10)

Group 4 HEK-293 nontransfected cells Pon (+) [via infusion catheter]
(N=10)

Group 5 (N=10) HEK-293 nontransfected cells Pon (+) [intraveneously]

Group 6 (N=10) HEK-293 nontransfected cells Pon (-)

Group 7 (N=10) Empty PLLA conduit

Group 8 (N=10) PLLA conduit filled with Vitrogen

Group 9 (N=10) hNGF-EcR-293 (TK+) induced with Pon (+) and treated with Ganciclovir (+) [via infusion catheter]

Group 10 (N=10) hNGF-EcR-293 (TK+) induced with Pon (+) and treated with Ganciclovir (+) [intraveneously]

Group 11 (N=10) hNGF-EcR-293 (TK+) noninduced with Pon (-) and treated with Ganciclovir (-)

Group 12 (N=10) Cultured Schwann cells

Group 13 (N=15) Isograft controls from 5 donor animals

270 nude rats will be utilized within this study in a multi-modal analysis to test the variables. The use of nude rats precludes potential immunologic reactions with the human NGF or HEK-293 cells. The cells suspended in media as outlined above for each group will be placed within PLLA conduits bridging a 10 mm nerve gap in the sciatic nerve. Cell concentration will be 1000 cells in the conduits after administration as determined from previous studies and the minimum amount of Ponasterone A will be determined from SA 1. We know from our preliminary data that further administration of Ponasteron A at later time points will improve the outcome. Therefore all groups but Group 5 and Group 10 will be locally reboostered with Ponasteron A at day 3, 5, 10,and 14 via a catheter placed directly at the conduit. The purpose of noninducible hNGF-EcR-293 cells are to determine the effect on nerve regeneration of potential secretory proteins produced by these cells alone. Additional control groups with empty PLLA conduits, conduits filled with collagen and isografts will be employed. In the control group with isografts from 5 donor animals the sciatic nerve of the right and the left leg of the donor animals will be harvested and surgically implanted in the right sciatic nerve of 10 control animals as a nerve graft. Alltogether for this group, 15 animals will be needed. In addition to the stimulatory animals, hNGF-EcR-293 cells transfected with a herpes simplex virus-thymidine kinase gene (HSV-TK) will be treated by Ganciclovir and placed at 1000 cells per conduits in additional animals. A final group of transfected but nontreated with Ganciclovir will be conducted. All cells will be placed within the PLLA conduits at the time of surgical intervention. The PLLA conduits will be harvested at days 3,5,10,14, and 21. The primary endpoint of this SA will be the NGF production by our cell line and will be determined by protein analysis using ELISA and immunohistochemistry and its gene expression using RT-PCR. The secondary endpoints are the expression of Gap-43, actin, myosin II, tubulin, fibronectin, laminin, trk A, B, C and p75. These variables will also be analyzed by ELISA, RT-PCR and immunohistochemistry to determine the extent of up or down regulation based on the delivery of NGF. The overall number of animals used for this SA is justified by the fact that this study is based upon preliminary studies and the need to obtain a minimum number of animals per group (n=10) to test the hypothesis as determined by statistical power analysis. To achieve a statistical power of 85% in our setting the minimum number to treat is n=19.

Specific Aim #4:

This SA will be conducted with 135 nude rats. Administration of Ponasterone-A dosing will be determined from SA 1. The animals will have the 15 mm PLLA conduits placed into a sciatic nerve defect in the right leg as outlined in SA 3 and the groups will include:

Group 1 (N=15)	Isograft controls from 5 donor animals
Group 2 (N=10)	hNGF-EcR-293 induced with Pon (+) [via infusion catheter]
Group 3 (N=10)	hNGF-EcR-293 induced with Pon (+) [intraveneously]
Group 4 (N=10)	hNGF-EcR-293 noninduced with Pon (-)
Group 5 (N=10)	HEK-293 nontransfected cells Pon (+) [via infusion catheter]
Group 6 (N=10)	HEK-293 nontransfected cells Pon (+) [intraveneously]
Group 7 (N=10)	HEK-293 nontransfected cells Pon (-)
Group 8 (N=10)	Empty PLLA conduit
Group 9 (N=10)	PLLA Conduit filled with Vitrogen
Group 10 (N=10)	hNGF-EcR-293 (TK+) induced with Pon (+) and treated with Ganciclovir (+) [via infusion catheter]
Group 11 (N=10)	hNGF-EcR-293 (TK+) induced with Pon (+) and treated with Ganciclovir (+) [intraveneously]
Group 12 (N=10)	hNGF-EcR-293 (TK+) noninduced with Pon (-) and treated with Ganciclovir (-)
Group 13 (N=10)	Cultured Schwann cells

Functional analysis will be conducted monthly through 4 months. This will be performed by walking track analysis as outlined below and will used as the primary endpoint. This analysis serves as an indirect measure of nerve reinnervation. At the end of 2 and 4 months, direct nerve to nerve stimulation will be performed on the sciatic nerve to assess conduction velocity and peak electrical amplitude. The gastrocnemius muscle will be harvested and weighed in order to assess nerve reinnervation following nerve stimulation. The gastrocnemius muscle is supplied by the posterior tibial branch of the sciatic nerve. Once the nerve is severed, the muscle will begin to atrophy. As the nerve regenerates into the muscle, it will regain its mass proportional to the amount of reinnervation. This will provide indirect measurements of nerve regeneration. Comparisons of the percentage will be performed between groups in order to potentially avoid normal differences in muscle weight between individual animals. By using this indirect technique for proportional measurements we will be able to save a complete group of animals. When muscle weight is compared between groups using absolute values instead of proportional changes another control group would first have to determine normal values of

the gastrocnemius muscle in these rats. In addition, the distal nerve and conduit/isografts will be harvested and histomorphologic analysis performed. The null hypothesis for statistical analysis in this SA is that there will be no significant difference between the functional parameters for the control isografts and the experimental groups. The secondary endpoints of this SA are changes in muscle weight and the histomorphological analysis of the distal nerve, conduit and isograft.

After 2 moths the first half of the animals will be conducted to terminal surgery for electrical nerve analysis and following muscle harvest. After 4 months the second half will be assessed and muscles will be harvested.

(135 for SA 3 and 135 for SA4; Group 13 in SA 3 and Group 1 in SA 4 will need 15 animals each [5 donor animals and 10 reciepient animals])

SECTION 4: ANIMAL REQUIREMENTS AND USDA PAIN CATEGORIES

Based upon the design above, provide the following information about the animals in this project:

- **Genus-Species or Common Name:** list the genus-species or common names of all vertebrate animals involved in the experimental design.
- **Strain:** List separately any special strains. Each animal should be accounted for once in the table.
- **Condition Code:** Assign a condition code for each species. These codes are used for animal purchase, transfer and reporting of animals numbers.
- **USDA pain category:** Assign a USDA pain/distress category for each species.
- **Total # required:** Indicate the total number of animals involved in the project for the duration of the project or 3 years, whichever is less.

SPECIES	STRAIN	CONDITION CODE	USDA PAIN CATEGORY (B, C, D, or E*)	TOTAL # REQUIRED
Rat	Nude	Mature	D	270
Rat	Sprauge Dowley	Mature	D	20

*Animals in Category E: Unrelieved pain, distress or discomfort requires strong scientific justification with particular attention to the significance, necessity, and potential benefits of the research.

- Investigators must perform euthanasia on all moribund experimental animals unless there is scientific justification that euthanasia would invalidate experimental data collection.
- If euthanizing a moribund animal would seriously harm the study, the scientific justification for using death as an endpoint must be provided below.
- Click here for additional information about UCI's euthanasia policy and alternative endpoints.

Scientific Justification for Animals in Category E: Type here

SECTION 5: DESCRIPTION OF NON-SURGICAL PROCEDURES

Describe **in detail** all non-surgical procedures to be performed on live animals.

- Indicate with an "**X**" in the bracket **[ ]** if non-surgical procedures will not be performed in live animals.
- Procedures described here must be referenced in Section 3.
- Animal monitoring and management (as applicable) must be addressed in Section 7.
- Each subsection below should be completed as it applies to the protocol.

- A ULAR veterinarian should be consulted in the planning of non-surgical procedures involving potential pain and/or distress.
- Click on “Section 5” above for detailed instructions.
- If a procedure does not apply state “N/A”.

[ ] Not applicable – Non-surgical procedures will not be performed on live animals. *Skip the rest of this section.*

1. Euthanasia followed by Tissue Harvest:

Harvest of conduits and nerves:
Tissue harvest will only occur during the terminal surgical procedure. Site of sciatic nerve defect and conduit implantation will be harvested at defined time points.

Gastrocnemius mascle harvest and weight:
Both the medial and lateral gastrocnemius muscle will be harvested. Muscle will be placed in preweighed sterile saline containers so that desiccation does not occur. The difference in weight of the containers before and after muscle placement will determine the muscle weight. Weights of the injured (experimental) and noninjured (control) leg will be compared to determine a percentage.

2. Blood and Tissue Collection in Live Animals:

N/A

3. Behavioral Studies:

Nerve regeneration functional analysis:
Walking track analysis (sciatic functional index - SFI) will be performed monthly through 2-4 months. Preoperatively, the animals are trained to walk down a 30 x 4 inch track into a darkened enclosure. Postoperatively, the rats’ hind paws are painted with water soluble ink and any changes in their paw prints caused by nerve injury and denervation will be recorded. Three different parameters of the rodents paw print are measured to determine the sciatic functional index. This number is traditionally expressed as a negative. Values tending toward zero indicate improved functional recovery:

Sciatic Functional Index = -38.3 (PLF) + 109.5(TSF) + 13.3 (ITF) - 8.8
PLF = Print Length Function = (Experimental PL - Normal PL)/Normal PL
TSF = Toe Spread Function = (Experimental TS - Normal TS)/Normal TS (1st to 5th Toe)
ITF = Intermedian Toe Spread Function = (Experimental IT-Normal IT)/Normal IT (2nd - 4th Toe)

4. Administration of Experimental Agents:

Ponasterone A is the agent, that when administered, will induce the transfected 293 cells to secrete NGF. To determine the optimal route of delivery of Ponasterone A will be administered through an infusion catheter [IC] or intravenously [IV] in the specified groups at day 3, 5, 10 and 14. Ganciclovir will only be administered locally at the time of surgery.

AGENT	DOSE (mg/kg body weight)	ROUTE	FREQUENCY
PURPOSE			
PonA	3 mL of 3 uM	intracathete	x4 administration
(inducing agent)			
PonA	3 mL of 3 uM	intravenous	x4 administration

(inducing agent)			
Ganciclovir (turn-off NGF)	150 mg/Kg	local	once

The catheter connected to the conduit will be placed during the first surgery. For iv administration we will use the femoral vein. We will clarify with the campus veterinarians if the volume of 3ml slowly injected is to high or not. We are open to adjust the volume for an optimal administration.

We consulted Dr. Roger Geertsema regarding the administration of 3ml volume iv. For a 400-500g rat, which we will use, 3ml volume for iv-administration is possible, but the upper limit.

5. Induction of Anesthesia/Sedation for Non-surgical Procedures:

- Indicate how anesthesia/sedation is induced:
- Describe how the level of anesthesia/sedation is assessed to be adequate to begin the procedure:
- Describe how animals are monitored (e.g., respiration pattern, response to noxious stimulation (e.g., paw pinch), heart rate/pattern, EKG, blood pressure, temperature, etc.) throughout the procedure and discuss any supplemental anesthesia dosing required:
- If animals will be placed on artificial ventilation, describe the range of respiration rates and tidal volumes.
- For survival procedures, describe how animals are monitored for recovery from anesthesia/sedation and when animals are returned to their home cages. Estimate how long it will take for the animal to recover from anesthesia/sedation (i.e., ambulatory and feeding).

6. Imaging Procedures:

Histomorphometric analysis:
The distal nerve will be harvested, fixed with 3% glutaraldehyde, embedded in epoxy resin, sectioned and stained with toluidine blue. Histomorphometric analysis will be performed by histology coupled with digital image processing and analysis. Briefly, nerve conduit sections stained with toluidine blue will be placed on the stage of an inverted microscope and viewed with bright field optics. Images of the histological sections will be digitized using a CCD camera and subsequently analyzed using standard and sophisticated image processing techniques. Images will be thresholded and segmented into individual axons. The number of axons per three randomly selected regions measuring 80 x 60 microns will be counted to give the number of axons/mm2. The area of each axon will be determined, summed, and expressed as axons/image area to give the nerve fiber density.

7. Cardiac Perfusion:

N/A

8. Other Non-surgical Procedures:

Conduit fabrication:
Poly(L-lactic acid) (PLLA) (Birmingham Polymers, Birmingham, AL) will be manufactured into porous biodegradable conduits using a combined solvent casting, extrusion, and particulate leaching technique. The PLLA conduits will be fabricated with a porosity of 90%, a pore size between 150 and 300 μM, and an extrusion temperature of 275°C. The resultant conduits will have an inner diameter of 1.6 mm, an outer

diameter of 3.2 mm, and a length of 15 mm. This portion of the proposals SAs will involve the assistance of consultant Charles Patrick, Jr. Ph.D. Previous studies with our transfected hDFBs have indicated degradation of the PLLA conduit does not cause cell death.

Protein Analysis:
To assess that the NGF protein is secreted in vivo, conduits will be harvested at 3, 5, 10, 14 and 21 days and fluid within the conduit will be aspirated with the help of a 30 gauge tuberculin syringe (Ethicon). Analysis for NGF production by ELISA using Emax NGF-ELISA kit (Promega) as per the manufacturer's protocol will be conducted. Protein expressions will also be assesed of Gap-43, actin, myosin II, tubulin, fibronectin, laminin, trk A, B, C and p75.

RT-PCR and Immunohistochemistry in tissue:
To characterize axonal/support cell interaction upon NGF production, RNA harvested from these conduits will be used to asses the status of Gap-43, actin, myosin II, tubulin, fibronectin, laminin, trk A, B, C, NGF expression and p75 by RT-PCR using primers specific to respective genes. Protein expression levels of these genes within the conduit will also be assessed by immunohistochemistry. The nerve conduits will be fixed, embedded and sectioned (5 micron) (see E.3.3.4). These sections will be used for immunohistochemical analysis of above mentioned support cell genes using labeled antibodies specific to respective proteins.

Electrical conduction studies:
At the end of 2 and 4 months, direct nerve to nerve stimulation will be performed on the sciatic nerve to assess conduction velocity and peak electrical amplitude. After deep intramuscular anesthesia as outlined above, ½ of the animals randomly selected in each subdivided group will be placed on a Harvard ventilator (New England Medical Instruments #122, Medway MA) delivering 300 ml of 100% O2 per minute through oral tracheal intubation with a 14 gauge angiocatheter (Terumo Medical Corp, Elkton, MD). Electrophysiologic testing will then be performed using an Advantage 3000 Series (London, Ontario Canada) nerve stimulator. At the conclusion of the electrical conduction studies, the medial and lateral gastrocnemius muscle will be harvested and weighed in order to assess nerve reinnervation as outlined above.

9. Post-procedural Care (as applicable):

N/A

SECTION 6: SURGICAL PROCEDURES

Describe **in detail** all surgical procedures to be performed.
- Indicate with an "**X**" in the bracket **[ ]** if surgical procedures will not be performed on live animals.
- Any procedures described here must be referenced in Section 3.
- Animal monitoring and management (as applicable) must be addressed in Section 7.
- Each subsection below should be addressed as it applies to the surgical procedure.
- Address each of the applicable subparts for **each** surgery to be performed.
- Click on "Section 6" above for detailed instructions.
- If a procedure does not apply, state "N/A".

[ ] Not applicable – Surgical procedures will not be performed on live animals.
Skip the rest of this section.

A. Pre-operative Care:

Food and water will be provided ad libitum

B. Induction of Anesthesia for Surgical Procedures:

- Indicate how anesthesia is induced:
  General anesthesia will be induced and maintained by a 0.4 ml intramuscular injection of a premixed solution containing 95 mg/kg ketamine HCL (Keta-StheticTM, Boehringer Ingelheim, St. Joseph, MO), 6 mg/kg xylazine (RompunTM, Miles, Shawnee Mission, KS), and 0.05 mg/kg atropine sulfate (Elkins-Sinn, Cherry Hill, NJ). If needed a supplemental dose of 0.1ml of the premixed solution will be given.

- Describe how the level of anesthesia is assessed to be adequate to begin the procedure:

- Describe how animals are monitored (e.g., respiration pattern, response to noxious stimulation (e.g., paw pinch), heart rate/pattern, EKG, blood pressure, temperature, etc.) throughout the procedure and discuss any supplemental anesthesia dosing required:

  Depth of anesthesia will be assessed intra-operatively by changes in muscle tone and, by changes in respiratory rate. Changes in muscle tone provides an earlier warning to changes in depth of anesthesia than toe-pinch. Changes in muscle flaccidity and/or changes in respiratory rate will indicate the need to adjust delivery of anesthetic.

- If animals will be placed on artificial ventilation, describe the range of respiration rates and tidal volumes.

  N/A

- For survival procedures, describe how animals are monitored for recovery from anesthesia and when animals are returned to their home cages. Estimate how long it will take for the animal to recover from anesthesia (i.e., ambulatory and feeding).

At the conclusion of surgery, buprenorphine will be given subcutaneously and bacitracin will be applied topically to the suture site. Animals will be monitored until ambulatory (2-4 hours after surgery) and before returning them to their home cages. Food and water will be given from the return on to their home cages.

C. Aseptic Techniques:

- Preparation of the surgical space:

  Topical sterilization with 70% ethanol

- Preparation of the surgeon(s):

  Standard surgical hand scrub and sterile gowning with masks, hats.

- Preparation of the animal(s):

  Topical betadine solution

- Sterilization of instruments:

  Autoclave

D. Surgical Procedure:

Surgical technique: Cells as outlined in the above groups will be seeded within the PLLA conduits with a seeding density of 103 suspended in Vitrogen and implanted into a surgically created nerve defect in the sciatic nerve of nude rats. Briefly, the right lower extremity of the animal will be shaved and prepared in an antiseptic fashion with betadine (AMSCO Medical Products, PA). The sciatic nerve will be exposed by a muscle splitting incision. The PLLA conduits, sterilized with ethylene oxide, will be placed into this sciatic nerve defect with 1 mm of the proximal and distal nerve ends invaginating into the conduit. Conduits will be sutured to the nerve using 10-0 nylon (Sharp Point) suture and microsurgical technique. One end of the nerve will be sutured within the conduit. Application of the cell suspended in Vitrogen will then be applied with a 27G needle (Becton Dickinson). Once this is completed, the other end of the nerve will be sutured in place allowing a "cap" to the filled conduit. This technique has worked for us in the past. One end of an infusion catheter will be connected to a conduit that will be interposed between the ends of a sciatic nerve defect. The injection port end will be placed on the dorsum subcutaneously. Ponasterone will be injected through the injection port at day 3, 5, 10, and 14 for all groups but Group 5 and Group 10. This will allow delivery of the agent to the conduit. In separate animals, Ponasterone A will be adiministered intravenously. The muscle of the leg will be closed using 4-0 Dexon sutures (Davis+Geck, Wayne, NJ) and skin staples used for wound approximation (Stoelting, Wood Dale, IL). At 3,5,10,14 and 21 days following conduit placement, 4 randomly selected animals at each time point for each group (total 10 per group) will again be anesthetized with the above intramuscular medications. Cells and contents within the PLLA conduit will be collected. In addition, sections of the distal nerve will be harvested for histomorphology. Staining and evaluation will proceed as outlined above.

Note: Animals in which a sciatic nerve defect will be created will undergo two surgical procedures:
During the 1st surgical procedure a sciatic nerve defect will be created and the PLLA conduit implanted [interposed over the ends of the sciatic nerve]. During the 2nd surgical procedure, the PLLA conduit will be harvested following direct nerve to nerve stimulation. This 2nd surgical procedure will be a terminal procedure.

E. Methods to Prevent Dehydration & Hypothermia:

Lactated Ringers or normal Saline will be given subcutaneously to prevent dehydration. A heating pad will be used to minimize hypothermia.

F. Surgical Endpoints and Post-operative Care:

Survival surgery will conclude with the closure of the skin incision [approximately 15 minutes following the iniating skin incision]. Terminal surgery will conclude with administration of an overdose of pentobarbital that will be given at the conclusion.
At the conclusion of surgery, buprenorphine will be given subcutaneously and bacitracin will be applied topically to the suture site. Animals will be monitored until ambulatory and before returning them to their home cages. Each animal will be monitored daily including weekends. Animals will be assessed for pain, distress and discomfort during daily monitoring.
Animals will be monitored daily during the 1st five post-operative days and buprenorphine and/or carprofen administered for pain management. The first dose of buprenorphine will be adminisered to the animals as they begin to recover from the procedural anesthetics. Injections of buprenorphine will be administered to each animal for the first 24 hours (q 8 to 12 hours) and on a PRN basis thereafter. After 24 hours the animals get Carprofen daily (q 12 to 24 hours) for 5 days, then as needed.

SECTION 7: ADVERSE EFFECTS & ANIMAL MONITORING AND MANAGEMENT

Please answer each of the questions below. **Note:** *A "not applicable" answer applies only to experiments in which naive animals will be euthanized for harvest of tissue only, without prior experimental intervention.*

A. Briefly summarize all possible adverse effects or phenotypic abnormalities that may present in the animals as a result of study procedures, agents, disease processes, genetic alterations, etc. (Example: tumor formation, ascites, neurologic deficits, moribundity, etc.)

See section B.

B. Describe the clinical signs and symptoms that may appear in the animals as a result of the experimental procedures or agents, including any associated pain, distress or discomfort.

Unrestricted weight-bearing activity will be allowed as tolerated postoperatively. Autonomy of the denervated foot can follow sciatic nerve resection resulting in walking impairment. Painting the foot with substances which are not harmful, such as cayenne pepper extract, quinine solution, or Biter Apple can assist in the prevention of this behavior.

C. Describe the monitoring parameters (i.e., signs, symptoms and species-specific behaviors) that will be used to assess pain, distress and discomfort in animals.

Retraction from observer, huddled in a fetal position, ruffled hair coat and excessive weightloss are warning sings for pain, stress and discomfort and should not have been detected during daily observation.

D. Describe the management plan that will be used to assess and treat pain, distress and discomfort in the animals, including any special procedures that will be used (e.g., periodic weighing of animals) and any interventions that will be performed to relieve pain, distress and discomfort in the animals (e.g., analgesics, antibiotics, special housing/bedding, etc.)

Animals will be monitored daily during the 1st five post-operative days and buprenorphine and/or carprofen administered for pain management. The first dose of buprenorphine will be adminisered to the animals as they begin to recover from the procedural anesthetics. Injections of buprenorphine will be administered to each animal for the first 24 hours (q 8 to 12 hours) and on a PRN basis thereafter. After 24 hours the animals get Carprofen daily (q 12 to 24 hours) for 5 days, then as needed.

Note: Analgesia will be administered during the first 5 post-operative days. Animals will be assessed for pain, distress and discomfort during daily monitoring and the Campus Veterinarian consulted if evidence of pain becomes apparent.

Every animal with a sciatic nerve defect will be observed daily, including weekends. If it can be predicted that an animal will mutilate it's foot within 24 hours, that animal will be euthanized immediately. Any animal presenting any evidence of foot mutilation will immediately be euthanized.

E. Indicate the frequency in which animals will be monitored to assess their well being.

Animals will be assessed for pain, distress and discomfort during daily monitoring.

F. Describe how the monitoring of animals (e.g., daily observations and treatments performed by research staff) will be documented. Monitoring records should be kept in the animal room and must be readily available to ULAR veterinary staff and IACUC members at all times.

Routine monitoring will be recorded with an animal protocol and indications on the cage cards.

G. Describe the criteria that will be used to determine that an animal must be removed from the study ahead of schedule and euthanized. (Click here for euthanasia criteria.)

Animals will be assessed for pain, distress and discomfort during daily monitoring. Any animal exhibiting unalleviated pain or distress [retraction from observer, huddled in a fetal position, ruffled hair coat] will be euthanized immediately.

SECTION 8: EXPERIMENTAL AGENTS AND THERAPEUTIC DRUGS

A. Table of Drugs/Agents Used in Live Animals

List all anesthetic, therapeutic drugs and experimental/study agents administered to live animals.

- **Drug/Agent**: list the name of the drugs or agents used in this project.
  - **Experimental agents** include placebos, viruses and other biological agents, tumor cells, gene markers, tracers, radioisotopes, etc.
  - **Therapeutic drugs** include anesthetics, analgesics, tranquilizers, antibiotics, fluids and other agents such as antimicrobials and paralytics.
  - **Do not list euthanasia drugs in this section**. Agents used to euthanize animals, including anesthetic overdoses, should be identified in Section 9.
  - Note: Rodent biological materials, including cell lines, may require testing for pathogens prior to use.
- **Controlled Substances**: Indicate with an "**X**" in the bracket **[ ]** if the drug is on the U.S. Drug Enforcement Agency's list of Controlled Substances
- **Purpose**: Use the following codes for the purpose column--Pre-anesthetic (PA); Anesthetic (A); Therapeutic (T); Experimental (E).
- **Dose Range**: Express dosages as a range and as mg/kg of body mass, wherever possible.
- **Route:** Use the following codes for routes of administration—intravenous (IV); intramuscular (IM); subcutaneous (SC); intraperitoneal (IP); *per os* –by mouth (PO); by inhalation (Inhl)
- **Frequency**: Specify how often the drug/agent will be administered in each animal in a 24 hour period
- **Period of Administration**: Specify how long the drug/agent will be used in each animal while it is in the study.

Note: Use the "Tab" key to create additional rows in a table by placing your cursor in the last cell of the table.

Species	Drug/Agent	Contr'd Subs?	Purpose	Dose Range	Route	Frequency	Period of Admin
Rat	Ketamine	[X]	Anesthesia	95mg/kg	IM	Once	
	Xylazine	[X]	Anesthesia	6mg/kg	IM	Once	
	Atropnie	[ ]	Anesthesia	0.05mg/kg	IM	Once	
	Buprenorphine	[X]	Analgesia	0.01 to 0.05 mg/kg	SC	Q 8 to 12 hrs	

	Cayenne pepper extract	[ ]	Prevent foot mutilation	Smear	Topical	As needed	
	Bitter apple	[ ]	Prevent foot mutilation	Smear	Topical	As needed	
	Quinine	[ ]	Prevent foot mutilation	Smear	Topical	As needed	
	Ponasterone A	[ ]	NGF production	2 uM/kg	Intra conduit	As needed	
	Ganciclovir		Stop NGF production	10 uM/kg	Intra conduit	Once	
	Bacitractin		Wound protection	Smear	Topical	Once	
	Betadine		Desinfection	Liquid	Topical	Once	
	Vitrogen		Cell carier	Gel/liquid	Intraconduit	Once	
	hNGF-EcR-293 cells		NGF production	Cells	Intracoduit	Once	
	Carprofen		Analgesia	4-5mg sc or 0.04mg/ml water po	Sc or po	Q 12-24 hrs	

SECTION 9: EUTHANASIA METHODS

A. Place an "**X**" in the bracket **[ ]** next to the method(s) of euthanasia to be used.

[X] Anesthetic Overdose (complete the table below)

SPECIES	AGENT	DOSE	ROUTE OF ADMINISTRATION
Rat	Eutha-6	150-200mg/kg animal body weight	IV

[ ] Physical Method

[ ] Decapitation (describe):

Type here

[ ] Cervical Dislocation (describe):

Type here

[ ] Cardiac Perfusion: (describe):

Type here

[ ] Other (describe):

Type here

B. Indicate how death of the animals will be confirmed:

[X] Direct (open chest) inspection of the heart

[ ] Decapitation

[ ] Exsanguination

[ ] Other (describe): Type here

SECTION 10: ROLES, RESPONSIBILITIES AND EXPERTISE OF THE STUDY TEAM

List below all study team members who will have contact with live animals.

1. Describe each person's **specific role and responsibility** on the project, including the **procedures** they will perform.
2. Indicate who will be responsible for the **daily care and monitoring** of the animals.
3. Provide a description of their **qualifications, level of training and expertise**.
4. If a study team member does not have relevant experience or training for a particular species or procedure they will perform, **describe how they will be trained**.

Lead Researcher:

Dr. Gregory Evans: Head of division and the PI on this project. Dr. Evans will oversee the project desing, procedure, and completion. He will conduct surgical teaching to the additional personnel through observation. Dr. Evans will be active in all surgical procedures. He has 5 years of general surgery training, 6 years of plastic surgery training, 1 year of microsurgery training, and over 15 years experience with rodent-based protocols.

Co-Researcher(s):

Garret Wirth, M.D.: Over 10 years of general and plastic surgery training. He will conduct surgical teaching to the additional personnel through observation. Dr. Wirth will be active in all surgical procedures.

Dr. Thomas Scholz: Will be involved in all surgical procedures as well as post-harvest processing and assays. He will be involved in the pre-intra- and post-operative care of the animals. He has 3 years general surgery training, and over 6 years of animal-based protocol experience including rats and pigs. Primarily responsible for conducting the behavioral studies.

Research Personnel:

Donald Mowlds: Medical student, available for assiting in Lab work and animal care.

Vita

Mireya Aidee Perez is a native of El Paso, TX and a 2003 graduate from Coronado High School. After that, she obtained a Bachelor of Science in Biological Sciences with a minor in Chemistry from the University of Texas at El Paso (UTEP) in May of 2007. During her undergraduate career, she was an active member of the Medical Professions Organization. As a member, she participated in various community service projects, including working as a volunteer at University Medical Center. She also conducted research at the Analytical Core Cytology Facility, directed by Dr. Joanne T. Ellzey. For two years, she was employed by Alternative Personal Care as Human Resources Coordinator and Staff Trainer. She decided to continue her education by re-enrolling at UTEP and pursuing a Master of Science in Biomedical Engineering. During her graduate studies, she participated in the Texas Tech-UTEP Collaborative Clinical Shadowing Program, enriching her exposure to the medical field. She was also employed as a graduate research assistant at the W.M. Keck Center for 3D Innovation, directed by Dr. Ryan B. Wicker, where she conducted research focused on the biomedical applications of additive manufacturing. Her research has been presented at international conferences such as the Solid Freeform Fabrication Symposium and the Biomedical Engineering Society's Annual Meeting.

Permanent address: 4445 Lazy Willow Dr.
El Paso, TX, 79922

This thesis was typed by Mireya Perez.